R. G. John

ADVANCED ELECTRIC PROPULSION RESEARCH

PREPARED FOR

NATIONAL AERONAUTICS AND SPACE ADMINISTRATION

GRANT NGR06-002-032

REPORT NO. 8

SPACE PROPULSION PROGRAM

ENERGY CONVERSION PROGRAM

COLLEGE OF ENGINEERING

COLORADO STATE UNIVERSITY

FORT COLLINS, COLORADO

MER 68-69WRM-11

FINAL REPORT

For the period July 1, 1968 to December 31, 1968

ADVANCED ELECTRIC PROPULSION RESEARCH

Prepared for

NATIONAL AERONAUTICS AND SPACE ADMINISTRATION

May, 1969

Grant NGR06-002-032

Technical Management

Mr. James Lazar
Nuclear Electric Systems Division
Office of Advanced Research Technology
NASA Headquarters
Washington, D.C. 20546

Prepared by: 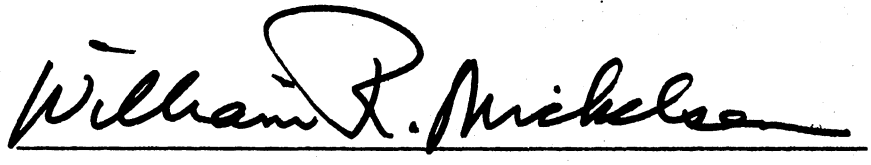

William R. Mickelsen, principal investigator
Professor of Mechanical Engineering
and Professor of Electrical Engineering
Engineering Research Center
Colorado State University
Fort Collins, Colorado 80521

CONTENTS

Paper presented at AIAA Seventh Electric Propulsion Conference, March 3-5, 1969, Williamsburg, Virginia.

THEORETICAL ANALYSES OF ELECTROTHERMAL THRUSTERS WITH SUPERSONIC HEAT ADDITION*

by Harry I. Leon+
and William R. Mickelsen++
Colorado State University

ABSTRACT

Theoretical performance analyses are presented for an electrothermal thruster using lithium propellant with a combination of radioisotope and electrical energy sources. This thruster concept allows the lithium propellant to condense in the nozzle and uses the latent heat of vaporization for increasing the exit velocity.

Specific impulses of greater than 500 seconds are predicted with plenum temperatures below 2250°K and with electric power/thrust ratios of less than 3 watt/mlb.

INTRODUCTION

The performance of existing resistojets is limited to specific impulses below 300 seconds with propellants of interest such as ammonia[1]. A higher specific impulse is required if resistojets are to be competitive with other propulsion systems for future applications. The analyses reported here show that resistojet specific impulse might be increased greatly by means of supersonic heat addition.

A fundamental limitation to the specific impulse of conventional resistojets is the practical limit for plenum temperature, which depends on the materials of construction and on the type of propellant. However, if more heat were added to the supersonic stream, it is theoretically possible to increase the exhaust velocity without incurring excessive materials temperature.

---

* Done under NASA Grant NGR06-002-032, Electric Thruster Systems, OART.
+ Pre-doctoral Graduate Research Assistant. Student Member, AIAA.
++ Professor of Mechanical Engineering. Assoc. Fellow, AIAA.

A number of means of supersonic heat addition were considered in the present study. Of these, the most attractive means appears to be the partial condensation of the vapor propellant in portions of the supersonic stream. For substantial amounts of heat addition by this means, the propellant must have a relatively high heat of vaporization. In addition the propellant molecular weight must be low in order to obtain a high exhaust velocity. A brief review of propellants indicated that lithium has superior properties for this thruster concept. For example, if 50% of the lithium vapor were condensed in the supersonic stream, the total temperature would be increased by about 3000°K. With a plenum temperature of 2000°K and 50% condensate, the ideal specific impulse would be approximately 550 seconds. Therefore, the present study was devoted exclusively to thruster designs with lithium propellant.

THE RADIOISOTOPE/RESISTOJET DESIGN CONCEPT

Only a fraction of the total propellant flow can be expected to condense, therefore an appreciable amount of heat of vaporization would leave the thruster in the vapor exhaust. Early studies[2] of the condensing-flow electrothermal thruster concept showed that the power/thrust would be high if the heat of vaporization were supplied by electric heaters. If the heat of vaporization were supplied by a thermal heater such as a radioisotope capsule, then the electric power/thrust would be competitive with conventional resistojets. A schematic diagram of the radioisotope/resistojet concept is shown in Figure 1.

The analyses reported here have been directed toward the radioisotope/resistojet concept, although much of the work is applicable to other thruster design concepts as well.

In addition to specifying lithium as the propellant, a nominal thruster mass flow rate of 0.0074 gm/sec was used throughout the analyses. At a specific impulse of 600 seconds, the thrust would be 10 millipounds.

BASIC THEORY OF HEAT ADDITION TO SUPERSONIC STREAM

The increase in velocity of a gas flowing through a nozzle follows the first law of thermodynamics:

$$h_o = h + v^2/2 \qquad (1)$$

where h_o is the total enthalpy, h is the stream static enthalpy and v is the velocity of the gas in the nozzle. With careful choice of nozzle geometry, heat may be added to the stream to increase the total enthalpy, thereby providing a velocity increase. Heating of the flow in the supersonic section of the nozzle was found to be more desirable than in the subsonic section since the overall size of the nozzle would be smaller.

It is well known that if heat is added to a constant area of supersonic flow, the Mach Number will decrease toward unity. However, if the nozzle area is increased at a sufficient rate, the additional energy will cause an increase in velocity, as given by[3]:

$$\frac{dv}{v} = \left(\frac{1}{M^2-1}\right)\left[\frac{dA}{A} - \left(1 + \frac{\gamma-1}{2} M^2\right)\frac{dT_o}{T_o} - \left(1 + \gamma M^2\right)\frac{d\dot{m}_v}{\dot{m}_v}\right] \qquad (2)$$

Where A is the cross section area of the stream, γ is the specific heat ratio, M is the Mach Number, T_o is the total temperature, and $\dot{m}_v$ is the mass flow rate of the vapor stream. From inspection of equation (2), it is evident that the stream velocity in supersonic flow will increase if:

$$\frac{dA}{A} > \left(1 + \frac{\gamma-1}{2} M^2\right)\frac{dT_o}{T_o} \qquad (3)$$

For condensing flow, $d\dot{m}_v$ is negative, therefore the stream velocity will increase if:

$$\frac{dA}{A} > \left(1 + \frac{\gamma-1}{2} M^2\right)\frac{dT_o}{T_o} - \left(1 + \gamma M^2\right)\left|\frac{d\dot{m}_v}{\dot{m}_v}\right| \qquad (4)$$

The theoretical improvement in exhaust-velocity using heat addition in the nozzle is shown on Figure 2, where T_{02}/T_{01} is the ratio of stagnation temperature in the nozzle to stagnation temperature in the plenum. It should be noted that although the total temperature in the nozzle can be several times greater than the total temperature in the plenum, the stream temperature T can be lower due to the increase in velocity. This is shown by the equation for the definition of total temperature:

$$T_o = T + \frac{v^2}{2c_p} \tag{5}$$

where c_p is the specific heat of the propellant.

BASIC THEORY OF NUCLEATION

By proper choice of plenum temperature and pressure, condensate nuclei will begin to form at an appreciable rate in the supersonic section of the nozzle. The plenum temperature and pressure must be chosen such that the conditions in the throat of the nozzle will be below the critical temperature and pressure of the propellant. The propellant vapor was assumed to be a perfect ideal gas with isentropic expansion to the point where nucleation begins, as shown in Figure 3.

For lithium vapor, an appreciable nucleation rate was found to begin at a saturation pressure ratio of about four. The critical-droplet radius r* for homogeneous nucleation is given by[4]:

$$r^* = \frac{2\sigma}{\rho_\ell RT \ln(p_v/p_s)} \tag{6}$$

where σ is the surface tension, ρ_ℓ is the liquid density, R is the gas constant, T is the vapor temperature, p_v is the stream static pressure, and p_s is the saturation pressure.

The critical-sized droplet can be thought of as the maximum of Gibbs free energy of a particle as shown in Figure 4. Thus, if a particle is less than critical size r*, it will reevaporate; on the other hand, if it is greater than r*, it will have the tendency to continue growing.

The rate of nucleation J_x of critical-sized droplets in a unit volume of vapor is[4]:

$$J_x = \left(\frac{p_v}{kT}\right)^2 \frac{1}{\rho_\ell} \left(\frac{2\mu\sigma}{\pi N_A}\right)^{\frac{1}{2}} \exp\left(-\frac{4\pi\sigma r^{*2}}{3kT}\right) \qquad (7)$$

Where k is Boltzmann's constant, N_A is Avogadro's number and μ is the molecular weight. The number of nuclei S_J formed per unit distance travelled in the nozzle is:

$$S_J = J_x \, \Delta V \, \Delta t \qquad (8)$$

where ΔV is the volume of an interval in the nozzle and Δt is the time required for the flow to traverse the interval $\Delta \ell$:

$$\Delta V = \bar{A} \, \Delta \ell \qquad (9)$$

$$\Delta \ell = \bar{v} \, \Delta t \qquad (10)$$

where $\bar{A}$ is the average cross-sectional area of the nozzle in the interval, and $\bar{v}$ is the average velocity in the interval.

GROWTH OF CONDENSATION NUCLEI

Once the critical-sized droplets are formed, they begin to grow as a result of collisions with the vapor molecules, some of which condense on the surface of the droplets. In a Maxwellian velocity distribution, the mass Γ_v of vapor droplets striking a unit area per second is[5]:

$$\Gamma_v = p_v/(2\pi RT)^{\frac{1}{2}} \qquad (11)$$

Only a small fraction of the atoms will stick to the nuclei, therefore the mass rate of arrival Γ_v must be multiplied by a sticking coefficient α to obtain the rate of mass increase Γ_a per unit area:

$$\Gamma_a = \alpha p_v/(2\pi RT)^{\frac{1}{2}} \qquad (12)$$

The sticking coefficient α is [5,6]:

$$\alpha = \frac{c_{p\ell} \quad (T_p - \bar{T})}{h_{fg} \left(1 - \frac{2\sigma}{r\rho_\ell h_{fg}}\right)} \tag{13}$$

where $c_{p\ell}$ is the specific heat of the liquid, T_p is droplet temperature, $\bar{T}$ is the average vapor temperature in the nozzle increment, h_{fg} is the heat of vaporization, σ is the surface tension, r is the droplet radius, and ρ_ℓ is the liquid density.

It should be noted here that the sticking coefficient α accounts for both the reflected incident atoms, and for atoms that are evaporated from the droplet. The expression for α given by Equation (13) is valid only for quasi-steady growth models.

The rate $\dot{m}_c$ at which nucleation and growth occurs in any particular nozzle interval n is:

$$\dot{m}_c = \dot{m}_J + \dot{m}_{ao} + \dot{m}_a \tag{14}$$

where $\dot{m}_J$ is the mass condensed due to fresh nucleation in the nozzle interval n, $\dot{m}_{ao}$ is the mass condensed in the nozzle interval n onto droplets which were originally formed by nucleation in the first nozzle interval, and $\dot{m}_a$ is the mass condensed in nozzle interval n onto droplets which were originally formed by nucleation in the nozzle intervals 2 to n-1.

Mass $\dot{m}_J$ due to fresh nucleation is:

$$\dot{m}_J = \rho_\ell \left(\frac{4}{3} \pi r^{*3}\right) \Delta V \, J_x \tag{15}$$

where r* is given by equation (6), ΔV is the volume of the nozzle interval n, and J_x is given by equation (7).

Mass $\dot{m}_{ao}$ condensed onto droplets that originated in the first nozzle interval is:

$$\dot{m}_{ao} = \Gamma_a S_{J1} \theta \tag{16}$$

where Γ_a is given by equation (12), S_{J1} is given by equation (8) evaluated in the first nozzle interval, and θ is the collision cross section:

$$\theta = 4\pi (r_m + r)^2 \tag{17}$$

where r_m is the lithium atom radius, and r is the drop radius accounting for the growth through nozzle intervals 2 to n-1.

Mass $\dot{m}_a$ condensed onto droplets that originated in nozzle intervals 2 to n-1 is:

$$\dot{m}_a = \Gamma_a \left(\sum_{i=2}^{n-1} S_{Ji} \right) \bar{\theta} \qquad (18)$$

where $\bar{\theta}$ is an average cross section for droplets in the nozzle interval n:

$$\bar{\theta} = 4\pi (r_m + \bar{r})^2 \qquad (17)$$

where $\bar{r}$ is an average of droplet radii for the drops originating in nozzle intervals 2 to n-1. By approximation, the radius $\bar{r}$ was determined by assuming that this class of drops had grown to 1/2 the mass of drops that originated in the first interval:

$$\bar{r} = (1/2)^{1/3} r \qquad (18)$$

When the vapor condenses, the latent heat of vaporization is released to the vapor stream. This heat causes the total temperature to rise, as given by the equation below:

$$T_o = \frac{\dot{m}_c h_{fg}}{\dot{m}_{tot} \bar{c}_p} \qquad (19)$$

where $\dot{m}_c$ is given by equation (14), $\dot{m}_{tot}$ is the total propellant flow rate, and $\bar{c}_p$ is an average specific heat for liquid and vapor:

$$\bar{c}_p = F\, c_{p\ell} + (1 - F)\, c_{pv} \qquad (20)$$

where F is the fraction of total propellant flow which has been condensed. In equations (19) and (20), it is assumed that the temperature rise of the droplet is the same as the increase in total temperature of the vapor stream. This approximation was considered adequate for the purposes of this preliminary analysis, but future work should include a detailed heat balance of the droplet growth process for determination of the actual rise in droplet temperature. According to a previous theoretical

analysis[6], the drop temperature should be close to the saturation temperature for the local stream static pressure. Since stream static pressure is continuously decreasing through the nozzle, the droplet temperature may actually decrease, and if this is true then the assumption used in equations (19) and (20) is conservative. In addition, future work should include the effect of momentum interchange between the droplets and the vapor stream on the stream total-temperature increase.

The combination of the total temperature change, the condensation fraction and the geometry (area change of the nozzle) can be used in Equation (2) to determine the velocity in an increment of the nozzle.

METHOD OF ANALYSIS

Analysis of the condensing nozzle flow was done on a CDC-6400 digital computer. An iterative method was used to solve the theoretical equations over many very small intervals of nozzle length:

1. A conical nozzle geometry was assumed, with switching controls to change the expansion angles at stations such as the onset of appreciable nucleation.

2. Plenum temperature and pressure were assumed.

3. Isentropic flow was calculated along the nozzle to the first interval where appreciable nucleation rate occurred.

4. The temperature T_1, the pressure p_1, and the Mach Number M_1 were assumed constant through the first interval during the first iteration.

5. For the first interval, the condensate mass, the total-temperature rise, and the velocity change were calculated based on the given nozzle area change.

6. From the velocity change, the temperature T_2, the pressure p_2, and the Mach Number M_2 were determined for the end of the first interval.

7. Returning to the start of the first interval, the condensate mass was re-calculated using the average values $(T_1 + T_2)/2$ and $(p_1 + p_2)/2$.

8. The iterative process was repeated until the average properties of the interval, $(T_1 + T_2)/2$ and $(M_1 + M_2)/2$ were negligibly different from those of the previous iteration.

A number of assumptions were made in the analysis:

a. The lithium vapor was assumed to be a perfect gas, which is very nearly correct since lithium is monatomic.

b. The drops were assumed to travel at the vapor stream velocity. Experimental measurements have shown that particles of less than 10^{-5} cm diameter move at stream velocity[5], and that particles as large as 10^{-4} cm diameter move at approximately 99% of the stream velocity[6]. Droplet diameters calculated in the present analysis were less than 10^{-6} cm; therefore, the stream-velocity assumption appears to be valid.

c. Boundary layer thickness and friction were assumed negligible. Because of the nozzle dimensions, the favorable pressure gradient, and the accelerating flow, this assumption may be valid but should be verified in future work.

d. Convective heat transfer from the stream to the nozzle walls was not considered. A regenerative propellant flow design might be used to prevent excessive nozzle wall temperature. Future work should include this heat transfer in the nozzle-flow heat balance.

e. Radiation heat transfer from the walls to the droplets in the stream was not considered. With high condensate fractions, this might return appreciable heat to the nozzle flow.

NOZZLE DESIGN AND PERFORMANCE ASSUMING NO PARTICLE GROWTH

In the early phases of the present study, a conical nozzle having a constant expansion angle was considered. It was soon found that the condensation fraction increased as the angle of the nozzle was decreased. In fact, it was found than an extremely small nozzle half-angle of about one-half degree gave the highest fraction of condensate. For example, a nozzle half-angle of 1/2-degree gave approximately twice the amount of condensation as a nozzle having a five-degree expansion. However, nozzle designs with these small expansion angles required

extremely long nozzle lengths to convert the thermal energy of the lithium propellant into kinetic energy. It was also found that since most of the condensation occurred in a relatively small section of the nozzle, the nozzle expansion could be increased after the high-condensation region. This increased angle after the condensation region greatly shortened the nozzle without much loss in performance. Furthermore, it was found that the nozzle could be shortened further if the angle upstream of the condensation was increased (to between 1 to 3 degrees) since it had no effect on the condensation. A typical nozzle design with these features is shown on Figure 5. The stations where these nozzle angle changes took place was found to have a strong effect on the total length of the nozzle. If the larger angle upstream of the nozzle-condensation region was allowed to penetrate the condensation region, the nucleation rate would increase faster than with the smaller angle in the condensation region. Thus, the nozzle would be further shortened if the upstream angle was continued to where the nucleation rate approached the maximum value. However, if this larger angle was continued too far, the region of condensation in the nozzle would be reduced in extent, thereby reducing the condensation fraction.

The effects of nozzle angles on the condensation fraction, the nozzle length, and the specific impulse for a particular set of plenum conditions is shown in Table I. In each case, the nozzle-angle change from θ_o to θ_c was done when the nucleation rate reached the values shown in the table. The nozzle angle was changed from θ_c to θ_E when the critical radius of the nuclei decreased to 1 angstrom. The nozzle length was terminated when the static temperature approached 60°K.

From inspection of Table I, it is evident that nozzle geometry has a marked effect on nozzle length. It is notable that the results reported here do not necessarily represent optimum nozzle geometries. A fully optimized nozzle geometry would be contoured rather than have the fixed cone angles shown in Table I.

A summary of nozzle performances is shown in Table II for ranges of plenum temperatures and pressures. The vaporizer

temperature is shown for each plenum pressure; that is, the vaporizer is assumed to generate the plenum pressure. Although these results do not represent fully optimized nozzle geometries, some general trends of nozzle performance can be seen. Nozzle length is greatly reduced when higher plenum pressures (corresponding to higher vaporizer temperatures) are assumed. As expected, specific impulse is increased by higher plenum temperature.

Electric power/thrust ratios, based on the radioisotope/resistojet concept shown in Figure 1, are also listed in Table II. In this concept electric power is used only to heat the propellant vapor from the vaporizer temperature to the plenum temperature. At a specific impulse of 500 seconds, an all-electric resistojet with an efficiency near 100% would have a power/thrust ratio of 11 watt/mlb; therefore, the theoretical performance of the radioisotope/resistojet concept is most attractive even with no particle growth.

NOZZLE DESIGN AND PERFORMANCE WITH PARTICLE GROWTH INCLUDED

Experiments[5,6,7,8] done on condensation in nozzles have shown that the droplets grow after nucleation. The growth of the droplets was found to considerably increase the total fraction of the condensate in designs of nozzles similar to those shown in the non-growth case. It was found, however, that the geometry for the non-growth case would not be the best design for the nozzle with growth.

After several attempts to modify slightly the geometry of the non-growth design, it was found that the optimum design of the nozzle with growth would be quite different from its non-growth counterpart. The required design changes in the nozzle are due to the following factors:

1. The overall rate of condensation is increased. In order to utilize the increased heating of the stream, the nozzle angles in the condensation region must be increased beyond those of the non-growth case.

2. Large nozzle exit angles cannot be used, because the rate of growth increases greatly when the stream temperature is low.

3. Nucleation and particle growth occur in different regions of the nozzle. The nucleation occurs as soon as the saturation pressure ratio is greater than 4, while growth occurs after nucleation. The heat released to the stream during growth tends to stop the nucleation. Further analyses may provide nozzle designs in which optimum conditions exist for both nucleation and growth.

As an initial step in developing the geometry for the nozzle, the performance was studied with a constant angle expansion. This analysis of a constant angle expansion-nozzle was made for a range of plenum temperatures and pressures. A summary of the results is shown in Table III.

The specific impulse was found to be greater by about 5 percent, while the required length of the nozzle was found to be considerably shorter than for the non-growth counterpart. It is noted that the effect of growth on improvement of performance was the greatest for the lower plenum temperature cases.

The best performance was found when the half-angle of the nozzle was around 1 degree. The best choice of the angle was a function of the plenum pressure. If the plenum pressure was low (below 1/2 atmosphere), a slightly larger angle would increase the performance; while for higher plenum pressure, a slight decrease in angle improved the performance.

It should be noted that the work on the nozzle with growth is in the preliminary stages. Based on past experience on the geometry study of the non-growth case, the specific impulse can be expected to increase by about 5 to 10 percent above those presented in Table III as the effects of geometry on the design are better understood. Thus, it is estimated that, with a plenum temperature as low as 2000°K, a theoretical specific impulse of 550 seconds will be possible.

SUMMARY OF RESULTS

Theoretical performance of the radioisotope/resistojet thruster concept with a lithium-condensing nozzle is shown in Figures 6 and 7 for vaporizer temperatures of 1300 and 1500°K respectively. Electric power/thrust ratios are shown for both the nucleation-only analysis, and for single-angle nozzles with particle growth. Although these results are preliminary, it is clear that particle growth provides markedly higher performance.

Also shown in Figures 6 and 7 are the power/thrust ratios for ideal all-electric thrusters with 100% thruster efficiency. From this comparison, it appears that the lithium-condensing radioisotope/resistojet concept has theoretical promise of high performance.

CONCLUSIONS

The theoretical analyses reported here indicate that the lithium-condensing radisisotope/resistojet thruster concept should have performance much superior to existing electrothermal thruster concepts. Specific impulse values of at least 500 seconds appear possible with ideal electric power/thrust values below 3 watt/mlb.

Particle growth provides definite improvement in theoretical performance. Further work is being done to develop nozzle geometries that optimize the competing processes of nucleation and ensuing particle growth. It is anticipated that theoretical specific impulse values as high as 550 seconds will be found for fully optimized nozzle geometries with realizable vaporizer and plenum temperatures.

REFERENCES

1. Page, R. J., and Short, R. A.: Ten-Millipound Resistojet Performance. AIAA Paper 67-664. September, 1967.

2. Mickelsen, W. R., and Isley, W. C.: Auxiliary Electric Propulsion - Status and Prospects. Paper presented at AFOSR Fifth Symposium on Advanced Propulsion Concepts, Chicago, Illinois, April, 1968.

3. Shapiro, H. A.: The Dynamics and Thermodynamics of Compressible Fluid Flow. Vol. 1. Ronald Press Company, 1953.

4. Griffin, J. L.: Digital Computer Analysis of Condensation in Highly Expanded Flows. Air Force Aerospace Research Laboratories ARL 63-206. November, 1963.

5. Buhler, R. D.: Condensation of Air Components in Hypersonic Wind Tunnels. Ph.D. dissertation, California Institute of Technology. 1952.

6. Wegener, P. P., and Mach, L. M.: Condensation in Supersonic and Hypersonic Wind Tunnels. Advances in Applied Mechanics, Vol. 1. Academic Press. 1958.

7. Hill, P. G.: Condensation of Water Vapour During Supersonic Expansion in Nozzles. Jour. Fluid Mechanics, 25, 593. 1966.

8. Crowe, C. T., and Willoughby, P. G.: A Study of Particle Growth in a Rocket Nozzle. AIAA Journal, 5, 1300. 1967.

Table I - Effect of nozzle geometry on nozzle length, with no particle growth.

Propellant = lithium

Vaporizer temp. = 1500°K

Plenum press. = 0.45 atmos

Plenum temp. = 2250°K

Throat area = 0.003675 sq. cm

Throat diam. = 0.06840 cm = 0.0269 in

Nominal thrust = 7.2 mlb

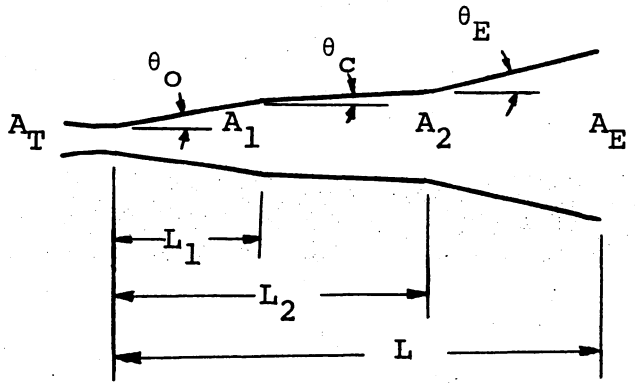

θ_o deg.	J_a #/cc-sec	L_1 cm	θ_c deg.	L_2 cm	θ_E deg.	cond. fract. F	L cm	I, sec
1.0	10^{18}	0.30	0.34	4.49	5.73	.271	10.20	485
2.0	10^{22}	1.04	0.57	1.55	0.57	.245	9.62	477
1.0	10^{21}	3.17	0.34	4.29	5.73	.269	5.87	484
1.0	10^{21}	0.46	0.57	3.07	11.46	.260	4.28	481
2.0	10^{22}	1.05	0.34	1.54	5.73	.235	2.98	473
2.0	10^{22}	1.04	.86	1.54	14.30	.224	2.19	470

TABLE II - Summary of nozzle performances with nucleation only

plenum temp. °K	plenum press. atmos.	vaporizer temp. °K	total temp. °K	fraction condensed	area ratio	nozzle length cm	specific impulse sec	power thrust watt/mlb
1600	.069	1300	3141	.260	41.7	78.1	437	.9
1800	.069	1300	3277	.247	49.2	43.0	447	1.5
1800	.3	1450	3480	.29	17.5	5.4	462	1.0
1800	.45	1500	3537	.303	14.5	4.2	468	0.9
2000	.069	1300	3252	.202	81.4	32.2	454	2.1
2000	.45	1500	3686	.291	14.1	5.9	475	1.4
2000	1.0	1600	3784	.313	5.4	4.9	480	1.1
2250	.039	1250	3358	.176	88.0	62.4	453	3.0
2250	.069	1300	3467	.196	74.5	28.0	460	2.8
2250	.116	1340	3608	.223	43.3	18.6	449	2.7
2250	.45	1500	3835	.269	14.9	5.9	485	2.1
2250	1.0	1600	3943	.29	8.2	3.5	491	1.8
2250	2.0	1670	4090	.308	5.4	2.9	477	1.6
2500	.069	1300	3658	.185	52.8	43.3	472	3.5
2500	.45	1500	3982	.249	15.7	5.7	494	2.7
2500	2.0	1670	4110	.274	7.5	1.7	502	2.2
2500	5.0	1860	4265	.31	2.3	1.3	510	1.7

TABLE III - Summary of nozzle performance with nucleation and growth

Constant nozzle angle expansion

Plenum Temp °K	Plenum Press. Atmos.	Vapor. Temp. °K	Total Temp. °K	Fraction Condensed	Area Ratio	Nozzle Half-angle Deg	Nozzle Length cm	Specific Impulse sec	Power/ thrust watts/mlb
1600	.0393	1250	3356	.307	5.25	1.0	7.9	454	1.05
1600	.0690	1300	3472	.334	3.49	1.0	4.0	462	.88
1800	.069	1300	3578	.312	3.77	1.0	4.46	469	1.45
1800	.30	1450	3725	.349	2.09	.34	2.84	476	1.00
1800	.30	1450	3700	.341	2.51	1.0	1.34	478	.98
1800	.45	1500	3741	.351	2.21	1.0	.92	480	.85
1800	.45	1500	3688	.338	2.61	2.0	.60	477	.86
2000	.069	1300	3732	.302	3.59	1.0	4.37	479	1.99
2000	.069	1300	3758	.308	3.47	2.0	2.11	481	1.98
2000	.45	1500	3868	.333	2.33	1.0	1.02	489	1.39
2000	1.0	1600	3865	.333	2.26	1.0	.66	488	1.52
2250	.069	1300	3960	.300	2.73	1.0	3.28	498	2.60
2250	.45	1500	3992	.304	2.55	1.0	1.19	496	2.06
2250	1.0	1600	4080	.326	1.86	1.0	.51	499	1.77
2250	1.0	1600	4013	.309	2.40	2.0	.38	498	1.78
2500	.069	1300	4028	.259	3.56	1.0	4.57	499	3.38
2500	.45	1500	4152	.284	2.62	1.0	1.26	506	2.69
2500	1.0	1600	4243	.3058	1.87	1.0	.52	508	2.41
2500	2.0	1670	4278	.313	1.92	1.0	.39	514	2.20

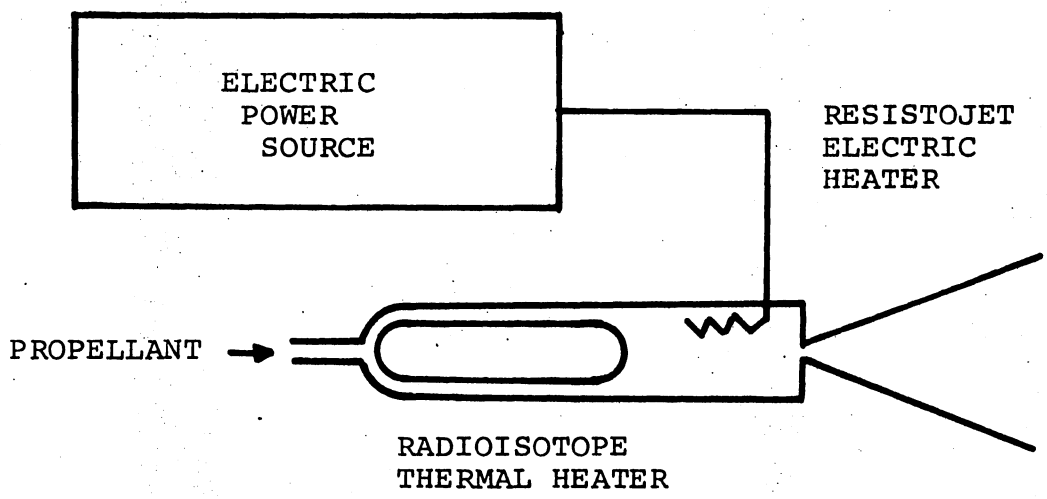

FIG. 1 - The radioisotope/resistojet concept.

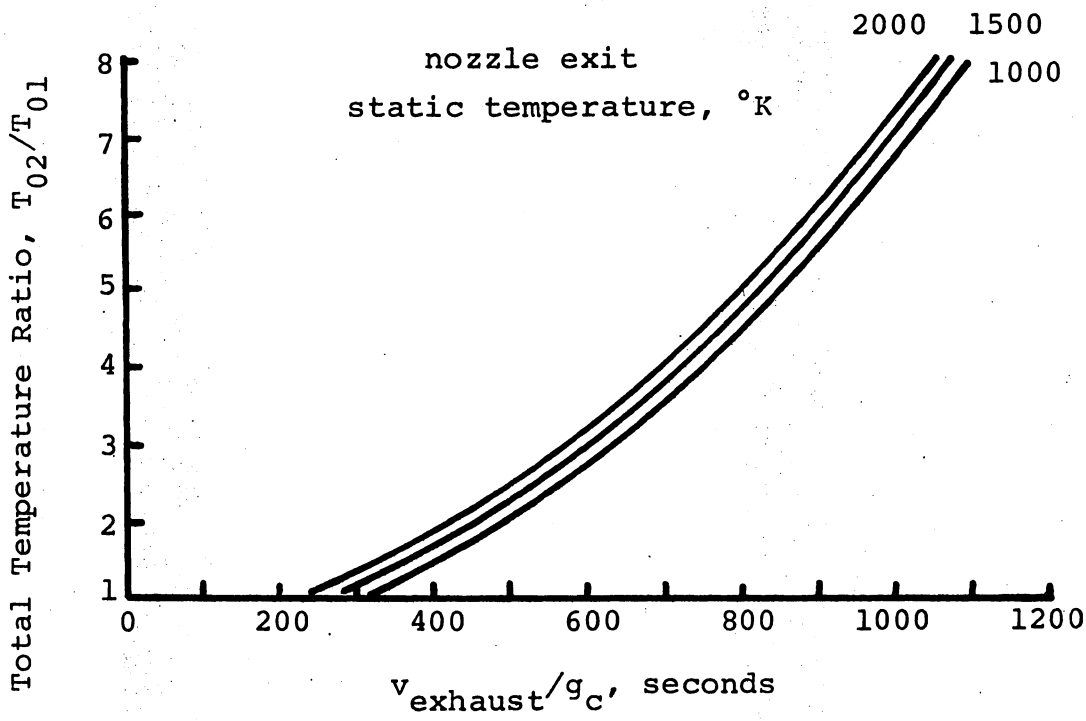

FIG. 2 - Theoretical exhaust velocity in supersonic flow of lithium with supersonic heat addition. Plenum total temperature, T_{01} = 2500°K; stream total temperature, T_{02}.

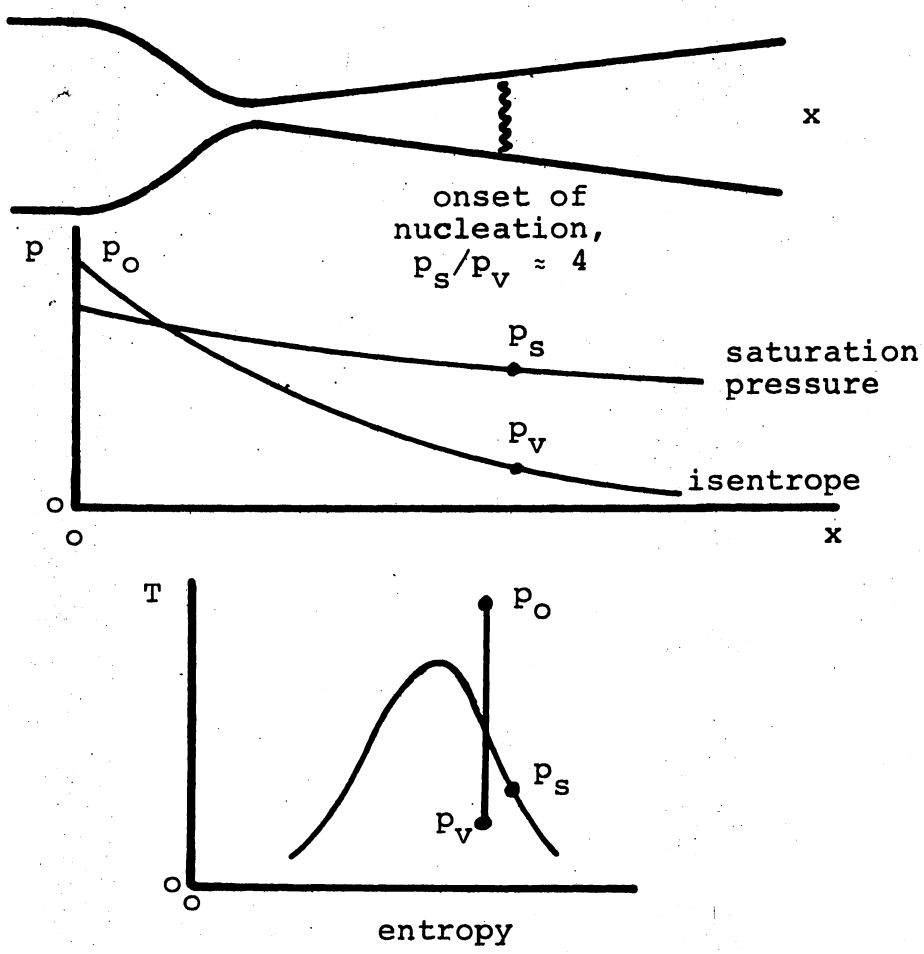

FIG. 3 - Onset of nucleation in condensing flow.

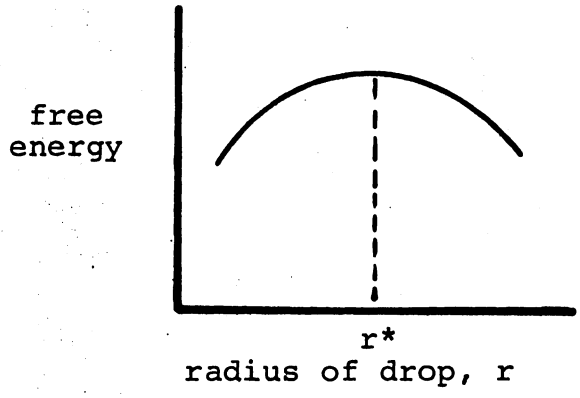

FIG. 4 - Gibbs free energy of liquid drops.

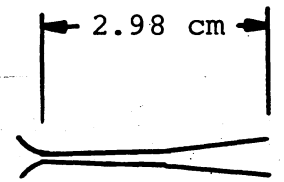

SCALE: 1/1

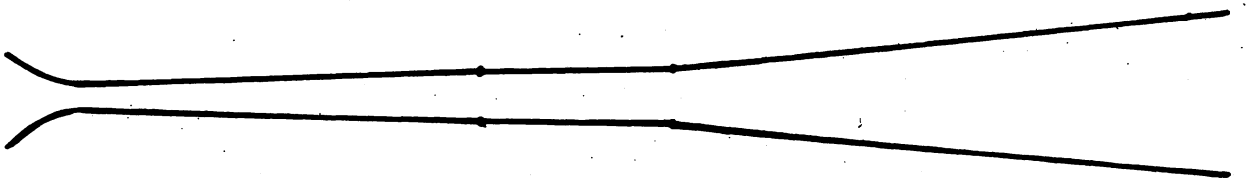

SCALE: 5/1

propellant: lithium
vaporizer temp.: 1500°K
plenum press.: 0.45 atmos
plenum temp.: 2250°K
throat diam.: 0.0684 cm (0.0269 in)
thrust: 7.2 mlb
specific impulse: 485 sec

FIG. 5 - Typical nozzle design based on nucleation with no particle growth.

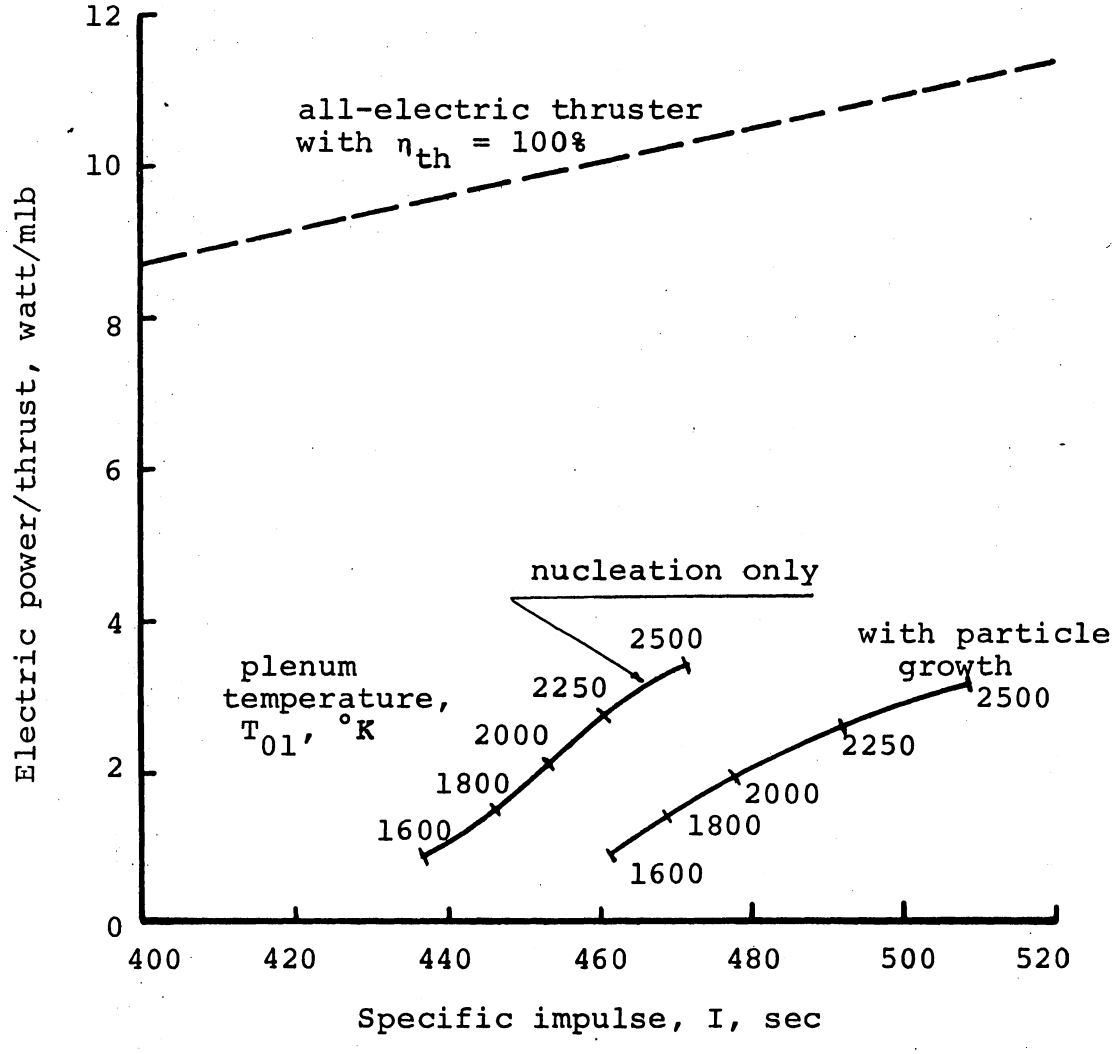

FIG. 6 - Comparison of theoretical performance of lithium-condensing nozzle electrothermal thrusters with vaporizer temperature of 1300°K.

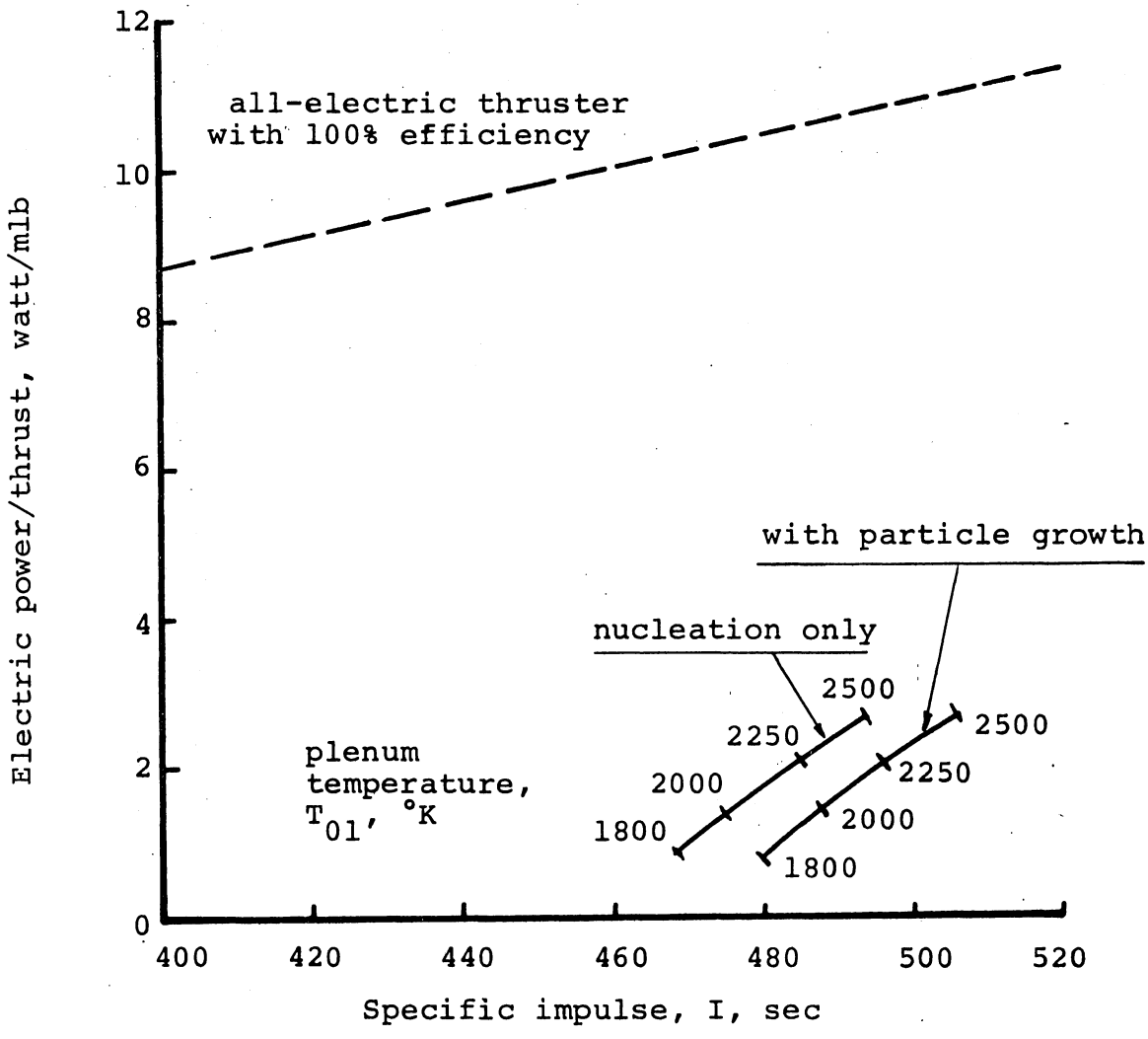

FIG. 7 - Comparison of theoretical performance of lithium-condensing nozzle electrothermal thrusters with vaporizer temperature of 1500°K.

ANALYSIS OF JUPITER FLY-BY MISSION WITH ELECTRIC PROPULSION*

by W. R. Mickelsen

This analysis has been done with the characteristic-length method. Because of the approximate nature of the C. L. method, the results of the analysis must be used only as rough indications of trends, and for specifying values of input parameters for more exact trajectory and mission calculations.

The results reported here are for the following mission-profile factors:

a. boost to hyperbolic excess velocity with SLV-3X/ Centaur/Burner II (2336) (Boeing growth version, propellant weight = 2336 lbs which is TE-364-4 being developed by NASA Goddard) (SLV-3X is available information on the 12-foot diameter currently being developed by General Dynamics/Convair).

b. 600-day heliocentric transfer to Jupiter

c. initial spacecraft weight W_Q of 630 lbs after boost to hyperbolic velocity V_H of 33,200 ft/sec (corresponds to inertial velocity V_c of 49,200 ft/sec).

d. on-board RTG with baseline power of 150 watts electric

e. hotel load of 50 watts electric during electric thrusting periods

f. 100 watts electric of "free" power for electric thruster system from baseline RTG

g. additional RTG units added as needed for electric propulsion

h. usable payload W_{pay} defined as:

$$W_{pay} = W_F - W_{th} - W_{addRTG} - W_c$$

where W_F = final spacecraft weight at Jupiter

W_{tank} = electric-propellant tank weight

W_{th} = weight of electric thruster system

W_{addRTG} = weight of additional RTG units

W_c = weight of power conditioning for electric thruster system

i. electric thruster system characteristics, from best available information, as shown in subsequent graphs.

---

* special report submitted to Mr. W. C. Isley, NASA Goddard Space Flight Center, June, 1968.

FIRST APPROXIMATION, CHARACTERISTIC-LENGTH METHOD

(assumes constant-mass vehicle, i.e., constant F and a)

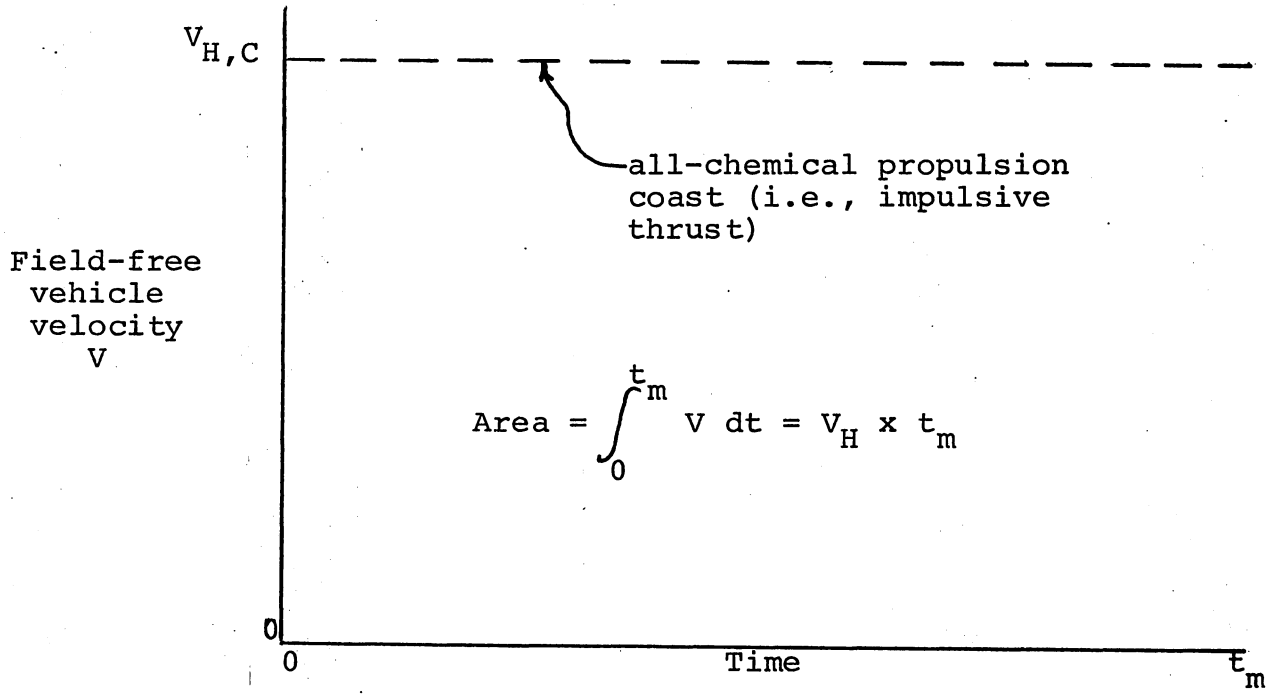

(a) velocity-time plot for all-chemical propulsion (i.e., impulsive thrust)

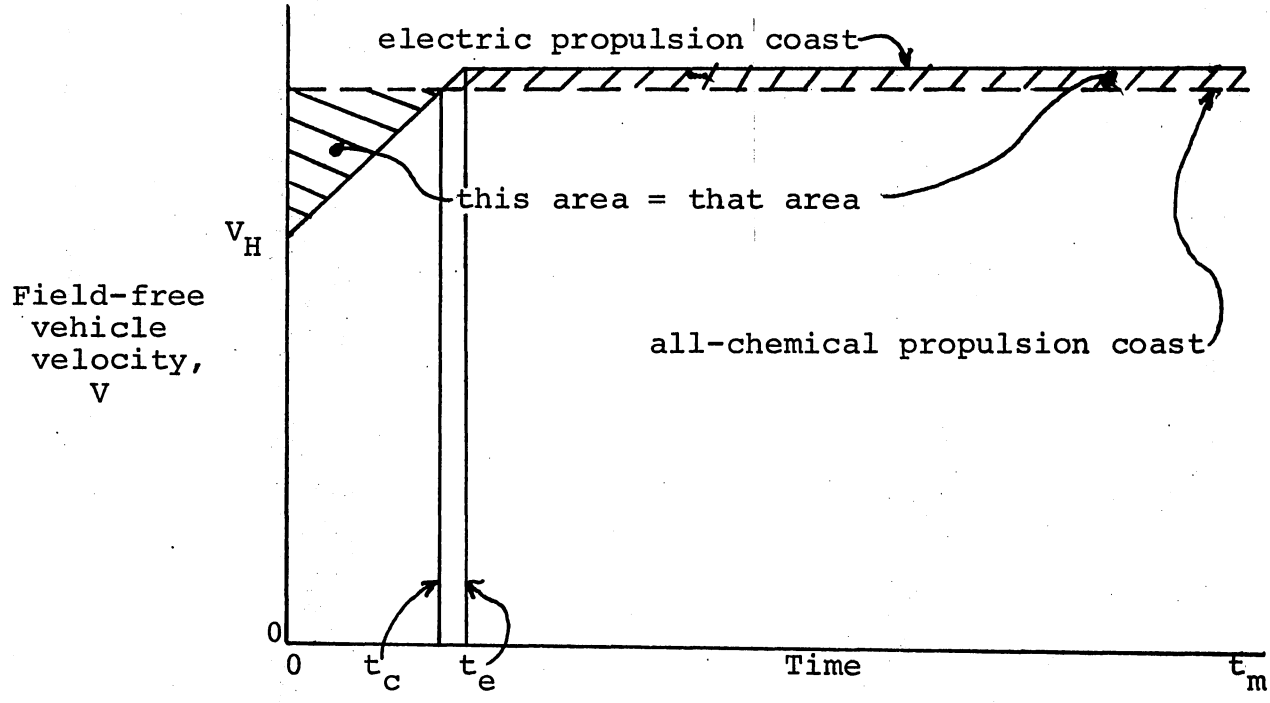

(b) velocity-time plot for electric propulsion after chemical-rocket boost to V_H.

DERIVATION OF EQUATIONS FOR CONSTANT THRUST HELIOCENTRIC TRANSFER, CHARACTERISTIC-LENGTH METHOD

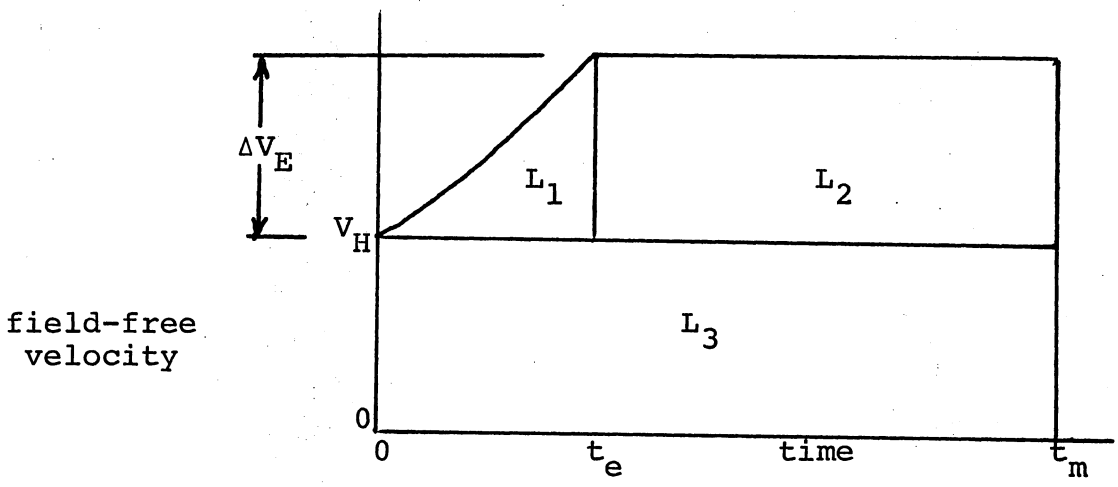

Mission profile:

a. chemical-rocket boost to V_H

b. electric-stage constant thrust, i.e., acceleration increases from a_0 at $t = 0$ to a_e at t_e

c. coast from t_e to t_m, where t_m is mission duration

Basic principle of characteristic-length method is that:

$$L_1 + L_2 + L_3 = V_{H,C}\, t_m$$

where $V_{H,C}$ is the hyperbolic excess velocity that an all-chemical rocket would need to accomplish the mission in time t_m

Calculation procedure:

a. choose launch vehicle

b. choose electric thrust, F, and specific impulse, I

c. assume several values of V_H, using the first approximation as a guide

d. for each value of V_H, find the t_e required for the mission, using the first approximation as a guide

e. from t_e and I, calculate propellant weight W_{pr}

f. from W_o for launch-vehicle V_H , and from propellant weight W_{pr} , calculate electric-stage final weight, $W_o - W_{pr}$.

Derivation of expressions for L_1, L_2, L_3

Instantaneous acceleration, a, is:

$$a = \frac{F}{M} = \frac{F}{M_0 - \dot{m}t} = \frac{1}{\frac{1}{F/M_0} - \frac{t}{v_j}} = \frac{a_0}{1 - \frac{a_0 t}{v_j}} \tag{1}$$

where M_0 = starting mass, $\dot{m}$ = propellant mass flow rate, a_0 = initial acceleration of electric stage, and:

$$v_j \equiv g_c I \tag{2}$$

The field-free velocity increase, ΔV_E , achieved by the electric stage is:

$$\Delta V_E = \int_0^{t_e} a\, dt = \int_0^{t_e} \frac{a_0\, dt}{1 - \frac{a_0 t}{v_j}} = -v_j \ln\left(1 - \frac{a_0 t}{v_j}\right)\Bigg|_0^{t_e}$$

$$= -v_j\left[\ln\left(1 - \frac{a_0 t_e}{v_j}\right) - \ln(1)\right] = -v_j \ln\left(1 - \frac{a_0 t_e}{v_j}\right)$$

$$= v_j \ln\left(\frac{1}{1 - \frac{a_0 t_e}{v_j}}\right) \tag{3}$$

The length increment L_1 is:

$$L_1 = \int_0^{t_e} dt \int_0^{t} a\, dt = \int_0^{t_e} dt \left[-v_j \ln\left(1 - \frac{a_0 t}{v_j}\right)\right]$$

$$= -v_j \int_0^{t_e} dt \ln\left(1 - \frac{a_0 t}{v_j}\right) \tag{4}$$

Let $y = 1 - \frac{a_0 t_e}{v_j}$, then $dy = -\frac{a_0}{v_j} dt$; and when $t = t_e$,

$y_e = 1 - \frac{a_0 t_e}{v_j}$; and when $t = 0$, $y_0 = 1$.

Using the preceding change of variable, eq. (4) becomes:

$$L_1 = -v_j \int_{y_o}^{y_e} \left(-\frac{v_j}{a_0}\right) \ln y \, dy = \frac{v_j^2}{a_0} \int_{y_0}^{y_e} dy \ln y$$

$$= \frac{v_j^2}{a_0} \, y \, (\ln y - 1) \Big|_{y_0}^{y_e}$$

$$= \frac{v_j^2}{a_0} \left\{ \left(1 - \frac{a_0 t_e}{v_j}\right) \left[\ln \left(1 - \frac{a_0 t_e}{v_j}\right) - 1\right] - (1) \left[\ln (1) - 1\right] \right\}$$

$$= \frac{v_j^2}{a_0} \left\{ \left(1 - \frac{a_0 t_e}{v_j}\right) \left[\ln \left(1 - \frac{a_0 t_e}{v_j}\right)\right] - 1 + \frac{a_0 t_e}{v_j} - 0 + 1 \right\} \tag{5}$$

But from eq. (3), $\ln \left(1 - \frac{a_0 t_e}{v_j}\right) = -\Delta V_E / v_j$, so eq. (5) becomes:

$$L_1 = \frac{v_j^2}{a_0} \left\{ \left(1 - \frac{a_0 t_e}{v_j}\right) \left(-\frac{\Delta V_E}{v_j}\right) + \frac{a_0 t_e}{v_j} \right\}$$

$$= \frac{v_j^2}{a_0} \left\{ \frac{a_0 t_e}{v_j} - \frac{\Delta V_E}{v_j} \left(1 - \frac{a_0 t_e}{v_j}\right) \right\} \tag{6}$$

The length increments L_2 and L_3 are simply:

$$L_2 = \Delta V_E \, (t_m - t_e) \tag{7}$$

$$L_3 = V_H \, t_m \tag{8}$$

The following graphs represent the results of calculations done with a simple program run on the CDC 6400 at Colorado State University. This information is presented in two forms:

a. electric-stage thrusts of .001, .002, .004, .006, .008, .010, .014, and .020 lb, each for a range of specific impulse values.

b. electric-stage specific impulse values of 400, 600, 800, 1000, and 2000 sec, each for a range of thrust levels.

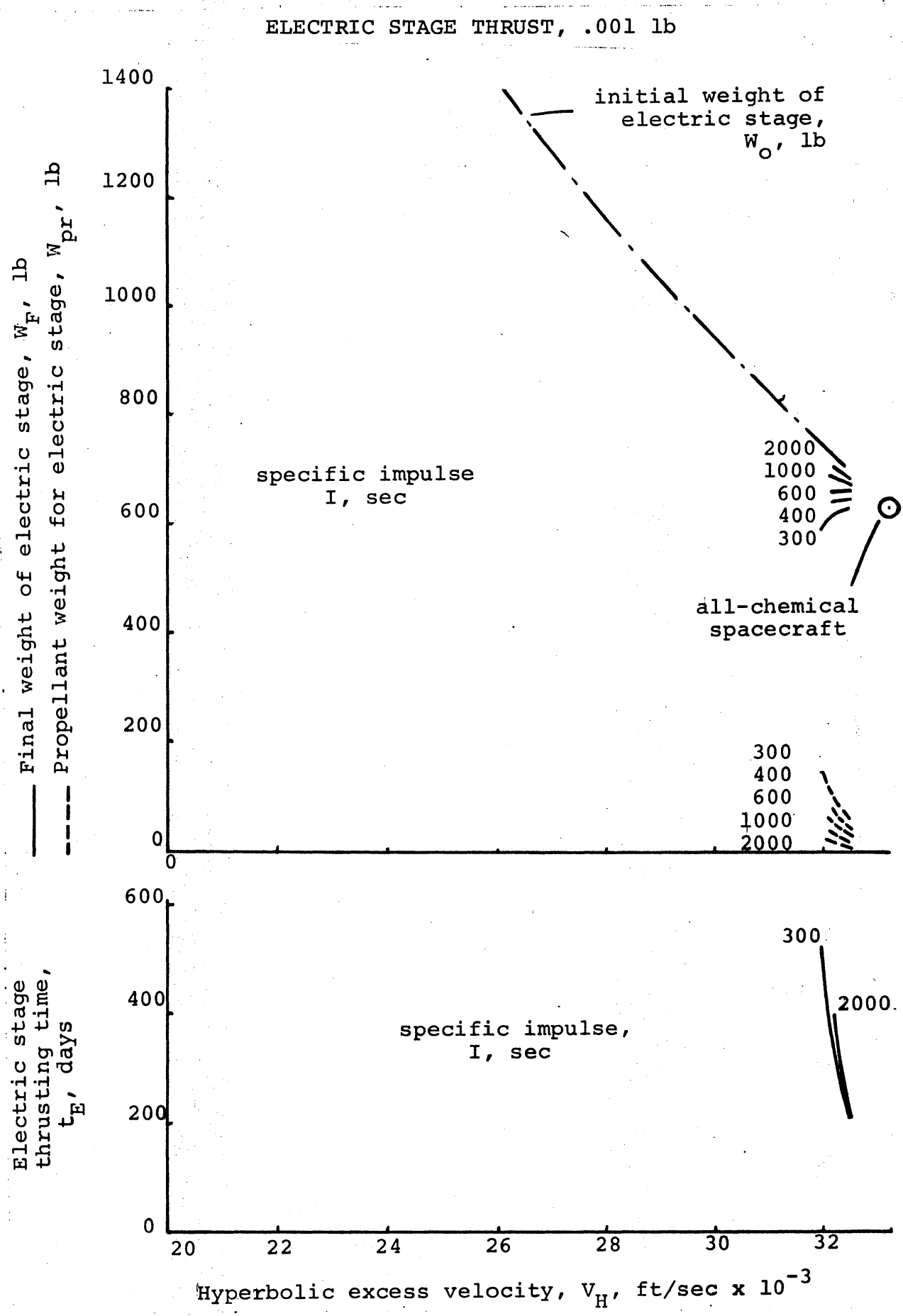
ELECTRIC STAGE THRUST, .001 lb
Final weight of electric stage, W_F, lb
Propellant weight for electric stage, W_{pr}, lb
1400
1200
1000
800
600
400
200
0
initial weight of electric stage, W_o, lb
specific impulse I, sec
2000
1000
600
400
300
all-chemical spacecraft
300
400
600
1000
2000
0
Electric stage thrusting time, t_E, days
600
400
200
0
300
2000
specific impulse, I, sec
20
22
24
26
28
30
32
Hyperbolic excess velocity, V_H, ft/sec x 10^{-3}

ELECTRIC STAGE THRUST, .002 lb

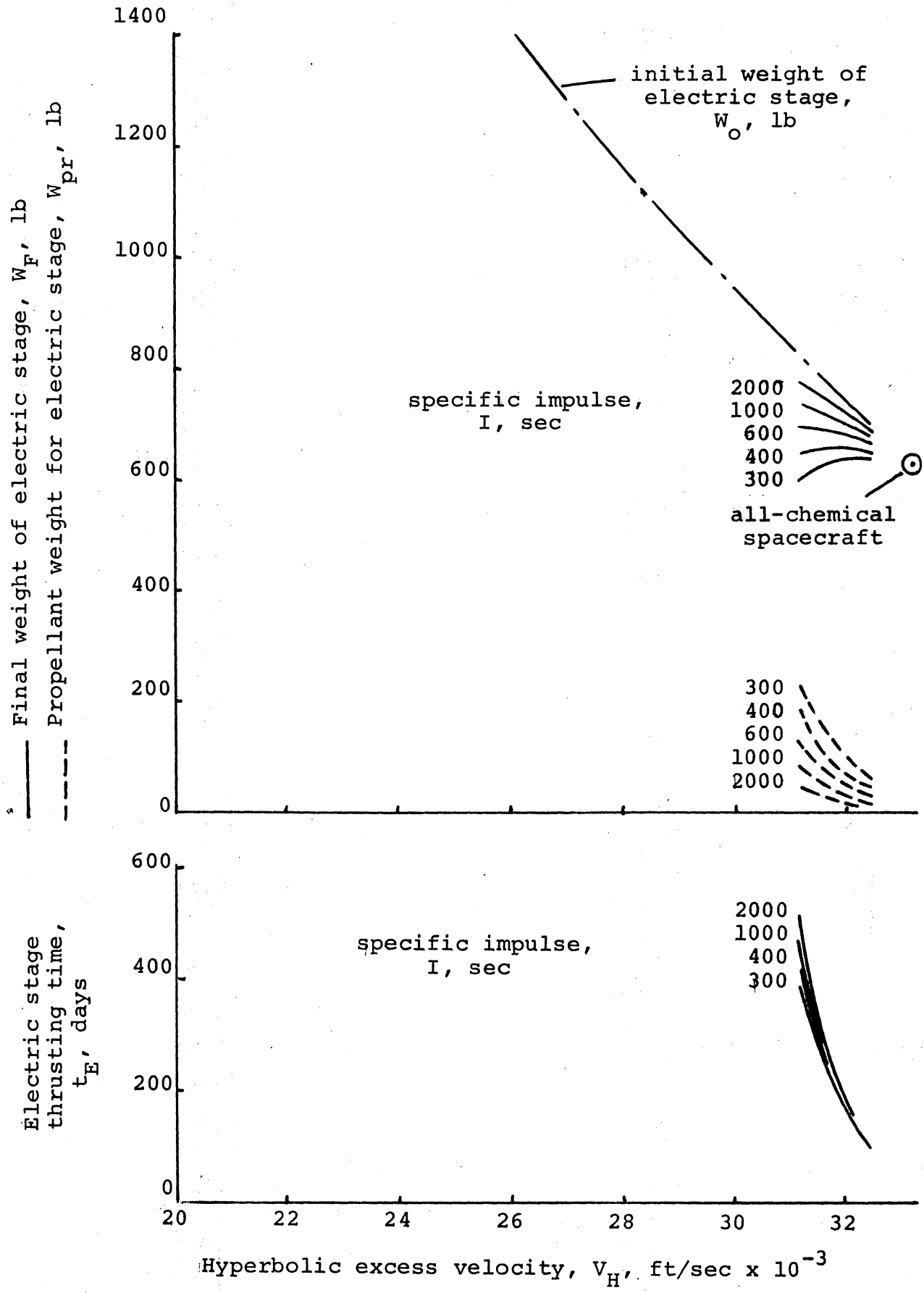

ELECTRIC STAGE THRUST, .004 lb

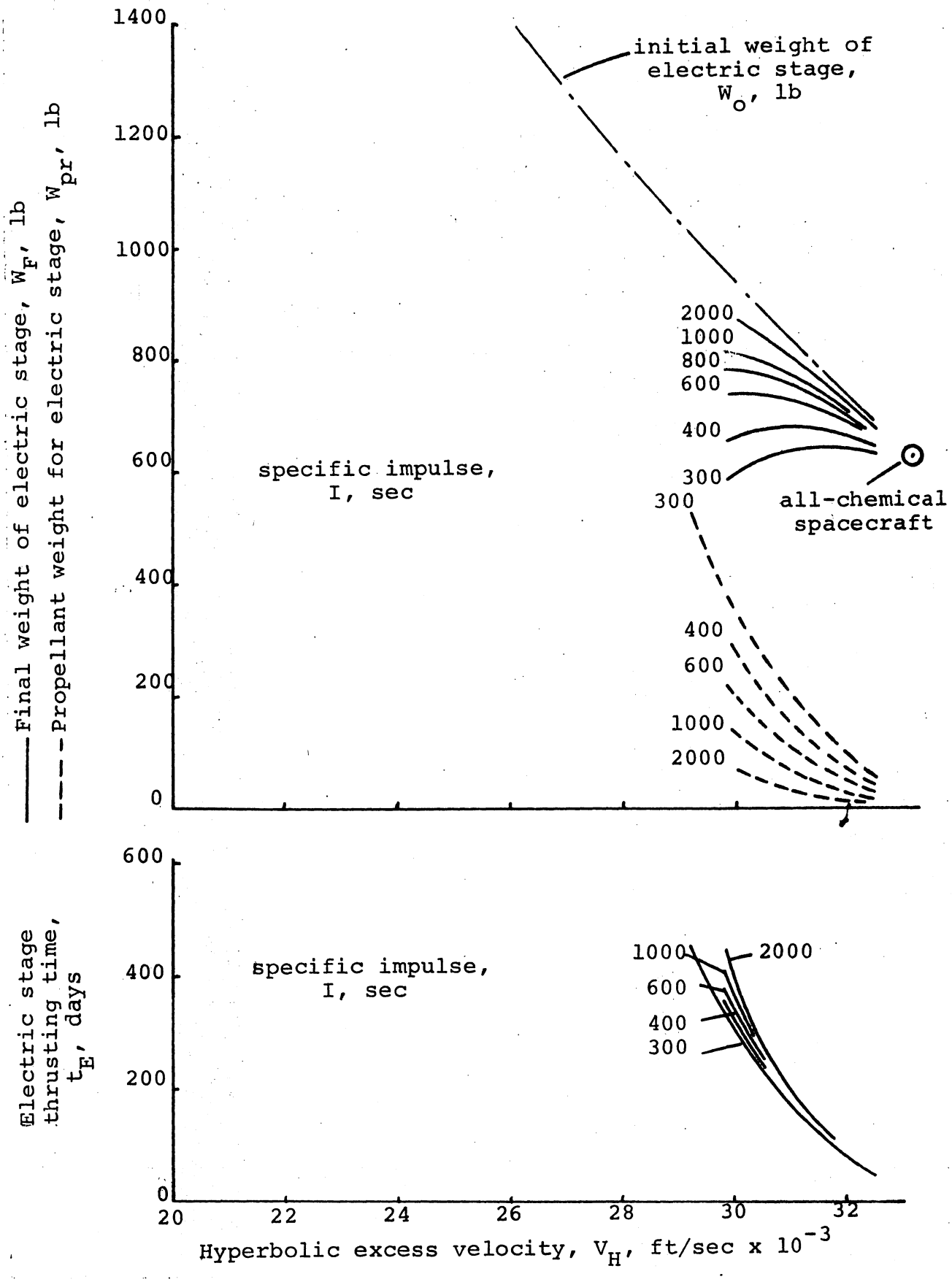

ELECTRIC STAGE THRUST, .006 lb

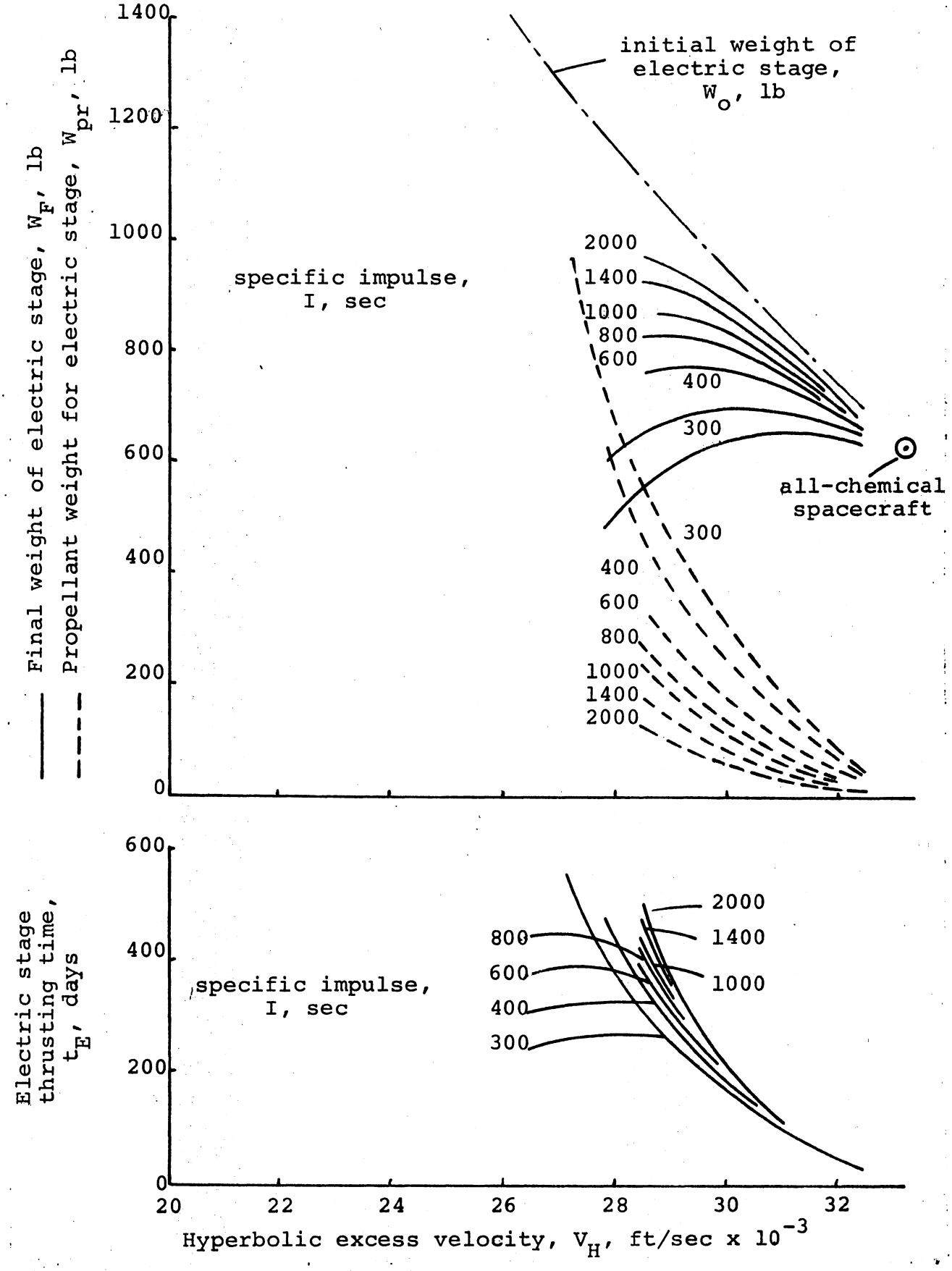

ELECTRIC STAGE THRUST, .008 lb

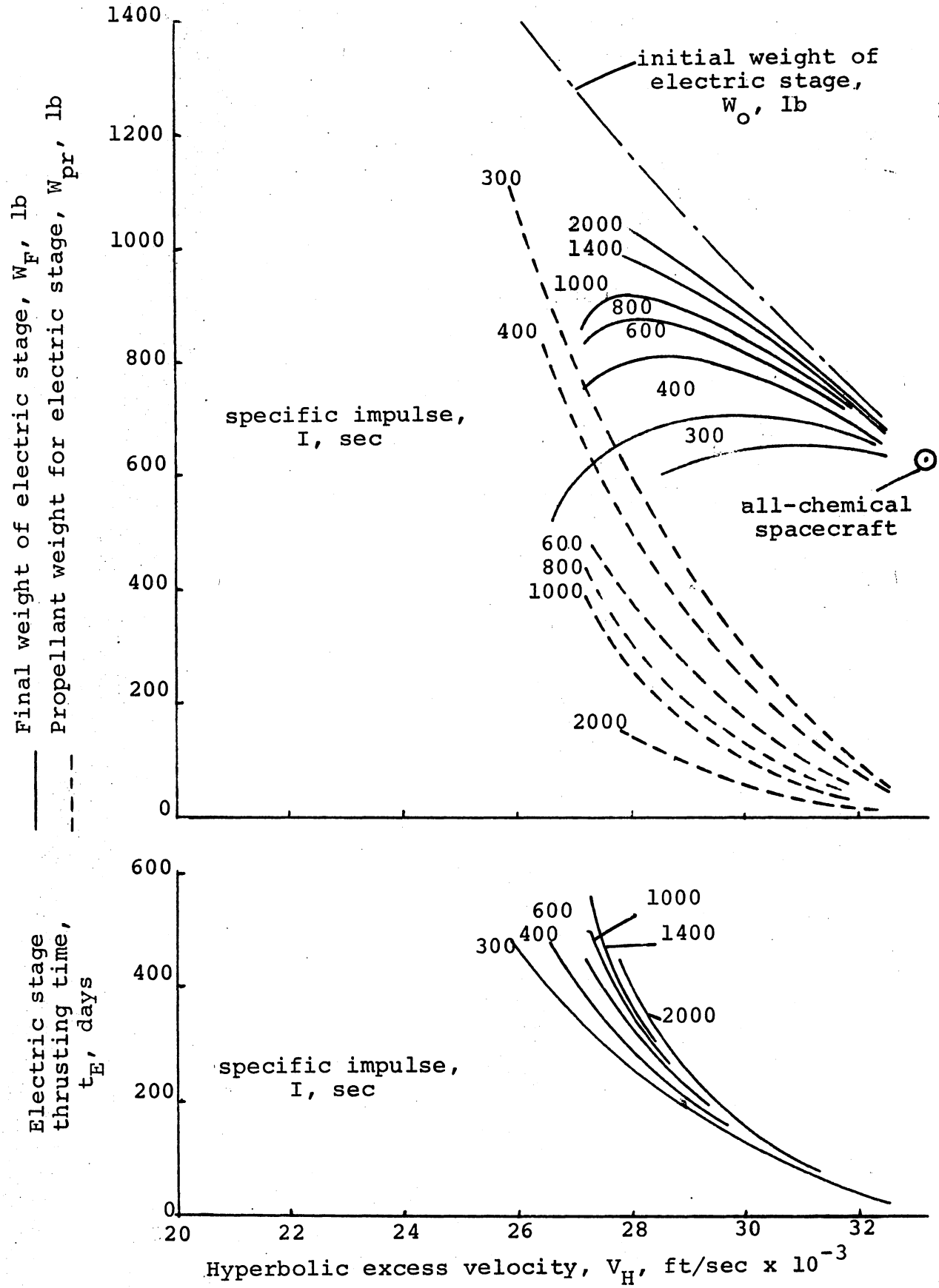

ELECTRIC STAGE THRUST, .010 lb

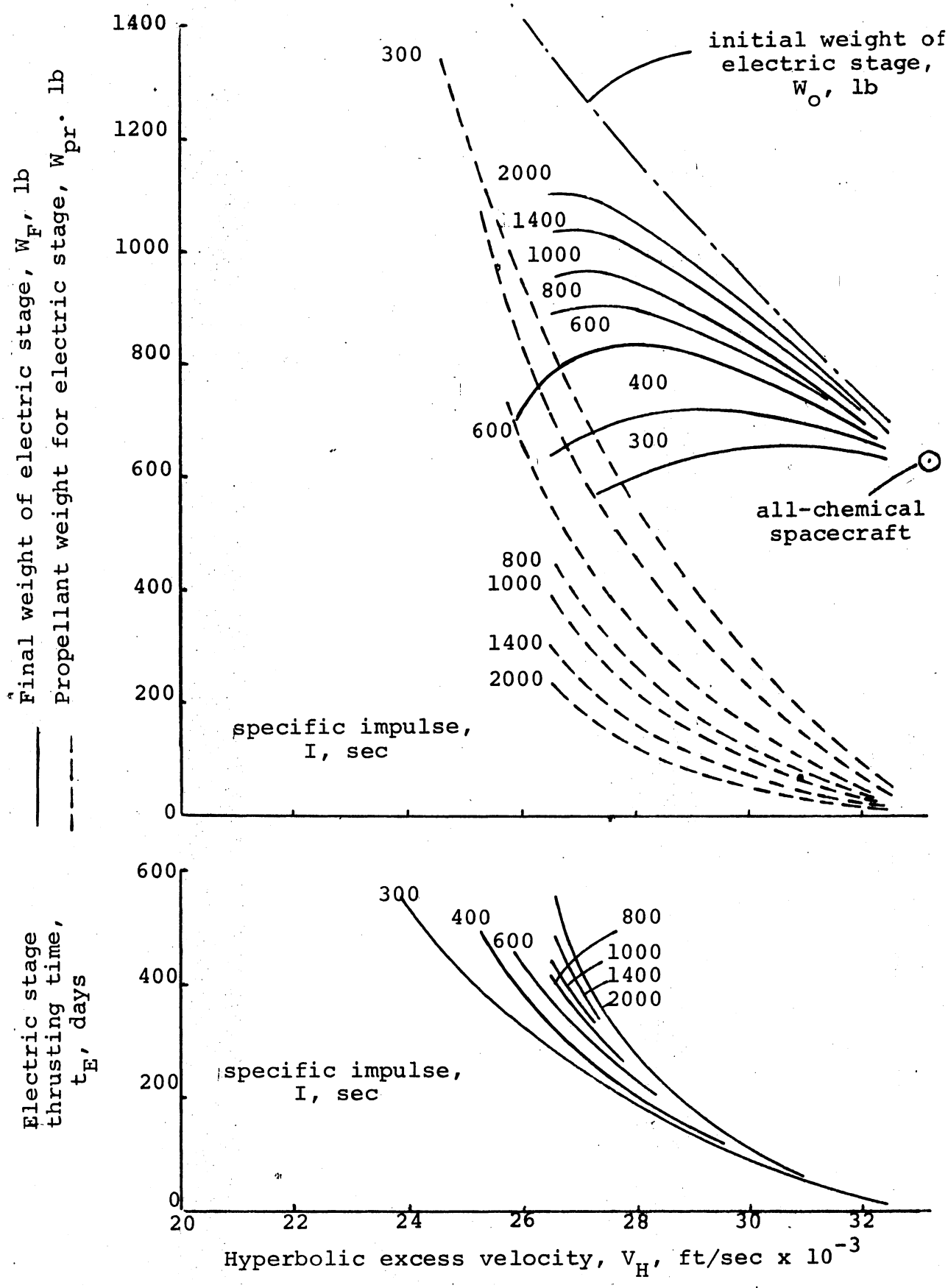

ELECTRIC STAGE THRUST, .014 lb

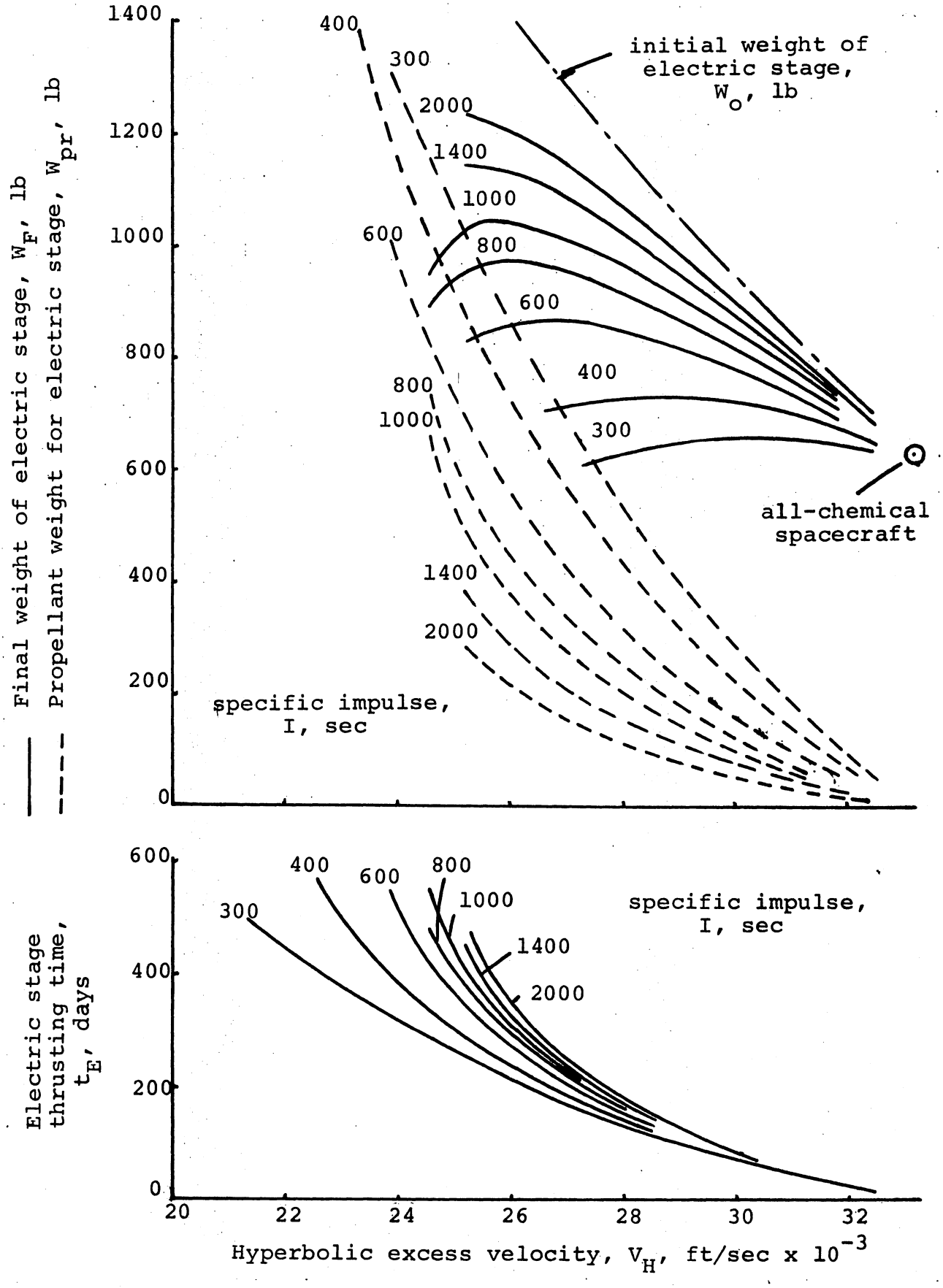

ELECTRIC STAGE THRUST, .020 lb

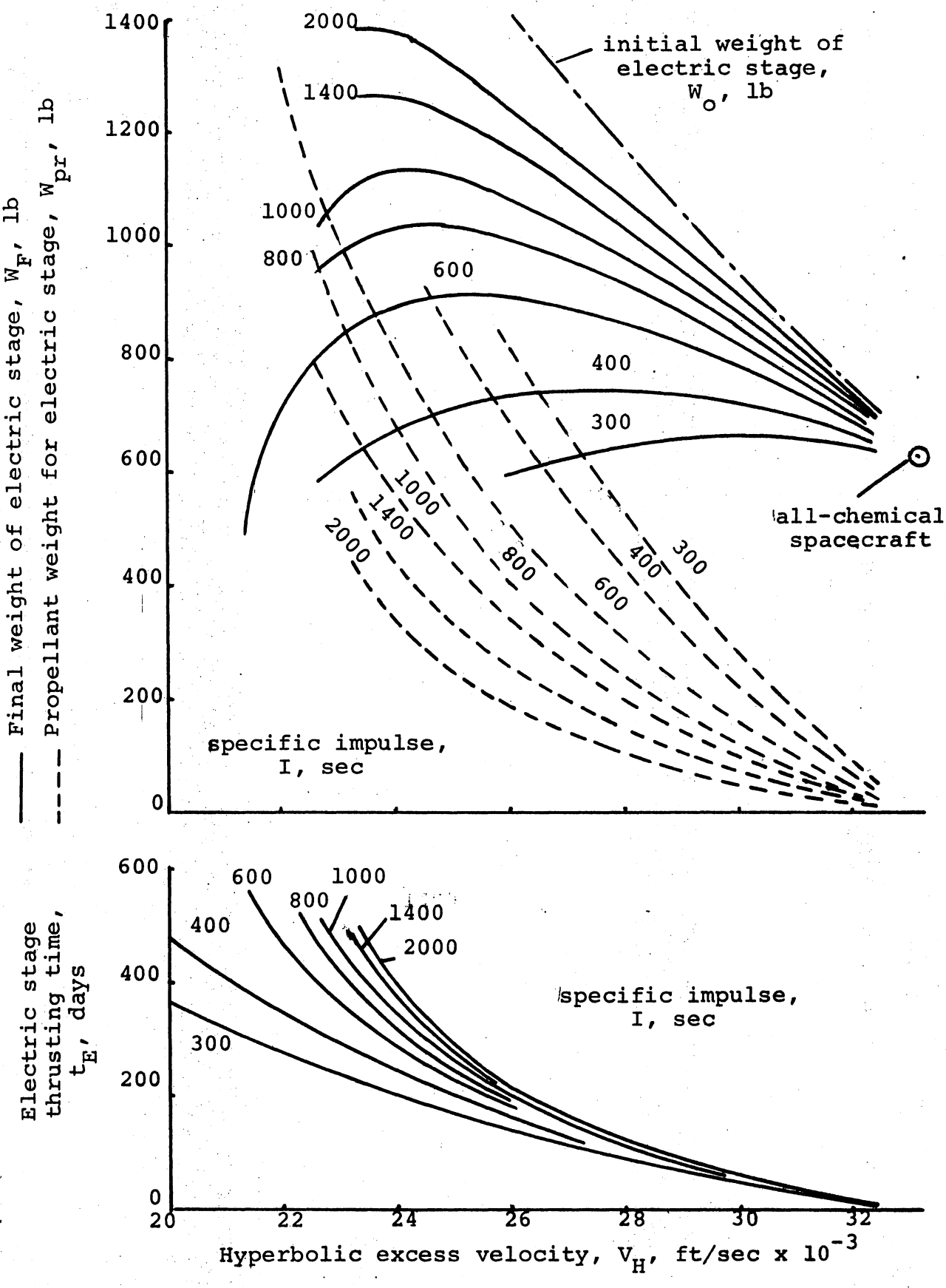

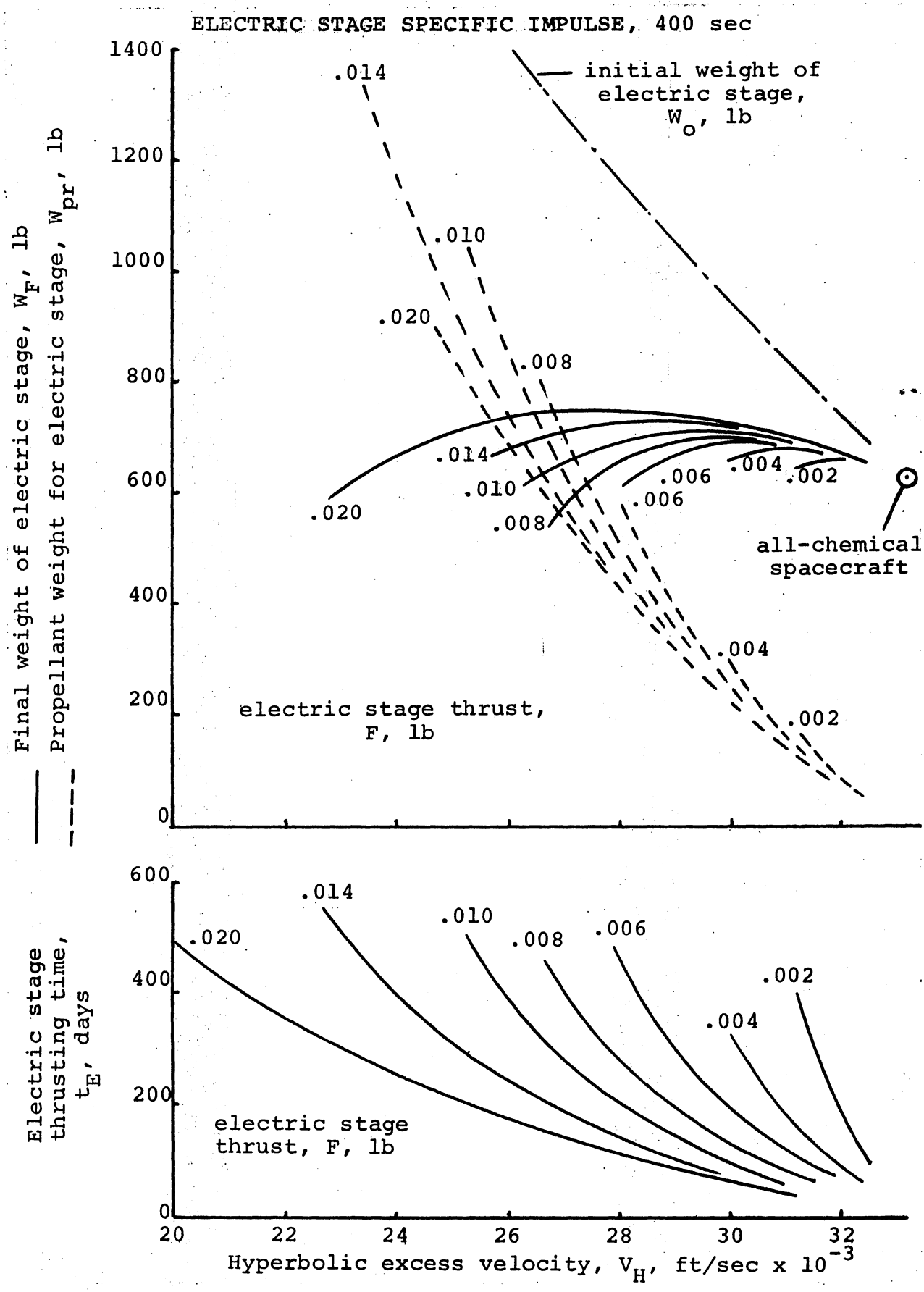
ELECTRIC STAGE SPECIFIC IMPULSE, 400 sec
Final weight of electric stage, W_F, lb
Propellant weight for electric stage, W_{pr}, lb
initial weight of electric stage, W_o, lb
.014
.010
.020
.008
.006
.004
.002
all-chemical spacecraft
electric stage thrust, F, lb
1400
1200
1000
800
600
400
200
0
Electric stage thrusting time, t_E, days
electric stage thrust, F, lb
20
22
24
26
28
30
32
Hyperbolic excess velocity, V_H, ft/sec x 10^{-3}

ELECTRIC STAGE SPECIFIC IMPULSE, 600 sec

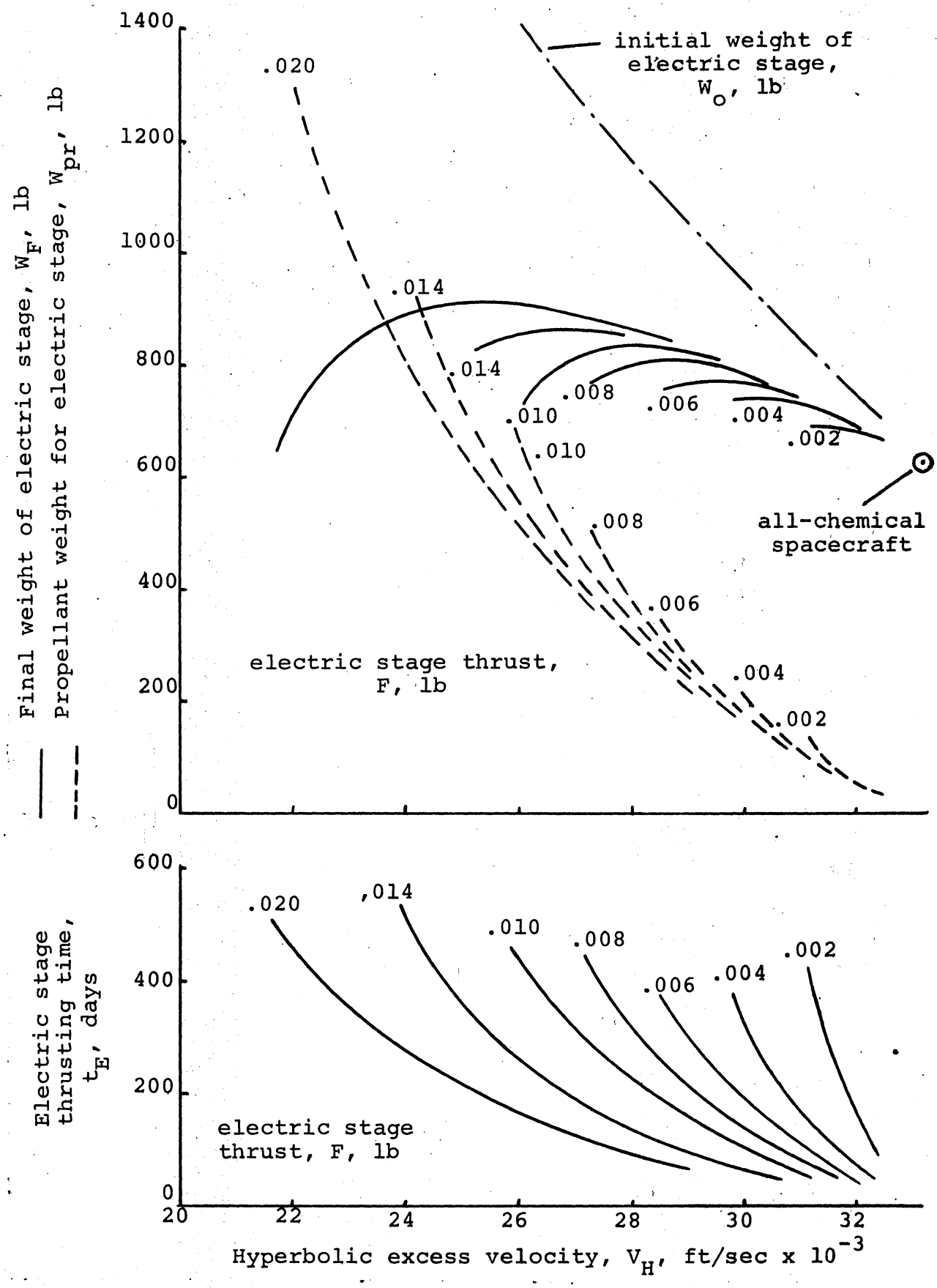

ELECTRIC STAGE SPECIFIC IMPULSE, 800 sec

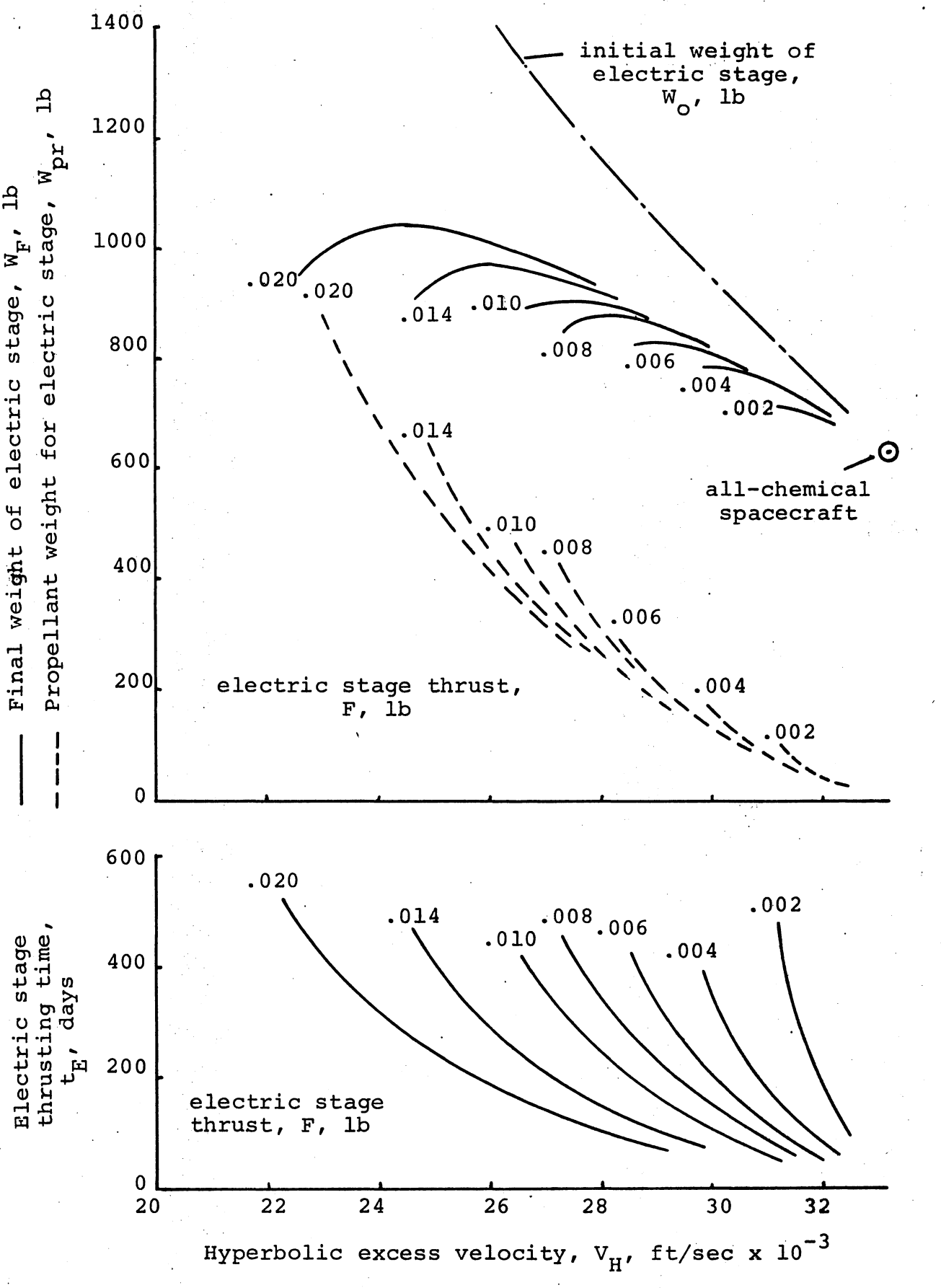

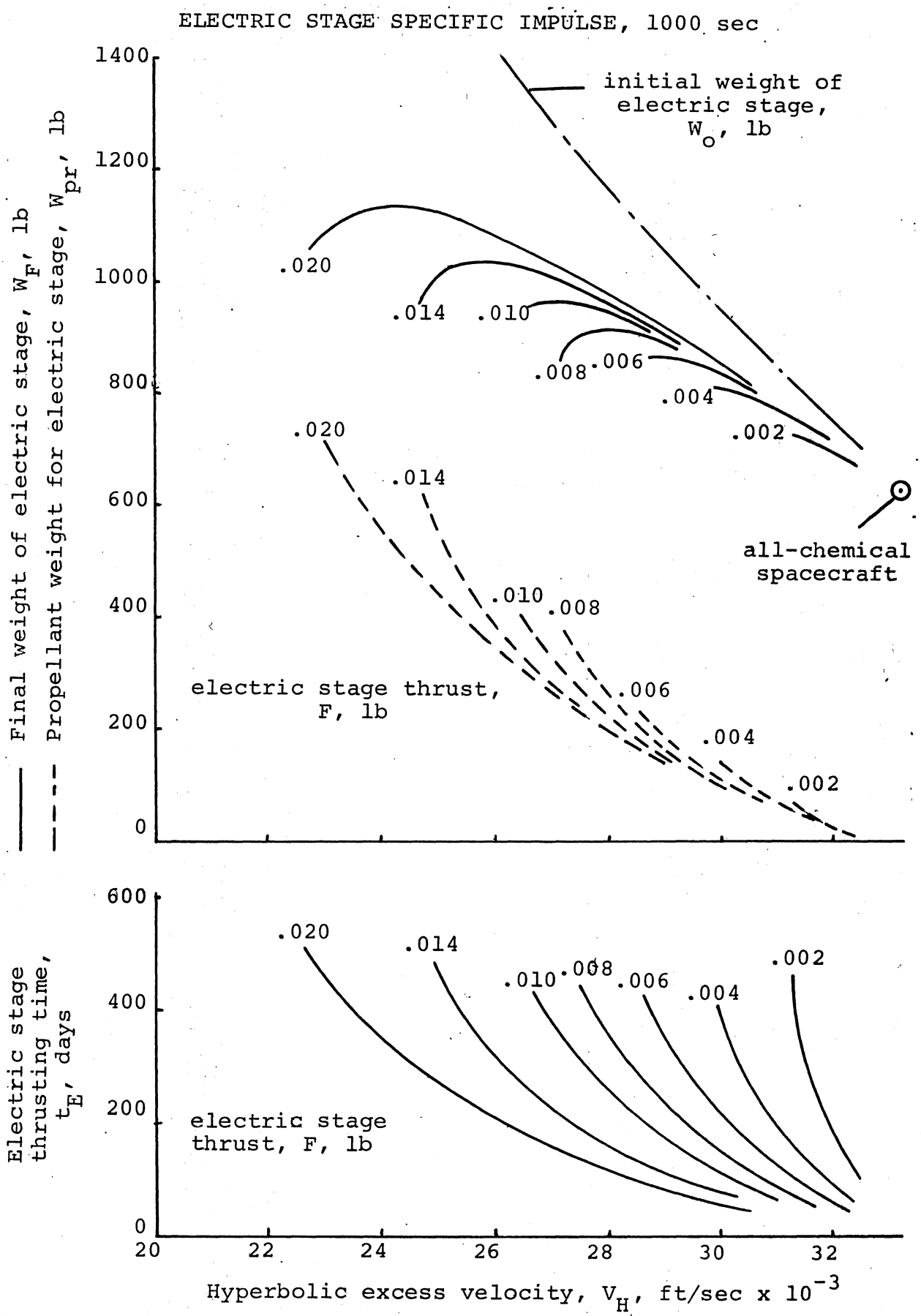
ELECTRIC STAGE SPECIFIC IMPULSE, 1000 sec
Final weight of electric stage, W_F, lb
Propellant weight for electric stage, W_{pr}, lb
1400
1200
1000
800
600
400
200
0
initial weight of electric stage, W_o, lb
.020
.014
.010
.008
.006
.004
.002
all-chemical spacecraft
electric stage thrust, F, lb
Electric stage thrusting time, t_E, days
600
400
200
0
electric stage thrust, F, lb
20
22
24
26
28
30
32
Hyperbolic excess velocity, V_H, ft/sec x 10^{-3}

ELECTRIC STAGE SPECIFIC IMPULSE, 2000 sec

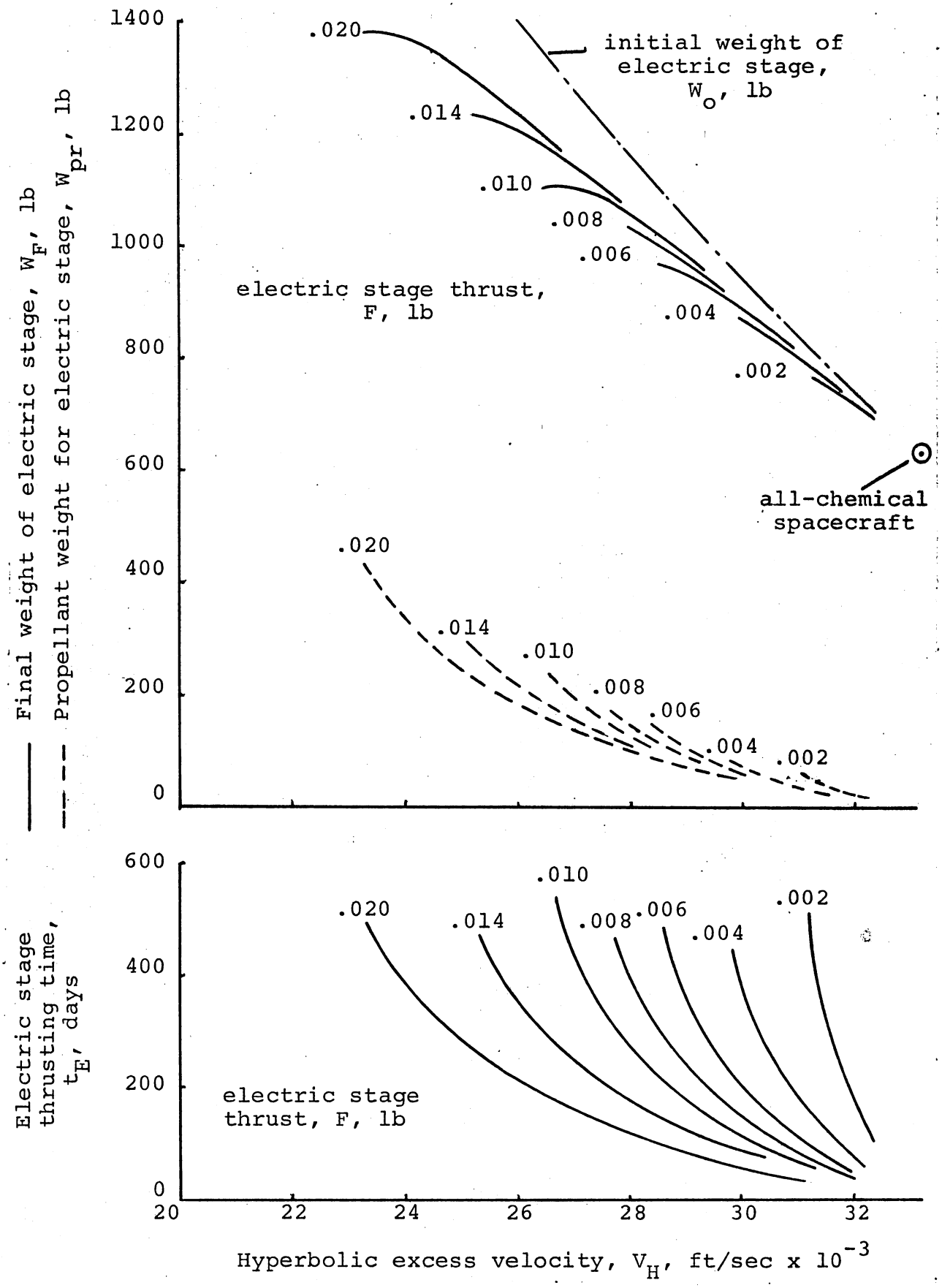

The following three graphs are the best available information on electric thruster systems. Each of the three graphs is accompanied with a page of reference information.

Following the three graphs is information regarding the electrostatic liquid-spray "colloid" thruster, and the lithium isotope/resistojet thruster concepts.

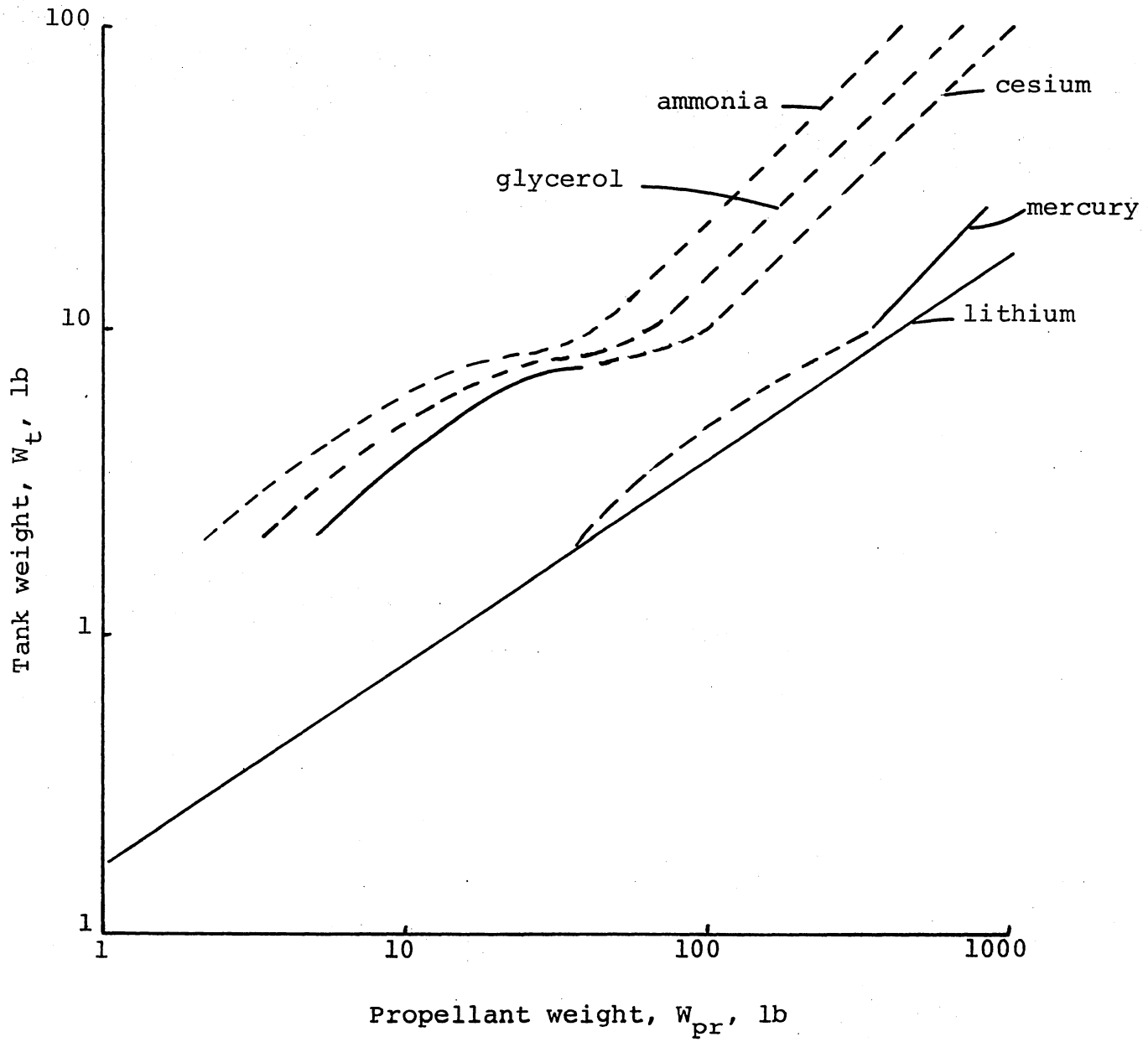
100
10
1
1
1
10
100
1000
Tank weight, W_t, lb
Propellant weight, W_{pr}, lb
ammonia
cesium
glycerol
mercury
lithium

Reference information for propellant tankage

all tanks spherical configuration

lithium

density, .53; m.p., 452°K; b.p., 1590°K. Tank assumed to be .010-inch stainless steel (note that titanium would be lighter). A 48-inch diameter tank would hold more than 1000 lb of lithium, and the .010-inch tank walls would be stressed to 60,000 psi by a 50 psi feed pressure.

mercury

density, 13.6; m.p., 234°K; b.p., 630°K. Tankage fraction assumed to be 3% in upper range, as reported in: 1965 Jupiter Flyby Mission Using a Solar Electric Spacecraft, JPL ASD 760-18, March 1, 1968. In lower range, mercury curve is extrapolated from cesium curve by using the density ratio.

cesium

density, 1.88; m.p., 302°K; b.p., 963°K. Tankage fraction in lower range from Worlock, R. M.: private communication, Electro-Optical Systems, Inc., May 19, 1967. This information is based on actual tank weights for 5- to 40-lb cesium propellant loadings, and on theoretical design calculations in the intermediate range.

glycerol

density, 1.26; m.p., 292°K; b.p., 563°K. Whole curve extrapolated from cesium curve by using the density ratio.

ammonia

density, .817; m.p., 195°K; b.p., 240°K. Whole curve extrapolated from cesium curve by using the density ratio.

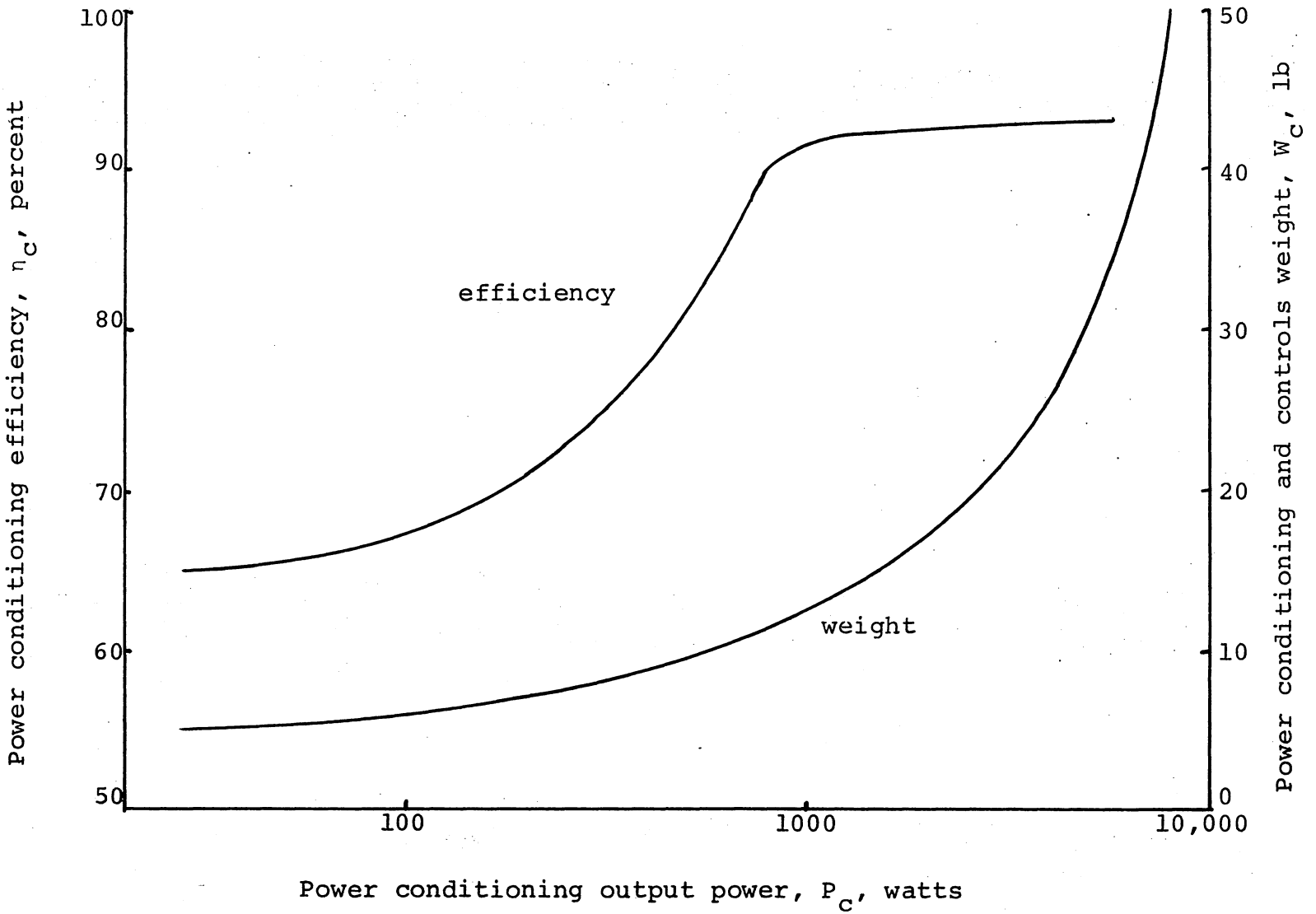
Power conditioning efficiency, η_c, percent
100
90
80
70
60
50
efficiency
weight
50
40
30
20
10
0
Power conditioning and controls weight, W_c, lb
100
1000
10,000
Power conditioning output power, P_c, watts

Reference information for power-conditioning and controls for electrostatic thrusters

This information published in:

1. Mickelsen, W. R.: Advanced Concepts in Electric Propulsion. AIAA Paper No. 67-426. July, 1967.

2. Mickelsen, W. R.: Auxiliary and Primary Electric Propulsion, Present and Future. Jour. Spacecraft and Rockets. November, 1967.

weight of power conditioning and controls. The weight at 30 watts is for the EOS contact microthruster system given in Worlock, R. M., Ramirez, P., Jr., Ernstene, M. P., and Beasly, W. E., Jr.: A Contact Ion Microthruster System. AIAA Paper No. 67-80, January, 1967. The weights above 1000 watts are given in Solar Powered Electric Propulsion Program, Program Summary Report, JPL Contract No. 951144, Hughes Aircraft Company SSD 6037R, December, 1966. The rest of the curve is an interpolation.

efficiency of power conditioning. The efficiency at 30 watts is for the EOS microthruster system referred to above. The efficiencies above 1000 watts are from the Hughes report referred to above. The rest of the curve is an interpolation.

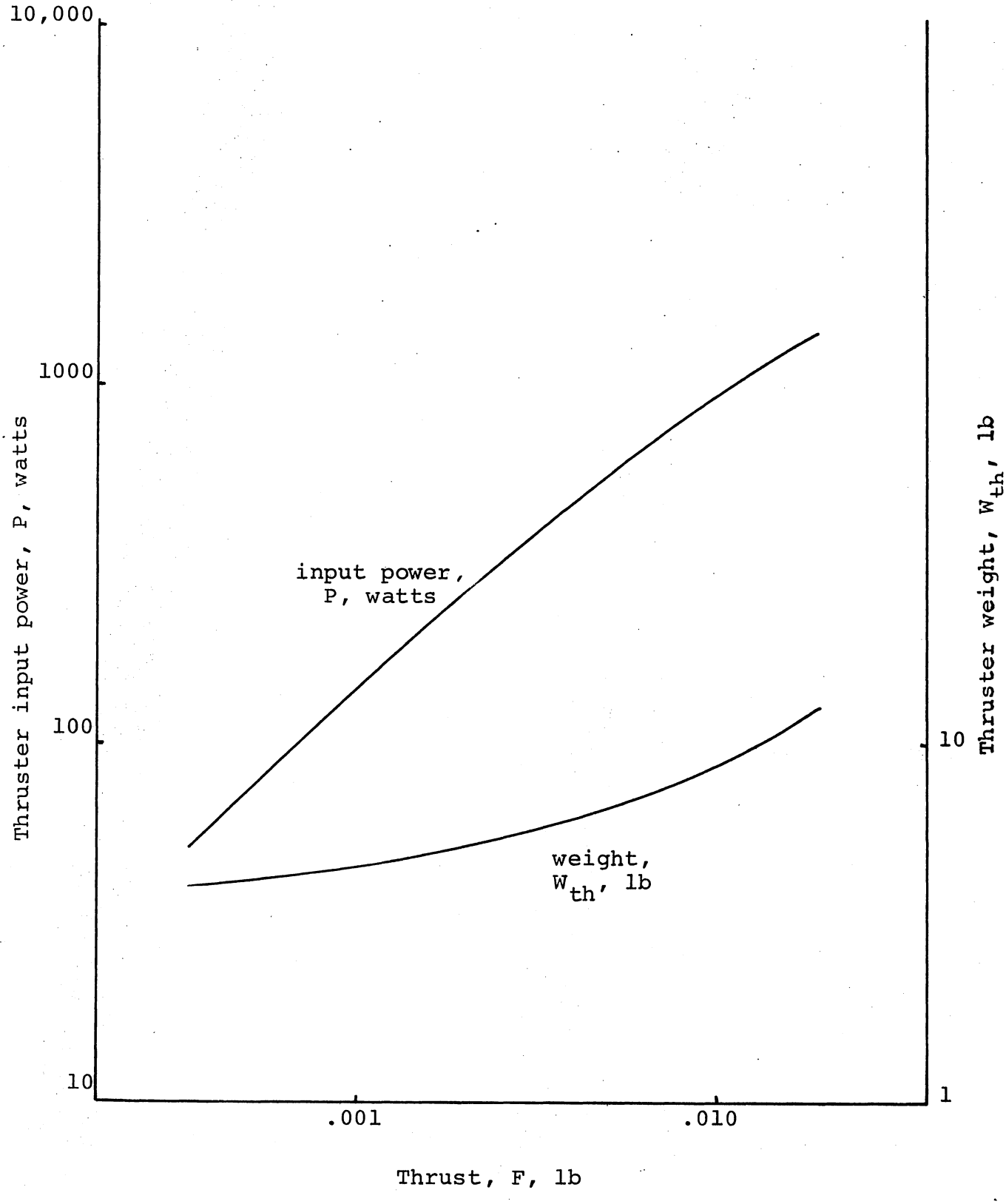
Mercury-bombardment thruster
I = 2000 sec
10,000
1000
100
10
Thruster input power, P, watts
input power,
P, watts
weight,
W_{th}, lb
10
1
Thruster weight, W_{th}, lb
.001
.010
Thrust, F, lb

Reference information for mercury bombardment thruster

references:

a. Richley, E. A., and Kerslake, W. R.: Bombardment Thruster Investigations at the Lewis Research Center. AIAA Paper No. 68-542. January, 1968.

b. 1975 Jupiter Flyby Mission Using a Solar Electric Spacecraft. JPL ASD 760-18. March 1, 1968.

5-cm thruster (ref. a). Thruster system weight assumed to be W_{th} = 4 lb. At I = 1700 sec, P = 54 watts, η_{th} = .2, F = 2 x .2 x 54/16,670 = .001295 newt = .000298 lb, and P_j = 10.8 watt. At I = 2000 sec, assuming beam current is the same as at I = 1700 sec, F = .000298 x 2000/1700 = .000351 lb. At I = 2000 sec, η_{th} = .3.

15-cm thruster (ref. a). Thruster system weight W_{th} = 3 kg = 6.6 lb. At I = 2400 sec, P = 600 watts, η_{th} = .53, F = 2 x .53 x 600/23,500 = .0271 newt = .0061 lb. At I = 2000 sec, assuming beam current is the same as at I = 2400 sec, F = .0061 x 2000/2400 = .00508 lb. At I = 2000 sec, η_{th} = .4.

30-cm thruster (refs. a and b). Thruster system weight W_{th} = 11 lb. At I = 2750 sec, η_{th} = .60, F = .022 lb. At I = 200 sec, assuming beam current is the same as at I = 2750 sec, F = .022 x 2000/2750 = 0.16 lb. At I = 2000 sec, η_{th} = .57.

summary

I, sec	F, lb	η_{th}	power to thruster, P. watts	W_{th}, lb
2000	.000351	.3	51	4
2000	.00508	.4	552	6.6
2000	.016	.57	1220	11.

Reference information for electrostatic glycerol liquid-spray "colloid" thruster

power to thruster, P is:

$$P = (FgI)/(2\eta_{th})$$

at I = 1000 sec, F in lbs:

$$P = 21{,}800\ F/\eta_{th}\ ,\ \text{watts}$$

for $\eta_{th} = 70\%$:

$$P = 31{,}200\ F,\ \text{watts}$$

Other power requirements, such as propellant feed and neutralizer, are assumed negligible. Thruster weight is assumed the same as the Hg-bombardment thruster.

Reference information for
lithium isotope/resistojet thrusters

This thruster concept has been briefly reported in:

Mickelsen, W. R., and Isley, W. C.: Auxiliary Electric Propulsion--Status and Prospects. Paper presented at AFOSR Fifth Symposium on Advanced Propulsion Concepts, Chicago, Illinois. April 8-10, 1968.

More detailed analyses of this concept are described in reports on NASA Grant NGR06-002-032. The analyses are for real gas one-dimensional flow, so the performance will be less than reported. However, conservative assumptions have been made in the analysis, such as no acceleration of condensate, which will tend to compensate for the one-dimensional-flow assumption.

Thruster weight has been assumed to be 6 lbs, which is probably optimistic.

It is assumed that radioisotope heating will supply the heat of fusion, and the heat of vaporization of lithium. At a radioisotope heater temperature of 1200°K, lithium has a vapor pressure of about 10 torr, which is probably too low. A radioisotope heater temperature of 1500°K would provide a vapor pressure of about 0.5 atmosphere, which is probably adequate.

The very high heat of vaporization of lithium provides an apparently practical method of heat addition by condensation in the supersonic flow. This supersonic heat addition would allow the high specific impulse values quoted below.

A plenum temperature of 2500°K after electric heating is assumed to be attainable in the light of resistojet developments by Marquardt.

thruster with I_{sp} = 400 sec

Expand to area ratio of 100 and a very low static temperature, i.e., non-equilibrium expansion along an isentrope to supersaturated conditions with no condensation.

Alternatively, expand to 1500°K static temperature at area ratio of about 4, condensate 15% of the lithium, then no further expansion.

With η_{th} = 50%, P/F = 8 watt/mlb

thruster with I_{sp} = 600 sec

Expand to an area ratio of 8, condense 40% of the lithium, then expand to an area ratio of 10. The condensate has a velocity of 2300 m/sec, and the vapor has a much higher velocity, to give a weighted-average exhaust velocity of 6000 m/sec.

With η_{th} = 50%, P/F = 26 watt/mlb

thruster with I_{sp} = 800 sec

Expand and condensate to an area ratio of 8, then free expansion to an area ratio of 34, and expand and condense to a final area ratio of 45. This might be accomplished by control of condensation rate, but probably will require a combination of heat addition by condensation and electric power addition to the supersonic flow.

With η_{th} = 50%, P/F = 34.8 watt/mlb

thruster with I_{sp} = 1000 sec

Same as for 800 sec, but final area ratio of 120, and more electric power addition to supersonic stream.

The following graphs and charts are summaries of the information presented in the previous portions of this report.

600-day Jupiter fly-by mission (with C. L. method)
launch vehicle, SLV-3X/Centaur/Burner II (2336)
hotel load during heliocentric transfer, 50 watts
THRUSTER SYSTEM, lithium isotope/resistojet, I = 400 sec

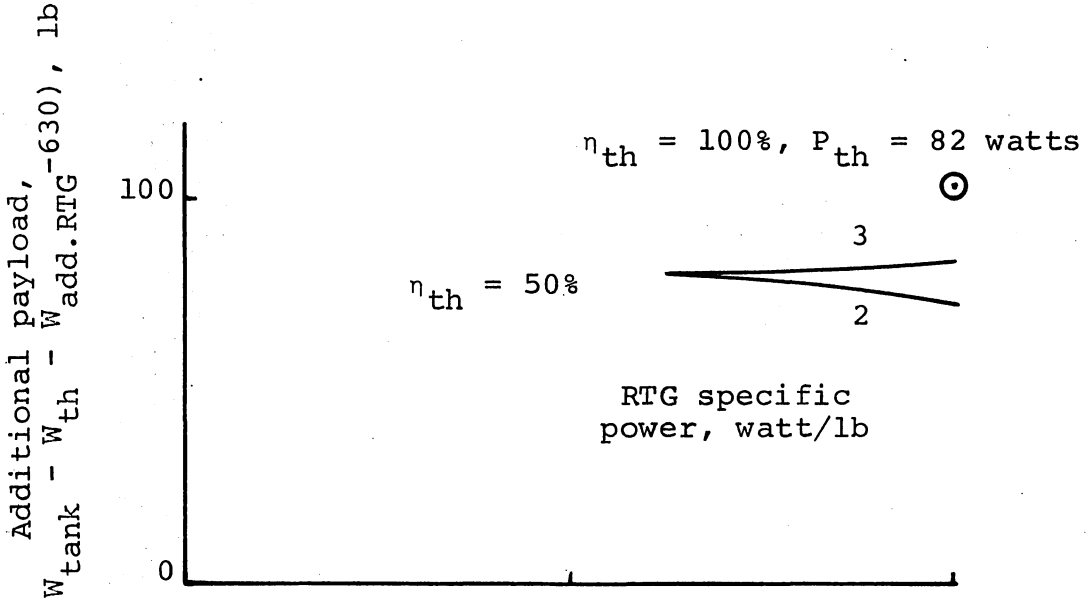

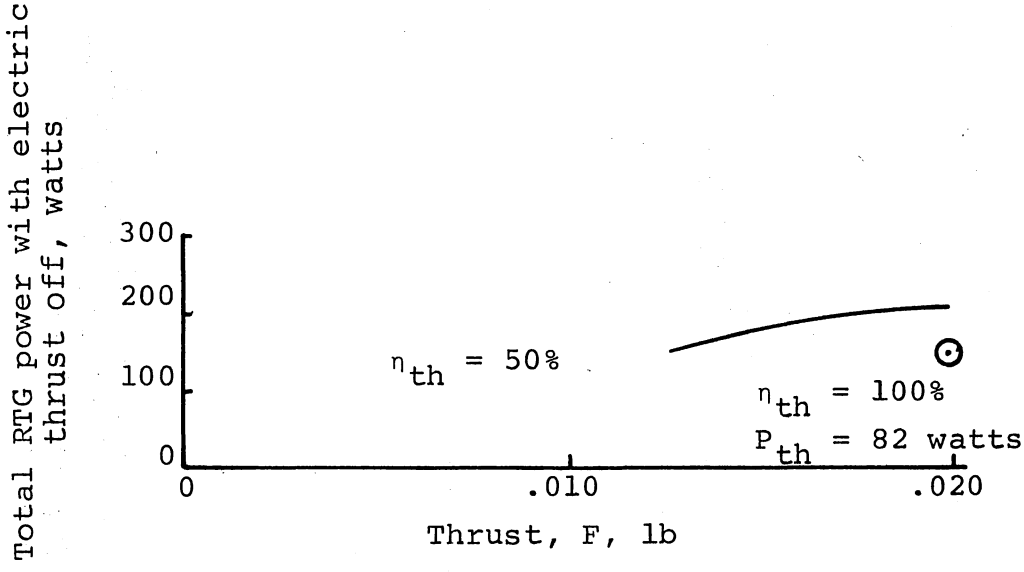

600-day Jupiter fly-by mission (with C. L. method)
launch vehicle, SLV-3X/Centaur/Burner II (2336)
hotel load during heliocentric transfer, 50 watts
THRUSTER SYSTEM, lithium isotope/resistojet, I = 600 sec

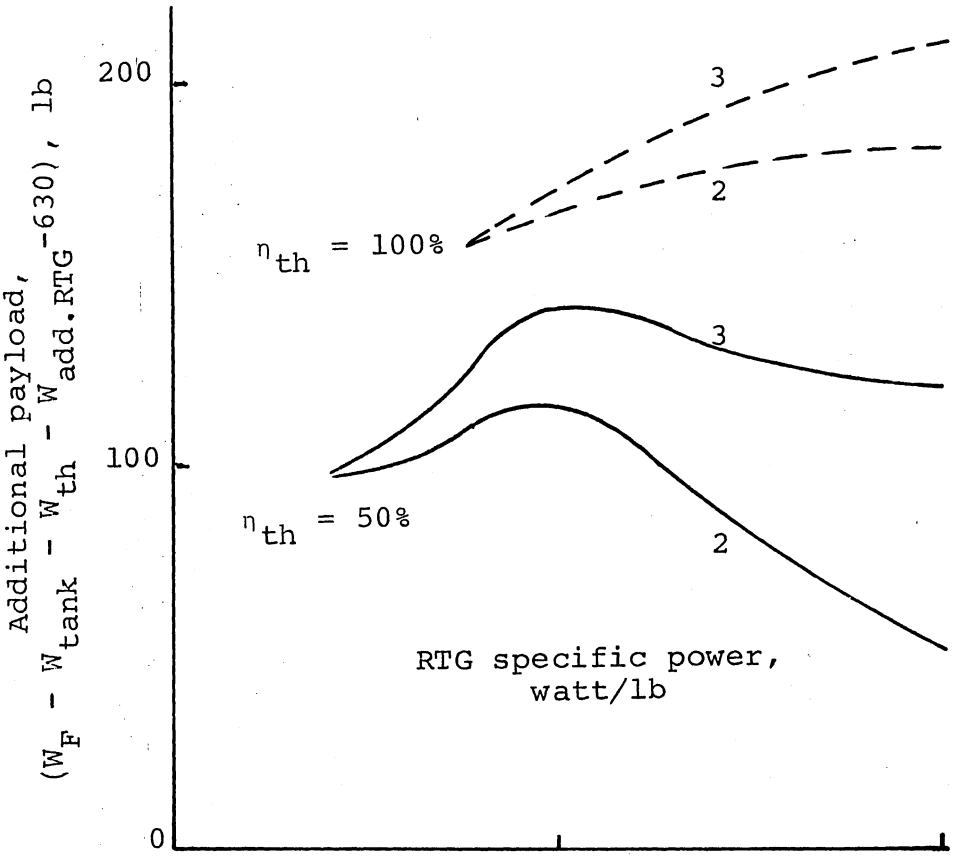

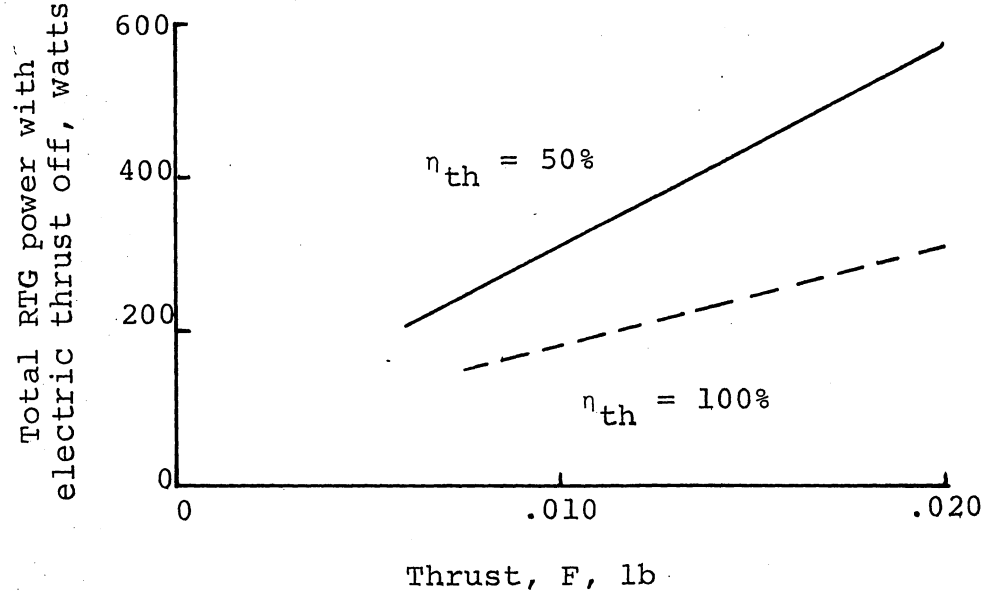

600-day Jupiter fly-by mission (with C. L. method)
launch vehicle, SLV-3X/Centaur/Burner II (2336)
hotel load during heliocentric transfer, 50 watts
THRUSTER SYSTEM, adv. lithium isotope/resistojet, I = 800 sec

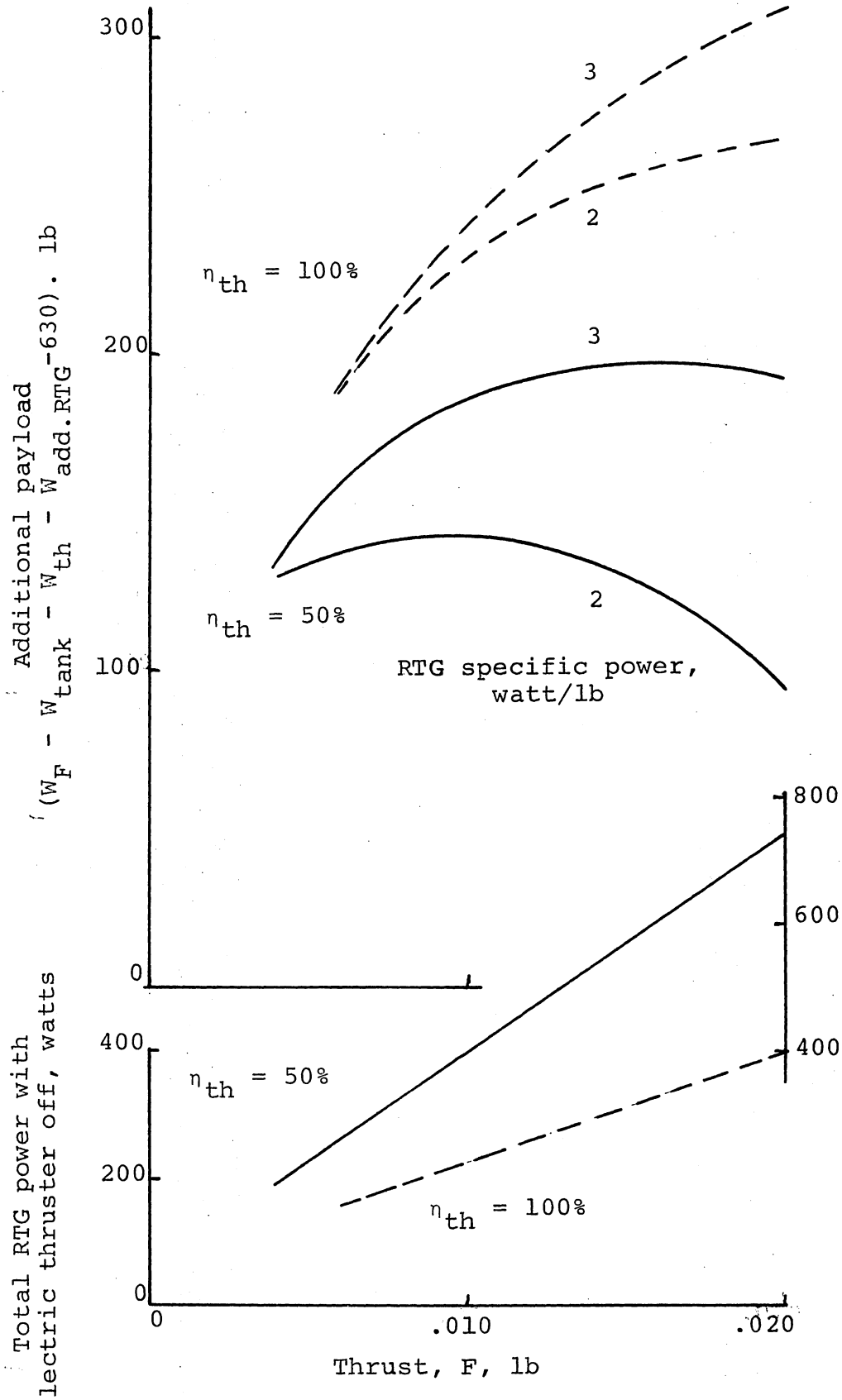

600-day Jupiter fly-by mission (with C. L. method)
launch vehicle, SLV-3X/Centaur/Burner II (2336)
hotel load during heliocentric transfer, 50 watts
THRUSTER SYSTEM, glycerol liquid-spray, η_{th} = .7, I = 1000 sec

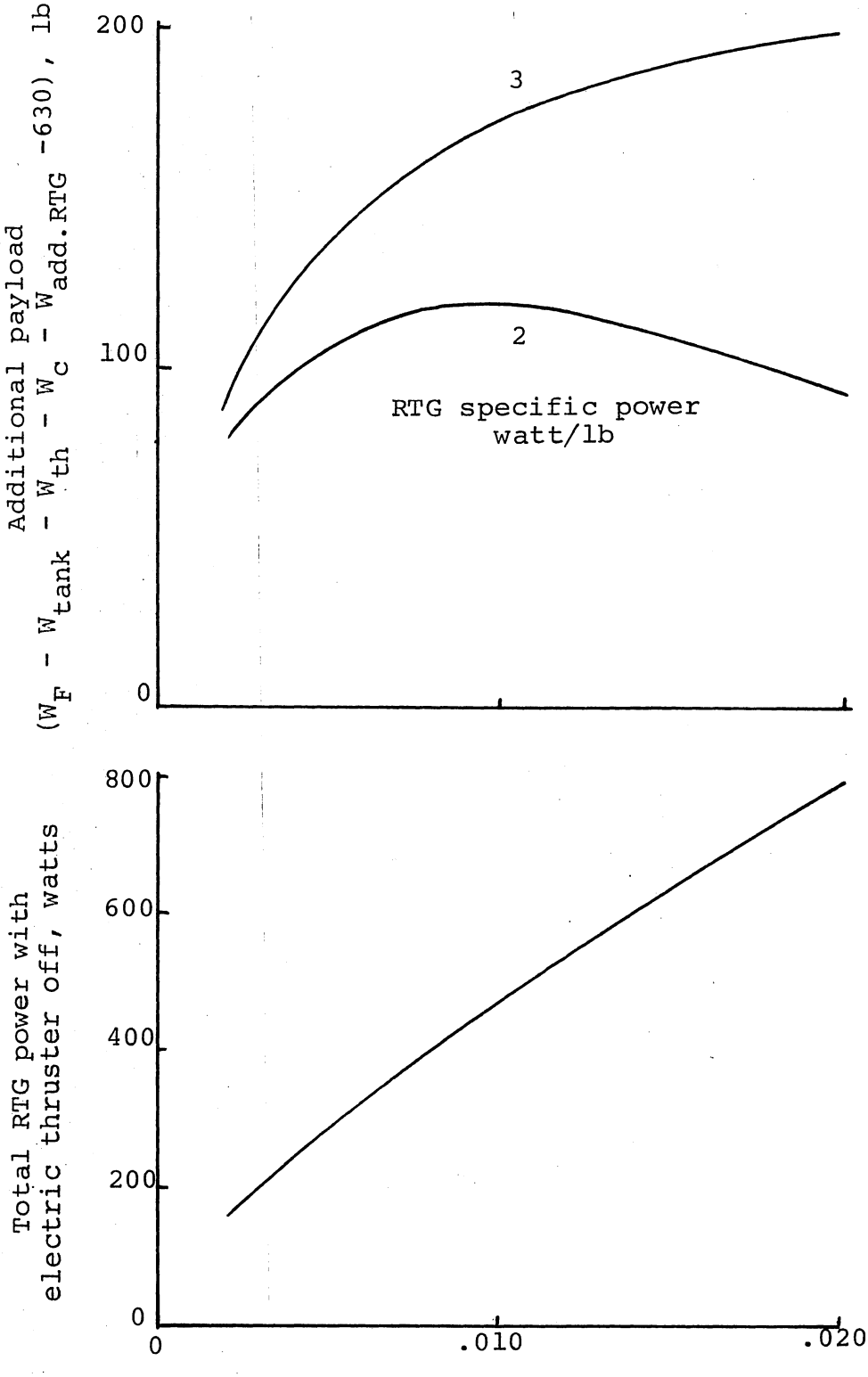

600-day Jupiter fly-by mission (with C. L. method)
launch vehicle, SLV-3X/Centaur/Burner II (2336)
hotel load during heliocentric transfer, 50 watts
THRUSTER SYSTEM, mercury-bombardment, I = 2000 sec

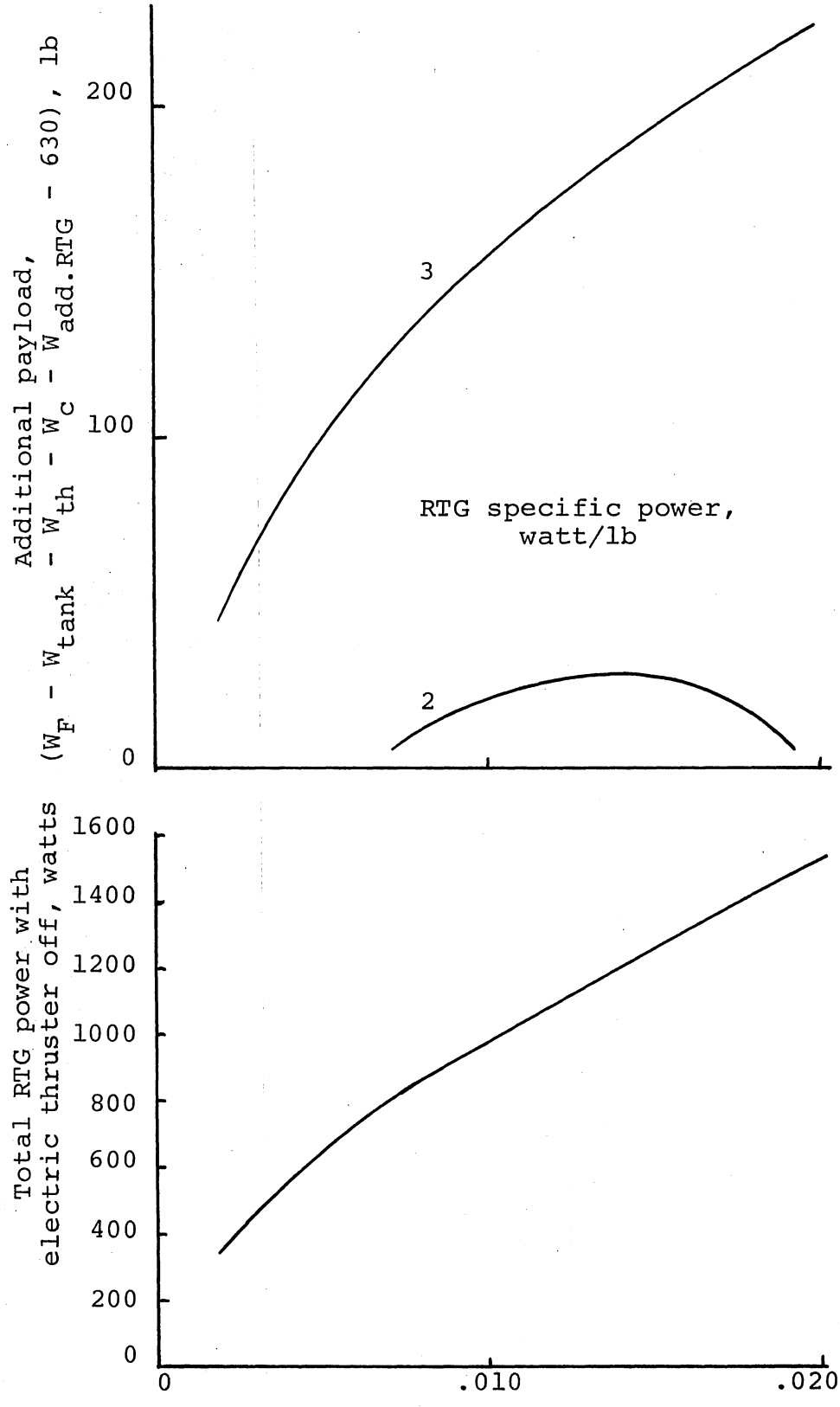

600-day Jupiter fly-by mission (with C. L. method)
launch vehicle, SLV-3X/Centaur/Burner II (2336)

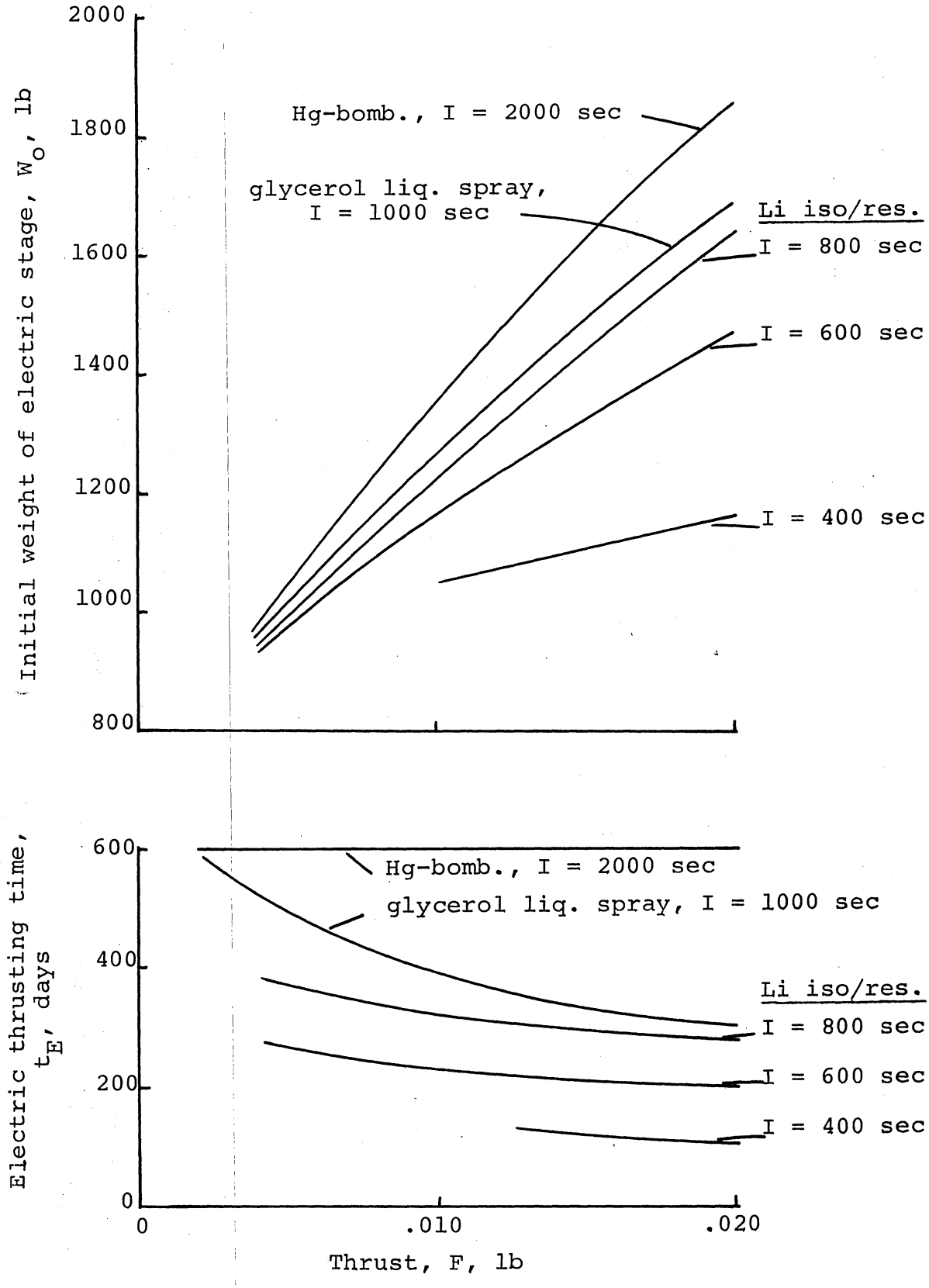

COMPARISON OF SPACECRAFT DESIGNS FOR JUPITER FLY-BY MISSION

FOR MAXIMUM ADDITIONAL PAYLOAD ($W_F - W_{tank} - W_{th} - W_{add.RTG} - W_c - 630$) (RTG, 2 watts/lb)

SPACECRAFT CONCEPT	GSFC					JPL
LAUNCH VEHICLE	SLV-3X/CENTAUR/BURNER II(2336)					SLV3C/CENT.
MISSION TIME, DAYS	600					900
BASELINE FINAL SPACECRAFT WT., LB	630					1553
ELECTRIC POWERPLANT	RTG					SOLAR CELLS
BASELINE USABLE PAYLOAD, LB	555					632
ELECTRIC THRUSTER SYSTEM	LI ISOTOPE/RESISTOJET			GLYC. LIQ. SP.	HG-BOMB.	HG-BOMB.
ELECTRIC THRUSTER I_{SP}, SEC	400	600	800	1000	2000	2700
THRUSTER SYSTEM THRUST, LB	.0125	.010	.010	.010	.014	.125
THRUSTER SYSTEM WT. ($W_{th} + W_c$), lb	6	6	6	17	21	180
PROPELLANT WEIGHT, LB	340	340	310	320	240	845
TANK WEIGHT, LB	9	9	8	46	8	25
TOTAL POWER AT JUPITER, WATTS	150	300	400	540	1200	483
ADDITIONAL PAYLOAD, LB	80	115	142	119	28	40
INITIAL WT. OF ELECTRIC STAGE, LB	1080	1140	1220	1280	1580	2398
ELECTRIC THRUSTING TIME, DAYS	140	230	320	360	600	470
TOTAL USABLE PAYLOAD, LB	635	670	697	674	583	672

COMPARISON OF SPACECRAFT DESIGNS FOR JUPITER FLY-BY MISSION

FOR MAXIMUM ADDITIONAL PAYLOAD ($W_F - W_{tank} - W_{th} - W_{add.RTG} - W_c - 630$) (RTG, 3 watts/lb)

SPACECRAFT DESIGN	GSFC					JPL
LAUNCH VEHICLE	SLV-3X/CENTAUR/BURNER II (2336)					SLV3C/CENT.
MISSION TIME, DAYS	600					900
BASELINE FINAL SPACECRAFT WT., LB	630					1553
ELECTRIC POWERPLANT	RTG					SOLAR CELLS
BASELINE USABLE PAYLOAD, LB	580					632
ELECTRIC THRUSTER SYSTEM	LI ISOTOPE/RESISTOJET			GLYC. LIQ. SP.	HG-BOMB.	HG-BOMB
ELECTRIC THRUSTER I_{SP}, SEC	400	600	800	1000	2000	2700
THRUSTER SYSTEM THRUST, LB	.020	.010	.014	.020	>.020	.125
THRUSTER SYSTEM WT. ($W_{th} + W_c$), lb	6	6	6	22	>27	180
PROPELLANT WEIGHT, LB	430	340	450	490	>500	845
TANK WEIGHT, LB	10	9	10	70	>15	25
TOTAL POWER OF JUPITER, WATTS	210	310	600	780	>1500	483
ADDITIONAL PAYLOAD, LB	84	142	198	198	>225	40
INITIAL WT. OF ELECTRIC STAGE, LB	1180	1160	1480	1690	>1860	2398
ELECTRIC THRUSTING TIME, DAYS	140	230	290	310	600	470
TOTAL USABLE PAYLOAD, LB	664	722	778	778	>805	672

COMPARISON OF SPACECRAFT DESIGNS FOR JUPITER FLY-BY MISSION
FOR 483 WATTS OF TOTAL POWER AT JUPITER (RTG, 2 WATT/LB)

SPACECRAFT DESIGN	GSFC					JPL
LAUNCH VEHICLE	SLV-3X/CENTAUR/BURNER II (2336)					SLV3C/CENT.
MISSION TIME, DAYS	600					900
BASELINE FINAL SPACECRAFT WT., LB	630					1553
ELECTRIC POWERPLANT	RTG					SOLAR CELLS
BASELINE USABLE PAYLOAD, LB	555					632
ELECTRIC THRUSTER SYSTEM	LI ISOTOPE/RESISTOJET			GLYC. LIQ. SP.	HG-BOMB	HG-BOMB
ELECTRIC THRUSTER I_{SP}, SEC	400	600	800	1000	2000	2700
THRUSTER SYSTEM THRUST, LB	-	.0163	.0154	.0104	-	.125
THRUSTER SYSTEM WT. $(W_{th} + W_c)$, lb	-	6	6	17	-	180
PROPELLANT WEIGHT, LB	-	530	500	326	-	845
TANK WEIGHT, LB	-	11	11	47	-	25
TOTAL POWER AT JUPITER, WATTS	-	483	483	483	-	483
ADDITIONAL PAYLOAD, LB	-	72	140	126	-	40
INITIAL WT. OF ELECTRIC STAGE, LB	-	1380	1330	1280	-	2398
ELECTRIC THRUSTING TIME, DAYS	-	210	310	380	-	470
TOTAL USABLE PAYLOAD, LB	-	627	695	681	-	672

COMPARISON OF SPACECRAFT DESIGNS FOR JUPITER FLY-BY MISSION
FOR 483 WATTS OF TOTAL POWER AT JUPITER (RTG, 3 WATT/LB)

SPACECRAFT DESIGN	GSFC					JPL
LAUNCH VEHICLE	SLV-3X/CENTAUR/BURNER II (2336)					SLV3C/CENT.
MISSION TIME, DAYS	600					900
BASELINE FINAL SPACECRAFT WT., LB	630					1553
ELECTRIC POWERPLANT	RTG					SOLAR CELLS
BASELINE USABLE PAYLOAD, LB	580					632
ELECTRIC THRUSTER SYSTEM	LI ISOTOPE/RESISTOJET			GLYC. LIQ. SP.	HG-BOMB	HG-BOMB
ELECTRIC THRUSTER I_{SP}, SEC	400	600	800	1000	2000	2700
THRUSTER SYSTEM THRUST, LB	-	.0163	.0154	.0104	.0032	.125
THRUSTER SYSTEM WT. $(W_{th} + W_c)$, lb	-	6	6	17	14	180
PROPELLANT WEIGHT, LB	-	530	500	326	60	845
TANK WEIGHT, LB	-	11	11	47	2	25
TOTAL POWER AT JUPITER, WATTS	-	483	483	483	483	483
ADDITIONAL PAYLOAD, LB	-	124	194	171	83	40
INITIAL WT. OF ELECTRIC STAGE, LB	-	1380	1330	1280	970	2398
ELECTRIC THRUSTING TIME, DAYS	-	210	310	380	600	470
TOTAL USABLE PAYLOAD, LB	-	704	774	751	663	672

PERFORMANCE MAPPING OF 20-CM HOLLOW-CATHODE MERCURY ION THRUSTER

by Dennis Fitzgerald
and
Richard Vahrenkamp

INTRODUCTION

This report summarizes work done the past year at the Space Propulsion Research Facility, Colorado State University. A discussion of the immediate goals of the present research effort is included, as well as proposal topics for future study. Preparations for experiments on a 20-centimeter mercury electron-bombardment thruster and present status of the facility are described. A detailed explanation of the procedure for starting and running the thruster with comments on typical experimental problems which may be encountered is included. Tables of experimental data and results are given in the final section.

In May of 1968, the final arrangements were made to borrow a current design, flight-type, electron-bombardment thruster from the Jet Propulsion Laboratory in Pasadena, California. The thruster is a 20-centimeter model utilizing a thin (0.076 centimeter) screen grid, and equipped with a hollow cathode as an electron source.

The primary research objective is to map the performance of the thruster over a range in mass utilization from 50 to 100 per cent. This will hopefully produce a set of curves which may be used as control parameters in an automatic control system. These parameters are necessary in order to control the value of mass utilization during a mission. This type of control must be used because of the present lack of an accurate mass flow meter. An example of a performance curve using arc current as a parameter is shown in Figure 1.

Studies have been made at the Jet Propulsion Laboratory[1] on an identical 20-centimeter thruster equipped with an oxide

cathode. These studies indicate that the arc current may be used as a control parameter at low thruster efficiencies (low magnet current). The use of the arc current is undesirable, however, at high efficiencies because the parametric curves become double-valued (identical beam current at two different values of mass flow). This problem makes it impossible to specify the exact operating point (mass utilization).

It is likely that similar characteristics are present when the thruster is equipped with a hollow cathode; therefore, it may be necessary to seek another control parameter to alleviate this problem. Other candidates include the arc voltage, and possibly the current to a Langmuir probe held at a fixed potential.

In addition to mapping the performance, there are several research topics which are tentatively planned. The thruster presently under study at C.S.U. is designed to give optimum performance ($\sim$100 eV/ion) when equipped with an oxide cathode. The results contained in this report support previous findings[1] which indicate that the thruster performance is worse ($\sim$200 eV/ion) when equipped with a hollow cathode as an electron source. An attempt will be made to improve the performance by changing the baffle configuration, and possibly by applying a potential to the baffle, pole piece, or both. In addition, the pole-piece geometry itself may be changed. An attempt will be made to relate the purely empirical changes in thruster performance with theory by means of probe measurements of the plasma parameters.

APPARATUS

This section contains a brief description of the equipment presently used at the vacuum facility for thruster operation.

The 4 x 15 tank, using mechanical pumps and an oil diffusion pump, is capable of vacuums to 10^{-6} torr. The main chamber is equipped with a stainless steel liquid nitrogen liner for use as a cold trap. Located on both ends of the tank

are air-operated valves separating the main chamber from the bell jars. These valves may be operated while the tank is under full vacuum for easy access to the thruster at any time. The bell jar presently being used is 16 inches in diameter and two feet in length. The mounting flange is hinged such that the thruster may be positioned as close to the bell jar valve as possible. The flange was machined such that single as well as multiple feed-throughs could be used at various positions. The thruster itself is mounted on four one-inch rods about 16 inches from the flange, thus making an easy access to all connections to the thruster.

The thruster and mounts are completely enclosed in a 20-gauge stainless steel ground screen. The end of the ground screen is positioned 3/8 in. from the accel grid. A plexi--glass container was installed on the outside of the mounting flange to isolate all electrical connections to the thruster. The connections were positioned for easy and rapid disconnection. Also mounted on the plexiglass container were two pipettes for mercury-flow calibration. The thruster mounting and flange set-up are shown in Figures 2 and 3.

Other work performed was the installation of a liquid nitrogen feed line to the vacuum facility. The nitrogen line itself is 1/2 in. stainless steel tubing suspended in the middle of a 1-1/2 in. copper vacuum line. Sections of the feed line that could not be insulated by vacuum were insulated by 1-1/4 in. Armaflex pipe insulation. A mirror was placed within the main chamber to observe thruster operation. The power supplies and control units were built by Electro Optical Systems, and donated to C.S.U. by NASA-Lewis.

Modifications had to be made to these controls and supplies since they were designed for a cesium thruster. Such modifications include changing transformers, increasing arc supply voltage while lowering the current capacity, and adding a keeper and baffle supply. Various automatic control systems were bypassed and additional capacitors were added to the high voltage supply to reduce ripple.

Originally, thermocouple meters were used to monitor the temperature of the vaporizers. These meters, however, proved to be very inaccurate, and were replaced with a potentiometer strip-chart recorder.

EXPERIMENTAL PROCEDURE

This section contains a detailed explanation of the start-up and running procedures followed in the operation of the 20-centimeter electron-bombardment thruster shown in Figure 3. Additional information and observations have been included in order to acquaint the reader with some of the characteristics peculiar to this type of thruster. An attempt has been made to give plausible explanations of the causes and cures of certain common problems that may be encountered by the experimenter.

The vacuum chamber is pumped down to approximately 10^{-5} torr by means of a 36-in. CVC diffusion pump and a liquid nitrogen baffle. The vacuum chamber liner is then filled with liquid nitrogen, which normally brings the vacuum down to about 10^{-6} torr. The entire pump-down operation usually takes about one hour, depending on the initial tank vacuum.

The thruster start-up procedure may begin when the vacuum has reached about 10^{-4} torr. This is possible because of the relatively long time ($\sim$25 minutes) necessary for the vaporizers to reach their operating temperatures. It is customary to apply extra power to the vaporizers during start-up in order to save time. The power is then reduced to a level necessary to maintain the proper mass flow. Typical values of operating power levels are 10 watts and 8 watts for the main vaporizer and hollow cathode vaporizer, respectively. The main vaporizer is generally the slower of the two to reach operating temperature, and is less responsive to power level changes during operation. This slow response is likely due to the large conduction path from the main vaporizer to the thruster body.

The flow is monitored by means of two 1-milliliter pipettes mounted on the side of the plexiglass flange cover shown in Figure 1. Access holes in the plexiglass allow the pipettes to be refilled with mercury during operation. Caution: the high voltage must always be shut off during refilling operations because the mercury column for the hollow cathode is at 2 KV. A small wire is placed in the pipette during filling in order to break up the capillary action of the mercury on the pipette wall.

While the vaporizers are coming up to temperature, the hollow cathode heater and the isolator heater are turned on. These heaters require about 45 watts and 5 watts respectively. At this point, the keeper starting power supply (refer to Figure 5) is turned on. The hollow cathode tip is generally hot enough to emit electrons; therefore, a few milliamperes of electron current will flow to the keeper. The keeper start supply is generally on the order of 200 volts, and must be capable of delivering at least 30 milliamperes. A series resistor is placed in the keeper start circuit in order to reduce the keeper voltage as the discharge commences. When the keeper voltage is less than 50 volts, the regular keeper power supply takes over, and the starting supply may be shut off. The keeper supply is usually turned up to about 50 volts beforehand in order to make the transition to the high current arc more rapid.

A discharge will usually commence in the keeper region when the mass flow through the hollow cathode has reached about one gram per hour. When this occurs, the keeper voltage will usually drop to about 10 volts, independent of the discharge current. At this point, the keeper current can be reduced to about one ampere and the cathode heater may be turned off. It is desirable to shut the cathode heater off during runs because a considerable amount of thermal power conducts to the hollow cathode vaporizer, making it impossible to control the mass flow by means of a vaporizer (mass flow versus temperature) calibration curve.

If the keeper discharge does not commence when the flowrate is adequate, increase the hollow cathode heater supply slowly, and note the keeper voltage. The keeper voltage should drop as more power is supplied to the cathode heater due to increased electron emission. Very often, a small amount of additional cathode heater power will initiate the keeper discharge. Caution: the cathode heater should not be operated for any sustained period at excessive power levels (greater than 70 watts for this system).

If the keeper discharge fails to ignite at maximum cathode power and maximum operational cathode flow ($\sim$2 grams per hour), it is generally an indication that the hollow cathode oxide coating is insufficient. The hollow cathode must be removed and the inside must be replenished with a barium carbonate coating. A solution is prepared by mixing a small amount of barium carbonate powder with amyl acetate (banana oil). A few drops of the solution in the hollow cathode tube is usually sufficient to provide a uniform coating. It is a good idea to put a piece of wire in the orifice of the cathode to prevent clogging. After the coating is dry, the wire is removed and the tube is inspected for clearance. Replace the hollow cathode in position on the thruster, and pump down the system again. This procedure can be accomplished in about one hour, including pump-down, because the system is mounted in a bell jar which is isolated from the main vacuum chamber by a 16-in. gate valve. The bell jar section is "roughed" down to about 10^{-3} torr by means of a pipeline to the high pressure side of the diffusion pump, then the gate valve is opened.

When the vacuum is at least 10^{-3} torr, and the vaporizers are off, turn the cathode heater on and let it sit for about one hour. The high temperature activates the barium carbonate and converts it to barium oxide (a low work-function material). After the activation period, the preceding directions for initiating the keeper discharge should be followed.

It is advisable to replenish the oxide coating beforehand

whenever the thruster has been exposed to atmosphere, or when the thruster start-up has become progressively more difficult (usually after several runs).

When the keeper discharge is going and the main vaporizer flow is adequate (greater than 2 grams per hour), it is possible to start the main discharge. Turn the arc voltage up to about 50 volts and turn the magnet current to about one ampere. The main discharge will start, normally, but occasionally the keeper current must be increased to help it ignite. The arc voltage should drop to a value between 25 and 40 volts, depending on the mass flow. The low voltage arc is indicative of high mass flow.

The final part of the start-up procedure is the ion beam extraction by application of high voltage. It is generally undesirable (and often impossible) to turn the high voltage up from zero when the main discharge is going. The accel electrode draws excessive impingement current because of the poor ion optics at lower than design voltages (less than 500 volts). The most expedient method is the following: set the high voltage variacs at the proper operating voltages (±2 KV) sometime before the main discharge begins. Shut off the high voltage and start the main discharge going. Set the main discharge at some low but stable operating point (usually between 2 and 5 amperes). The magnet should be set at about 0.5 amperes. The beam should commence as soon as the high voltage is applied. The low discharge current and magnet current are necessary in order to keep the plasma density low. The plasma tends to bulge out of the thruster at high plasma densities, thereby making it difficult to turn on the high voltage without overloading the accel power supply.

If the thruster electrodes are contaminated due to long exposure to the atmosphere, or to a buildup of mercury, there may be difficulty in achieving the operational high voltage immediately, due to excessive impingement. In this case, the thruster should be run at lower values of high voltage until the thruster has decontaminated itself. The electrodes are

decontaminated by ion impingement (bombardment); therefore, the clean-up time can be minimized by keeping the impingement at a maximum. The impingement should be down in the typical operating range (5 to 20 milliamperes) before any tests are run.

When the thruster is operating smoothly (stable beam and discharge), there are several things that can be done to optimize the beam current at a given mass flow. The keeper current may be reduced to improve the beam, but it should be kept at a level that will maintain the keeper discharge in spite of any changes in the arc performance. The optimizing effect of reducing the current seems to approach a point of diminishing returns below about 0.5 amperes, but this relationship has not been firmly established. If the keeper current is too low, however, there is a possibility that the keeper discharge will go out when the arc goes out; therefore, some optimization of the beam must be traded for more reliable keeper performance. All the experimental data in this report were carried out at 0.5 amperes keeper current.

When the mass flow through the hollow cathode is low (less than 0.8 grams per hour), the keeper and arc discharges appear to be strongly coupled. In other words, rapid changes in the main discharge current (oscillations, pulsing, etc.) appear to have considerable influence on the keeper current. It is known from previous experience that reducing the percentage of the total mass flow through the hollow cathode must be weighed against the desirability of maintaining a stable keeper discharge.

The most significant changes in the ion beam are controlled by the arc current and the magnet current. These are essentially the two parameters that are varied in the data included in this report. Their influence on the operation of the thruster is shown quite well in the data and the corresponding results.

EXPERIMENTAL DATA AND RESULTS

The following data were taken primarily to gain familiarity with the thruster operation and general charac-- teristics. Although care was taken to calibrate the meters beforehand, there were certain discrepancies noticed in the arc voltage and current meters after the experiments were run. In addition, the beam and accel currents were measured on relatively small meters; therefore, the last significant digits were interpolated. Although the data may be in slight error, it should nevertheless provide information on the general trend of certain parameters. These facts should help the experimenter design an enlightened experimental approach in future studies.

The data are tabulated in nearly graphical form with the arc current and magnet current as coordinates. The blank areas are indicative of highly unstable or totally inoperative regions. The thruster was not operated above 1.0 ampere beam current; therefore, a small region on the table has no recorded data. These high beam current regions are indicated by cross-hatched spaces, and should not be considered as unstable operating points.

The results indicate that the thruster operates at very high efficiency when the magnet current is large. Unfortunately, it is difficult to maintain this operating level due to difficulty in re-cycling the high voltage after arcing; therefore, some of this data was also excluded.

These experiments suggest that several things be done to improve the speed and accuracy of data-taking. Certain critical parameters will be measured in the future by means of digital voltmeters in order to reduce the possibility of error. Periodic calibration checks will be made during the course of an experiment as an additional precaution. A system of rapid data accumulation is near completion at this time. Scaled-down samples of pertinent data coming from appropriately designed voltage dividers and shunt resistors are fed to the

contacts of a stepping relay and recorded in sequence on an FM tape recorder. After many runs are recorded, the data will be converted to computer punch cards by means of an analog to digital converter. This data is in turn processed by the digital computer, which is programmed to perform some rather simple calculations and print out a record of the data and corresponding results.

REFERENCES

1. Masek, T. D., and Pawlik, E. V.: Thrust System Technology for Solar Electric Propulsion. AIAA Paper No. 68-541. June, 1968.

Additional References pertinent to the thruster presently under study at C.S.U.

1. Masek, T. D.: Plasma Properties and Performance of Mercury Ion Thrusters. AIAA Paper No. 69-256. March, 1969.

2. Mueller, P. A., and Pawlik, E. V.: Control Analysis of an Ion Thruster with Programmed Thrust. AIAA Paper No. 69-239. March, 1969.

3. Pawlik, E. V., Macie, T. W., and Ferrara, J.: Electric Propulsion System Performance Evaluation. AIAA Paper No. 69-236. March, 1969.

4. Macie, T. W., Pawlik, E. V., Ferrara, J. D., and Costogue, E.: Solar-Electric Propulsion System Evaluation. AIAA Paper No. 69-498. June, 1969.

run number 1	DATE: 5/5/69 TIME: 1300 H.V. = ±2 K.V. KEEPER = 0.5 amp @ 10 v					$\dot{M}_{H.C.}$ = 0.89 g/hr $\dot{M}_{Main}$ = 7.10 g/hr $\dot{M}_{total}$ = 7.99 g/hr					
I_{arc} \ I_{mag}	0.2	0.4	0.6	0.8	1.0	1.2	1.4	1.6	1.8	2.0	2.2
0.5	I+ I-										
1.0			110 8								
1.5			170 11								
2.0		200 12	220 12	240 13	240 13						
2.5		260 13	270 14	300 15	300 15						
3.0		310 15	330 15	360 16	365 16						
3.5		350 16	380 16	420 17	430 17						
4.0		400 16	430 17	480 17	490 18	500 16					
4.5		440 16	480 17	540 17	540 18	560 16					
5.0		490 16	530 17	590 17	590 18	610 16	640 15				
5.5		520 16	580 16	640 16	650 17	660 15	700 14				
6.0		580 16	620 16	700 15	700 16	710 14	760 13	790 12			
6.5		620 16	680 16	750 14	760 15	760 14	810 12	840 11			
7.0		660 15	730 14	800 13	810 14	810 13	860 11	890 10	940 10		
7.5		690 15	780 13	850 12	860 13	860 12	910 10	940 9	980 9		
8.0		720 14	820 12	890 11	910 12	910 11	950 10	990 9			
8.5		740 14	850 12	940 10	960 11	960 10	990 9				
9.0		760 13	890 11	980 9	1000 10	1000 9					
9.5		790 13	920 10								
10.0	I+ I-	810 12	950 10								

run number 1	DATE: 5/5/69 TIME: 1300 H.V. = ±2 K.V. KEEPER = 0.5 amp @ 10 v					$\dot{M}_{H.C.}$ = 0.89 g/hr $\dot{M}_{Main}$ = 7.10 g/hr $\dot{M}_{total}$ = 7.99 g/hr					
I_{arc} \ I_{mag}	0.2	0.4	0.6	0.8	1.0	1.2	1.4	1.6	1.8	2.0	2.2
0.5	V_{arc}										
1.0			22.1								
1.5			22.2								
2.0		22.4	22.4	22.7	23.0						
2.5		22.6	22.6	22.9	23.1						
3.0		22.8	22.8	23.2	23.3						
3.5		23.0	23.0	23.5	23.5						
4.0		23.2	23.2	23.8	23.7	24.1					
4.5		23.3	23.4	24.0	23.9	24.3					
5.0		23.5	23.7	24.2	24.0	24.5	25.2				
5.5		23.7	23.9	24.4	24.1	24.6	25.4				
6.0		24.0	24.1	24.5	24.4	24.7	25.8	26.3			
6.5		24.2	24.4	24.7	24.6	25.0	26.0	26.7			
7.0		24.6	24.7	25.0	24.9	25.2	26.2	27.1	28.5		
7.5		24.8	25.0	25.3	25.2	25.6	26.8	27.7	29.3		
8.0		25.0	25.2	25.8	25.8	26.1	27.5	28.5			
8.5		25.1	25.4	26.4	26.4	26.8	28.1				
9.0		25.2	25.8	27.2	27.3	27.5					
9.5		25.4	26.2								
10.0	V_{arc}	25.6	26.6								

run number 1	DATE: 5/5/69 TIME: 1300 H.V. = ±2 K.V. KEEPER = 0.5 amp @ 10 v					$\dot{M}_{H.C.}$ = 0.89 g/hr $\dot{M}_{Main}$ = 7.10 g/hr $\dot{M}_{total}$ = 7.99 g/hr					
I_{arc} \ I_{mag}	0.2	0.4	0.6	0.8	1.0	1.2	1.4	1.6	1.8	2.0	2.2
0.5	eV/ion η_m(%)										
1.0			246 10.3								
1.5			225 15.9								
2.0		249 18.8	226 20.6	210 22.5	212 22.5						
2.5		236 24.4	228 25.3	208 28.1	208 28.1						
3.0		237 29.1	223 31.0	207 33.8	205 34.2						
3.5		244 32.8	225 35.6	208 39.4	203 40.3						
4.0		245 37.6	228 40.4	212 45.1	204 46.0	202 46.8					
4.5		250 41.3	229 45.0	208 50.6	207 50.6	203 52.6					
5.0		249 46.0	232 49.7	214 55.3	212 55.3	208 57.2	205 60.0				
5.5		260 48.8	235 54.4	217 60.0	211 61.0	212 61.9	207 74.1				
6.0		257 54.4	242 58.2	217 65.7	216 65.7	214 66.6	210 71.2	207 74.1			
6.5		261 58.2	241 63.8	221 70.4	217 71.3	219 71.3	215 75.9	212 78.7			
7.0		268 62.0	244 68.5	225 75.0	221 76.0	217 76.0	218 80.6	219 83.4	218 88.1		
7.5		277 64.8	246 73.2	229 79.8	226 80.6	229 80.6	227 85.3	227 88.1	230 91.8		
8.0		285 67.5	252 76.9	237 83.5	232 85.3	235 85.3	237 89.0	235 92.8			
8.5		294 69.5	260 79.7	243 88.2	239 90.0	243 90.0	246 92.8				
9.0		304 71.3	267 83.5	254 92.0	250 93.8	253 93.8					
9.5		312 74.0	276 86.3								
10.0	eV/ion η_m(%)	316 76.0	280 89.2								

run number 1	DATE: 5/5/69 TIME: 1300 H.V. = ±2 K.V. KEEPER = 0.5 amp @ 10 v					$\dot{M}_{H.C.}$ = 0.89 g/hr $\dot{M}_{Main}$ = 7.10 g/hr $\dot{M}_{total}$ = 7.99 g/hr					
I_{arc} \ I_{mag}	0.2	0.4	0.6	0.8	1.0	1.2	1.4	1.6	1.8	2.0	2.2
0.5	η_t(%)										
1.0											
1.5			7.9								
2.0		15.1	12.7	18.4	18.6						
2.5		21.3	20.9	23.5	23.5						
3.0		24.1	26.0	28.6	28.9						
3.5		27.2	29.9	33.5	34.4						
4.0		31.4	34.1	38.6	39.5	40.3					
4.5		34.6	38.3	43.6	43.6	45.6					
5.0		38.9	42.4	47.7	47.7	49.7	52.4				
5.5		41.2	45.8	51.9	53.0	53.8	57.0				
6.0		46.2	49.8	57.2	57.3	58.1	62.4	65.4			
6.5		49.4	54.8	61.4	62.2	62.3	66.6	69.3			
7.0		52.8	59.2	65.4	66.3	66.6	70.8	73.4	77.6		
7.5		55.1	63.3	69.7	70.5	70.5	74.4	77.4	80.7		
8.0		57.3	66.6	73.0	74.5	74.6	77.8	81.5			
8.5		58.8	68.8	76.8	78.5	78.6	81.0				
9.0		60.5	72.1	80.0	81.7	81.7					
9.5		62.2	74.5								
10.0	η_t(%)	64.0	76.6								

run number 2	DATE: 5/5/69 TIME: 1600 H.V. = ±2 K.V. KEEPER = 0.5 amp @ 10 v					$\dot{M}_{H.C.}$ = 1.23 g/hr $\dot{M}_{Main}$ = 5.60 g/hr $\dot{M}_{total}$ = 6.83 g/hr					
I_{arc} \ I_{mag}	0.2	0.4	0.6	0.8	1.0	1.2	1.4	1.6	1.8	2.0	2.2
0.5	I+ I-										
1.0		120 7									
1.5		170 8	190 9	190 9	190 9						
2.0		220 9	250 10	260 10	260 10						
2.5		270 10	310 10	330 11	330 11						
3.0		320 10	370 11	400 11	400 11						
3.5		370 11	420 11	460 11	460 11						
4.0		420 11	480 10	510 10	520 11	530 10	560 9				
4.5		470 10	530 10	560 10	580 10	590 10	620 9				
5.0		520 10	580 9	620 9	630 9	640 9	660 8				720 7
5.5		560 10	620 9	670 8	680 8	690 8	710 8	740 7	750 7	760 7	760 7
6.0		590 9	660 8	710 8	720 8	730 8	750 7	780 6	780 6	790 6	790 6
6.5		610 9	690 8	740 7	760 7	760 7	780 6	810 6	810 6	820 6	830 6
7.0		640 9	720 7	770 7	780 7	800 6	810 6	840 6	840 6	850 5	860 5
7.5		660 8	750 7	790 6	800 6	820 6	840 6	860 6	870 5	880 5	890 5
8.0		680 8	770 6	820 6	830 6	840 6	860 5	890 5	890 5	900 5	910 5
8.5		700 8	790 6	840 6	850 5	870 5	890 5	910 5	920 5		
9.0		720 7	800 6	860 5	880 5	890 5	900 5				
9.5		730 7	820 6	880 5	910 5	910 5					
10.0	I+ I-	740 7	840 5								

run number 2	DATE: 5/5/69 TIME: 1600 H.V. = ±2 K.V. KEEPER = 0.5 amp @ 10 v					$\dot{M}_{H.C.}$ = 1.23 g/hr $\dot{M}_{Main}$ = 5.60 g/hr $\dot{M}_{total}$ = 6.83 g/hr					
I_{arc} \ I_{mag}	0.2	0.4	0.6	0.8	1.0	1.2	1.4	1.6	1.8	2.0	2.2
0.5	V_{arc}										
1.0		23.3									
1.5		23.5	23.3	23.6	23.9						
2.0		23.7	23.7	23.8	24.0						
2.5		24.0	24.0	24.0	24.1						
3.0		24.1	24.3	24.5	24.3						
3.5		24.2	24.4	24.8	24.7						
4.0		24.5	24.7	25.0	24.9	25.1	25.8				
4.5		24.7	25.0	25.2	25.0	25.3	26.0				
5.0		25.0	25.1	25.5	25.3	25.6	26.3				28.1
5.5		25.2	25.4	25.8	25.6	26.0	26.7	27.8	28.0	28.6	28.6
6.0		25.5	25.7	26.2	26.0	26.2	27.1	28.3	28.6	29.1	29.5
6.5		25.7	26.0	26.6	26.6	26.9	27.8	29.0	29.6	30.0	30.3
7.0		25.8	26.3	27.2	27.7	27.5	28.6	30.0	30.6	31.5	32.0
7.5		26.0	26.7	27.7	27.9	28.3	29.5	31.5	32.0	33.0	33.8
8.0		26.1	27.2	28.3	28.6	29.4	31.0	33.0	34.0	35.0	35.3
8.5		26.5	27.7	29.3	30.0	31.0	32.6	35.3	36.0		
9.0		26.7	28.2	30.6	31.7	32.4	34.5				
9.5		27.0	28.9	32.0	33.0	34.0					
10.0	V_{arc}	27.2	29.9								

run number 2	DATE: 5/5/69 TIME: 1600 H.V. = ±2 K.V. KEEPER = 0.5 amp @ 10 v					$\dot{M}_{H.C.}$ = 1.23 g/hr $\dot{M}_{Main}$ = 5.60 g/hr $\dot{M}_{total}$ = 6.83 g/hr					
I_{arc} \ I_{mag}	0.2	0.4	0.6	0.8	1.0	1.2	1.4	1.6	1.8	2.0	2.2
0.5	eV/ion η_m(%)										
1.0		236 13.2									
1.5		237 18.7	210 20.8	212 20.8	216 20.8						
2.0		239 24.2	210 27.4	203 28.5	204 28.5						
2.5		238 29.6	210 34.0	197 36.2	198 36.2						
3.0		242 35.1	211 40.6	196 43.8	195 43.8						
3.5		243 40.6	216 46.0	200 50.5	199 50.5						
4.0		245 46.1	217 52.6	206 56.0	201 57.0	197 58.1	193 61.4				
4.5		247 51.6	221 58.1	210 61.4	202 63.6	201 64.7	197 68.0				
5.0		250 57.0	224 63.6	213 68.0	208 69.0	206 70.2	198 72.5				203 79.0
5.5		257 61.5	234 68.0	219 73.5	215 74.6	214 75.7	214 77.9	214 81.2	212 82.2	213 83.5	213 83.5
6.0		267 64.6	241 72.4	227 78.0	223 79.0	221 80.1	224 82.3	225 85.5	227 88.9	228 90.0	230 91.0
6.5		282 66.9	252 75.7	240 81.2	234 83.5	237 83.5	238 85.5	239 88.9	245 88.9	244 90.0	246 91.0
7.0		291 70.1	263 79.0	253 84.4	255 85.5	247 87.6	253 89.0	256 92.0	261 92.0	266 93.3	266 94.5
7.5		303 72.5	273 82.3	270 86.6	269 87.8	266 90.0	269 92.3	281 94.5	281 95.5	287 96.5	291 97.6
8.0		314 74.6	290 84.4	283 90.0	282 91.0	286 92.0	295 94.3	303 97.6	312 97.6	316 98.6	316 99.6
8.5		329 76.8	305 86.6	302 92.2	306 93.5	309 95.5	317 97.6	336 99.6	337 101.2		
9.0		342 79.0	324 87.8	325 94.2	331 96.5	333 97.6	351 98.9				
9.5		357 80.1	341 90.0	351 96.5	350 99.6	360 99.6					
10.0	eV/ion η_m(%)	375 81.2	362 92.1								

run number 2	DATE: 5/5/69 TIME: 1600 H.V. = ±2 K.V. KEEPER = 0.5 amp @ 10 v					$\dot{M}_{H.C.}$ = 1.23 g/hr $\dot{M}_{Main}$ = 5.60 g/hr $\dot{M}_{total}$ = 6.83 g/hr					
I_{arc} \ I_{mag}	0.2	0.4	0.6	0.8	1.0	1.2	1.4	1.6	1.8	2.0	2.2
0.5	η_t (%)										
1.0		10.2									
1.5		15.1	17.1	17.1	17.0						
2.0		19.8	23.0	24.0	24.0						
2.5		24.6	28.8	31.0	30.9						
3.0		29.5	34.7	37.8	37.8						
3.5		34.2	39.5	43.9	44.0						
4.0		39.1	45.5	48.7	49.6	51.0	53.9				
4.5		44.1	50.5	53.4	55.7	56.7	59.8				
5.0		48.3	55.3	59.6	60.5	61.5	63.8				
5.5		52.6	59.2	64.5	65.5	66.5	68.4	71.5	72.5	73.5	73.8
6.0		55.0	62.9	68.3	69.3	70.2	72.0	75.0	75.0	76.0	76.0
6.5		57.0	65.6	71.0	73.2	73.0	74.5	77.5	77.3	78.3	79.2
7.0		59.4	68.2	73.3	74.2	76.3	77.3	79.9	79.6	80.6	81.5
7.5		61.3	71.3	74.8	76.2	77.6	79.6	81.4	82.3	82.7	83.5
8.0		62.8	72.2	77.2	78.1	78.9	80.6	83.4	83.0	83.6	84.5
8.5		64.4	72.3	78.6	79.6	81.4	82.6	83.8	84.0		
9.0		65.7	74.0	79.5	81.5	82.5	82.7				
9.5		66.5	75.4	80.8	83.6	83.0					
10.0	η_t (%)	66.8	76.7								

run number 3	DATE: 5/6/69 TIME: 1400 H.V. = ±2 K.V. KEEPER = 0.5 amp @ 10 v					$\dot{M}_{H.C.}$ = 1.6 g/hr $\dot{M}_{Main}$ = 5.9 g/hr $\dot{M}_{total}$ = 7.5 g/hr					
I_{arc} \ I_{mag}	0.2	0.4	0.6	0.8	1.0	1.2	1.4	1.6	1.8	2.0	2.2
0.5											
1.0											
1.5											
2.0			190 12								
2.5			240 13	260 14							
3.0			300 15	310 16							
3.5			340 25	360 17	380 17						
4.0		340 16	390 16	420 17	430 18						
4.5		380 17	430 17	470 18	490 18						
5.0		420 17	470 17	520 18	540 18						
5.5		450 17	500 17	560 18	580 18	580 18					
6.0		480 17	550 17	600 17	620 18	630 18					
6.5		510 18	580 17	640 17	670 18	680 18	700 17				
7.0		540 18	620 17	690 17	710 17	720 17	740 16	780 15			
7.5		560 18	650 17	720 16	740 17	760 17	790 16	820 14	840 13		
8.0		600 17	680 16	760 15	790 16	800 16	830 15	860 13	860 12	870 12	
8.5		620 17	720 16	800 14	820 15	840 15	860 14	900 13	900 11	900 11	
9.0		640 17	740 15	820 14	850 15	870 15	900 14	920 12	920 11		
9.5		660 17	770 15	840 13	880 14	900 14	930 13	940 11	940 10		
10.0		680 17	790 15	870 12	910 13	920 13	950 12	960 11	960 10		

run number 3	DATE: 5/6/69 TIME: 1400 H.V. = ±2 K.V. KEEPER = 0.5 amp @ 10 v							$\dot{M}_{H.C.}$ = 1.6 g/hr $\dot{M}_{Main}$ = 5.9 g/hr $\dot{M}_{total}$ = 7.5 g/hr			
I_{arc} \ I_{mag}	0.2	0.4	0.6	0.8	1.0	1.2	1.4	1.6	1.8	2.0	2.2
0.5	V_{arc}										
1.0											
1.5											
2.0			21.0								
2.5			21.5	21.6							
3.0			21.7	21.8							
3.5			21.8	22.0	22.3						
4.0		20.7	22.0	22.0	22.4						
4.5		21.0	22.0	22.1	22.5						
5.0		21.3	22.0	22.3	22.6						
5.5		21.6	22.0	22.4	22.7	23.0					
6.0		21.7	22.0	22.5	22.6	23.0					
6.5		21.7	22.1	22.5	22.6	23.0	23.7				
7.0		21.7	22.1	22.6	22.6	23.0	23.8	24.6			
7.5		21.7	22.1	22.5	22.7	23.0	23.9	24.7	25.1		
8.0		21.7	22.1	22.7	22.9	23.1	24.0	25.0	25.5	25.8	
8.5		21.9	22.2	22.8	23.0	23.3	24.1	25.3	25.7	26.0	
9.0		22.0	22.2	23.0	23.0	23.6	24.3	25.6	26.0		
9.5		22.0	22.3	23.1	23.3	23.9	24.7	26.0	26.4		
10.0	V_{arc}	22.0	22.3	23.4	23.6	24.0	25.0	26.3	27.0		

run number 3	DATE: 5/6/69 TIME: 1400 H.V. = ±2 K.V. KEEPER = 0.5 amp @ 10 v					$\dot{M}_{H.C.}$ = 1.6 g/hr $\dot{M}_{Main}$ = 5.9 g/hr $\dot{M}_{total}$ = 7.5 g/hr					
I_{arc} \ I_{mag}	0.2	0.4	0.6	0.8	1.0	1.2	1.4	1.6	1.8	2.0	2.2
0.5	eV/ion η_m(%)										
1.0											
1.5											
2.0			248 19.0								
2.5			246 24.0	227 26.0							
3.0			233 30.0	229 31.0							
3.5			240 34.0	227 36.0	219 38.0						
4.0		259 34.0	239 39.0	222 42.0	220 43.0						
4.5		262 38.0	242 43.0	223 47.0	216 49.0						
5.0		266 42.0	244 47.0	225 52.0	219 54.0						
5.5		276 45.0	252 50.0	228 56.0	224 58.0	228 58.0					
6.0		281 48.0	249 55.0	233 60.0	227 62.0	227 63.0					
6.5		286 51.0	257 58.0	233 64.0	227 67.0	228 68.0	227 70.0				
7.0		289 54.0	258 62.0	236 69.0	229 71.0	230 72.0	233 74.0	227 78.0			
7.5		300 56.0	263 65.0	242 72.0	238 74.0	233 76.0	233 79.0	232 82.0	229 84.0		
8.0		299 60.0	267 68.0	246 76.0	239 79.0	238 80.0	238 83.0	239 86.0	243 86.0	244 87.0	
8.5		308 62.0	270 72.0	248 80.0	245 82.0	242 84.0	244 86.0	245 90.0	248 90.0	251 90.0	
9.0		317 64.0	277 74.0	259 82.0	249 85.0	251 87.0	149 90.0	157 92.0	261 92.0		
9.5		323 66.0	282 77.0	268 84.0	258 88.0	257 90.0	259 93.0	269 94.0	273 94.0		
10.0	eV/ion η_m(%)	332 68.0	289 79.0	274 87.0	265 91.0	270 92.0	268 95.0	279 96.0	286 96.0		

run number 3	DATE: 5/6/69 TIME: 1400 H.V. = ±2 K.V. KEEPER = 0.5 amp @ 10 v					$\dot{M}_{H.C.}$ = 1.6 g/hr $\dot{M}_{Main}$ = 5.9 g/hr $\dot{M}_{total}$ = 7.5 g/hr					
I_{arc} \ I_{mag}	0.2	0.4	0.6	0.8	1.0	1.2	1.4	1.6	1.8	2.0	2.2
0.5	$\eta_{t(\%)}$										
1.0											
1.5											
2.0			15.2								
2.5			19.5	21.4							
3.0			24.8	25.7							
3.5			28.3	30.1	32.0						
4.0		28.1	32.7	35.6	36.4						
4.5		31.4	36.1	40.0	41.8						
5.0		34.9	39.6	44.4	46.2						
5.5		37.3	42.2	48.0	49.8	49.6					
6.0		39.9	46.6	51.5	53.2	54.2					
6.5		42.5	49.1	55.0	57.8	58.5	60.5				
7.0		45.0	52.6	59.5	61.2	62.2	64.0	67.9			
7.5		46.5	55.1	62.0	63.8	65.8	68.5	71.4	73.1		
8.0		50.0	57.8	65.5	68.2	69.2	72.0	75.0	75.8	75.5	
8.5		51.6	61.3	69.0	70.8	72.6	74.5	78.1	78.2	78.1	
9.0		53.1	63.0	70.5	73.5	75.0	78.0	79.4	79.4		
9.5		54.6	65.5	72.2	76.0	77.6	80.0	81.0	81.0		
10.0	$\eta_{t(\%)}$	56.1	67.0	74.5	78.5	79.1	81.5	82.4	82.6		

run number 4	DATE: 5/7/69 TIME: 1300 H.V. = ±2 K.V. KEEPER = 0.5 amp @ 10 v					$\dot{M}_{H.C.}$ = 1.5 g/hr $\dot{M}_{Main}$ = 5.8 g/hr $\dot{M}_{total}$ = 7.3 g/hr					
I_{arc} \ I_{mag}	0.2	0.4	0.6	0.8	1.0	1.2	1.4	1.6	1.8	2.0	2.2
0.5	I+ I-										
1.0											
1.5											
2.0				190 12							
2.5				250 14							
3.0				300 15	320 15						
3.5			320 15	350 16	370 16						
4.0			380 16	400 17	430 17	450 17					
4.5		400 16	430 17	450 17	480 17	500 17					
5.0		440 16	460 17	490 18	530 17	550 17					
5.5		470 16	500 17	540 18	570 17	600 17	620 17				
6.0		510 16	540 17	580 18	610 17	650 17	670 16	700 15			
6.5		540 16	580 17	620 17	660 17	690 16	720 15	750 15			
7.0		570 16	620 17	660 17	700 16	730 15	770 15	800 14			
7.5		600 16	650 16	700 17	740 16	780 15	810 14	840 13	850 13		
8.0		630 16	680 16	730 16	780 15	810 14	840 13	870 12	880 12	890 12	
8.5		650 16	720 15	770 15	810 15	850 14	880 13	900 12	900 12	920 12	
9.0		670 16	750 15	800 15	840 14	880 13	900 12	930 12	930 11	950 12	
9.5		700 16	770 15	840 14	870 13	900 13	930 12	950 11	950 11	970 11	
10.0	I+ I-	710 16	790 14	860 14	900 13	920 12	950 11	970 11	970 11	990 11	

run number 4	DATE: 5/7/69 TIME: 1300 H.V. = ±2 K.V. KEEPER = 0.5 amp @ 10 v					$\dot{M}_{H.C.}$ = 1.5 g/hr $\dot{M}_{Main}$ = 5.8 g/hr $\dot{M}_{total}$ = 7.3 g/hr					
I_{arc} \ I_{mag}	0.2	0.4	0.6	0.8	1.0	1.2	1.4	1.6	1.8	2.0	2.2
0.5	V_{arc}										
1.0											
1.5											
2.0				21.2							
2.5				21.4							
3.0				21.6	22.0						
3.5			21.0	21.8	22.2						
4.0			21.4	22.0	22.4	23.0					
4.5		22.2	21.8	22.2	22.5	23.1					
5.0		22.4	22.3	22.3	22.7	23.2					
5.5		22.5	22.5	22.4	22.7	23.2	24.0				
6.0		22.6	22.6	22.6	22.7	23.4	24.1	24.8			
6.5		22.7	22.7	22.7	22.8	23.5	24.2	25.0			
7.0		22.8	22.8	22.7	22.9	23.7	24.4	25.2			
7.5		22.8	23.0	22.8	23.0	23.8	24.6	25.4	25.8		
8.0		22.8	23.0	22.9	23.1	24.0	24.7	25.7	26.1	26.0	
8.5		22.8	23.0	23.0	23.2	24.3	25.0	26.2	26.3	26.5	
9.0		22.8	23.0	23.1	23.4	24.5	25.2	26.7	26.7	27.0	
9.5		22.8	23.1	23.3	23.6	24.8	25.6	27.1	27.3	27.5	
10.0	V_{arc}	22.8	23.1	23.5	23.9	25.0	26.0	27.6	27.8	28.0	

run number 4	DATE: 5/7/69 TIME: 1300 H.V. = ±2 K.V. KEEPER = 0.5 amp @ 10 v					$\dot{M}_{H.C.}$ = 1.5 g/hr $\dot{M}_{Main}$ = 5.8 g/hr $\dot{M}_{total}$ = 7.3 g/hr					
I_{arc} \ I_{mag}	0.2	0.4	0.6	0.8	1.0	1.2	1.4	1.6	1.8	2.0	2.2
0.5	eV/ion η_m(%)										
1.0											
1.5											
2.0				253 19.5							
2.5				234 25.7							
3.0				234 30.8	222 32.9						
3.5			245 32.9	232 36.0	224 38.0						
4.0			239 39.0	233 41.1	221 44.2	213 46.2					
4.5		263 41.1	239 44.2	233 46.3	221 49.3	220 51.4					
5.0		266 45.2	253 47.2	238 50.3	224 54.5	220 56.5					
5.5		275 48.3	258 51.3	239 55.5	229 58.6	222 61.6	221 63.7				
6.0		276 52.2	261 55.7	243 59.6	231 62.6	223 66.9	224 68.9	220 71.9			
6.5		282 55.0	264 59.8	247 63.6	232 67.8	229 70.8	225 74.0	224 77.0			
7.0		289 58.6	266 63.9	247 67.8	236 71.9	234 75.0	229 79.1	277 82.2			
7.5		291 61.8	272 67.0	250 71.9	241 76.0	236 80.1	235 83.2	233 86.2	234 87.3		
8.0		296 65.0	278 70.0	258 75.0	244 80.1	243 83.2	242 86.2	243 89.4	247 90.5	239 91.5	
8.5		306 66.9	279 74.0	261 79.2	252 83.2	248 87.5	246 90.4	254 92.5	255 92.5	250 94.6	
9.0		314 69.0	282 77.0	265 82.2	259 86.2	256 90.4	258 92.5	265 95.5	265 95.6	261 97.6	
9.5		317 72.0	292 79.2	270 86.3	263 89.2	268 92.5	267 95.6	276 97.6	277 97.6	274 99.5	
10.0	eV/ion η_m(%)	328 73.0	299 81.2	279 88.4	271 92.5	277 94.5	279 97.6	289 99.6	292 99.5	287 102.0	

run number 4	DATE: 5/7/69 TIME: 1300 H.V. = ±2 K.V. KEEPER = 0.5 amp @ 10 v					$\dot{M}_{H.C.}$ = 1.5 g/hr $\dot{M}_{Main}$ = 5.8 g/hr $\dot{M}_{total}$ = 7.3 g/hr					
I_{arc} \ I_{mag}	0.2	0.4	0.6	0.8	1.0	1.2	1.4	1.6	1.8	2.0	2.2
0.5	η_t (%)										
1.0											
1.5											
2.0				15.5							
2.5				21.0							
3.0				25.5	27.4						
3.5			27.2	30.0	32.0						
4.0			32.6	34.5	37.5	39.4					
4.5		34.1	37.2	39.1	42.0	43.9					
5.0		37.7	39.6	42.6	46.6	48.5					
5.5		40.3	43.3	47.2	50.1	53.0	54.9				
6.0		43.8	47.0	50.6	53.7	59.4	59.5	62.5			
6.5		46.2	50.6	54.3	58.3	61.2	64.2	66.8			
7.0		49.2	54.1	58.0	61.9	64.6	68.7	71.4			
7.5		52.0	56.6	61.5	65.5	69.3	72.2	75.0	76.0		
8.0		54.5	59.3	64.2	69.0	72.0	74.9	77.6	78.9	79.5	
8.5		56.0	62.9	67.6	71.7	75.6	78.3	80.0	80.0	81.8	
9.0		57.4	65.5	70.5	74.2	78.2	79.7	82.3	82.5	84.1	
9.5		60.0	67.3	73.9	77.0	79.5	82.5	83.6	83.6	85.5	
10.0	η_t (%)	60.9	69.1	75.5	79.5	83.9	83.5	85.1	85.0	85.5	

run number 5	DATE: 5/7/69 TIME: 1500 H.V. = ±2 K.V. KEEPER = 0.5 amp @ 10 v					$\dot{M}_{H.C.}$ = 1.5 g/hr $\dot{M}_{Main}$ = 4.9 g/hr $\dot{M}_{total}$ = 6.4 g/hr					
I_{arc} \ I_{mag}	0.2	0.4	0.6	0.8	1.0	1.2	1.4	1.6	1.8	2.0	2.2
0.5	I+ I-										
1.0											
1.5											
2.0		180 9	200 10	210 10	200 10						
2.5		240 11	260 11	270 11	270 11						
3.0		280 12	310 12	330 12	330 12						
3.5		320 12	360 13	380 12	390 12	400 12					
4.0		360 12	400 13	430 12	440 12	470 12					
4.5		400 12	450 13	480 12	490 12	520 12	540 11				
5.0		430 12	490 13	520 12	540 12	560 12	590 11				
5.5		460 12	530 12	560 12	580 11	600 11	630 10	560 11			
6.0		500 12	570 12	600 11	610 10	650 10	670 10	690 10			
6.5		520 12	600 12	630 11	650 10	670 10	700 10	720 10			
7.0		550 12	630 11	660 10	670 9	700 10	720 9	740 10			
7.5		560 11	650 11	680 10	690 9	720 9	740 9	760 10	770 10		
8.0		580 11	680 11	710 10	710 9	730 9	760 9	780 9	790 9		
8.5		600 11	690 10	730 10	720 8	750 9	780 9	800 9	800 9	820 9	
9.0		610 11	710 10	740 9	740 8	760 9	790 9	810 9	820 9	830 9	
9.5		620 10	720 10	760 9	750 8	780 8	810 8	830 9	840 9	840 9	
10.0	I+ I-	630 10	740 10	770 9	760 8	790 8	820 8	840 9	850 9	850 9	

run number 5	DATE: 5/7/69 TIME: 1500 H.V. = ±2 K.V. KEEPER = 0.5 amp @ 10 v					$\dot{M}_{H.C.}$ = 1.5 g/hr $\dot{M}_{Main}$ = 4.9 g/hr $\dot{M}_{total}$ = 6.4 g/hr					
I_{arc} \ I_{mag}	0.2	0.4	0.6	0.8	1.0	1.2	1.4	1.6	1.8	2.0	2.2
0.5	V_{arc}										
1.0											
1.5											
2.0		21.6	21.8	22.1							
2.5		21.7	21.9	22.0	22.2						
3.0		22.0	22.0	22.3	22.5						
3.5		22.2	22.2	22.6	22.7	23.4					
4.0		22.3	22.4	22.7	23.0	23.5					
4.5		22.5	22.6	23.0	23.1	23.6	24.2				
5.0		22.6	22.7	23.0	23.2	23.7	24.4				
5.5		22.7	22.8	23.1	23.4	23.9	24.6	25.0			
6.0		22.7	22.9	23.2	23.6	24.0	24.8	25.2			
6.5		22.7	23.0	23.3	23.7	24.2	25.0	25.5			
7.0		22.8	23.1	23.4	24.0	24.4	25.3	26.0			
7.5		22.9	23.1	23.6	24.2	24.7	25.7	26.4	27.0		
8.0		22.9	23.1	23.8	24.5	25.0	26.1	26.9	27.4		
8.5		23.0	23.2	24.0	24.8	25.6	26.7	27.4	28.2	28.6	
9.0		23.0	23.3	24.2	25.1	26.0	27.4	28.1	29.1	29.8	
9.5		23.0	23.5	24.4	25.6	26.7	28.1	29.0	30.0	30.6	
10.0	V_{arc}	23.0	23.6	24.7	26.1	27.5	29.2	30.0	30.5	31.8	

run number 5	DATE: 5/7/69 TIME: 1500 H.V. = ±2 K.V. KEEPER = 0.5 amp @ 10 v					$\dot{M}_{H.C.}$ = 1.5 g/hr $\dot{M}_{Main}$ = 4.9 g/hr $\dot{M}_{total}$ = 6.4 g/hr					
I_{arc} \ I_{mag}	0.2	0.4	0.6	0.8	1.0	1.2	1.4	1.6	1.8	2.0	2.2
0.5	eV/ion η_m(%)										
1.0											
1.5											
2.0		267 21.1	241 23.4	231 24.6	246 23.4						
2.5		247 28.2	230 30.5	222 31.6	224 31.6						
3.0		253 32.8	229 36.3	218 38.7	220 38.7						
3.5		258 37.5	230 42.2	221 44.6	217 45.7	220 46.9					
4.0		262 42.3	236 46.8	225 50.4	221 51.6	210 55.1					
4.5		268 46.9	237 52.7	226 56.2	222 57.4	214 60.9	211 63.3				
5.0		274 50.4	242 57.4	231 60.9	224 63.4	220 65.6	215 69.2				
5.5		283 53.9	245 62.2	236 65.6	231 68.0	228 70.3	222 79.8	218 76.2			
6.0		282 58.7	251 66.8	240 70.3	241 71.5	229 76.2	230 78.5	226 80.8			
6.5		292 61.0	258 70.3	249 73.8	244 76.2	242 78.5	240 82.0	238 84.4			
7.0		300 64.4	264 73.9	256 77.4	258 78.5	251 82.0	252 84.4	252 86.7			
7.5		320 65.6	275 76.3	268 79.7	270 80.9	264 84.4	268 86.7	267 89.0	270 90.2		
8.0		326 68.0	279 79.7	274 83.2	283 83.2	281 85.5	281 89.0	282 91.4	284 92.6		
8.5		335 70.4	293 80.8	286 85.5	300 84.4	298 87.9	310 91.4	297 93.7	291 93.7	302 96.0	
9.0		348 71.5	303 83.3	302 86.7	312 86.7	314 90.0	319 92.6	318 94.9	325 96.0	330 97.2	
9.5		361 72.6	316 84.5	312 89.0	330 87.9	332 91.4	336 94.9	337 97.2	345 98.5	352 98.5	
10.0	eV/ion η_m(%)	373 73.8	331 86.7	327 90.2	350 89.0	353 92.6	362 96.0	363 98.5	364 99.6	380 99.6	

run number 5	DATE: 5/7/69 TIME: 1500 H.V. = ±2 K.V. KEEPER = 0.5 amp @ 10 v					$\dot{M}_{H.C.}$ = 1.5 g/hr $\dot{M}_{Main}$ = 4.9 g/hr $\dot{M}_{total}$ = 6.4 g/hr						
I_{arc} \ I_{mag}	0.2	0.4	0.6	0.8	1.0	1.2	1.4	1.6	1.8	2.0	2.2
0.5	$\eta_{t(\%)}$										
1.0											
1.5											
2.0		17.1	19.3	20.3	19.1						
2.5		23.3	25.4	26.6	26.8						
3.0		27.2	30.6	32.8	32.8						
3.5		31.3	35.6	38.0	39.4	41.2					
4.0		35.6	39.8	43.2	44.5	47.8					
4.5		39.4	45.1	48.8	49.2	53.2	55.3				
5.0		42.3	49.2	52.6	54.8	57.2	60.4				
5.5		45.5	53.2	56.7	59.0	61.0	64.2	66.6			
6.0		49.7	57.3	60.7	62.0	66.5	68.5	70.6			
6.5		51.4	60.3	63.0	66.0	68.2	71.4	73.6			
7.0		54.3	63.3	66.7	68.0	70.9	73.3	75.0			
7.5		54.8	64.3	68.4	69.5	72.8	74.3	77.4	77.5		
8.0		56.7	68.3	71.4	71.0	73.3	76.5	78.3	79.3		
8.5		58.5	68.9	73.0	71.8	74.7	77.3	79.7	79.5	79.8	
9.0		59.4	70.6	73.5	73.4	75.5	78.0	80.0	81.0	81.4	
9.5		59.7	71.3	75.2	73.8	76.8	79.4	81.3	82.3	82.0	
10.0	$\eta_{t(\%)}$	60.5	72.7	75.6	74.5	76.9	79.8	81.5	82.6	82.0	

Figure 1 Typical Performance Map, Ion Thruster*

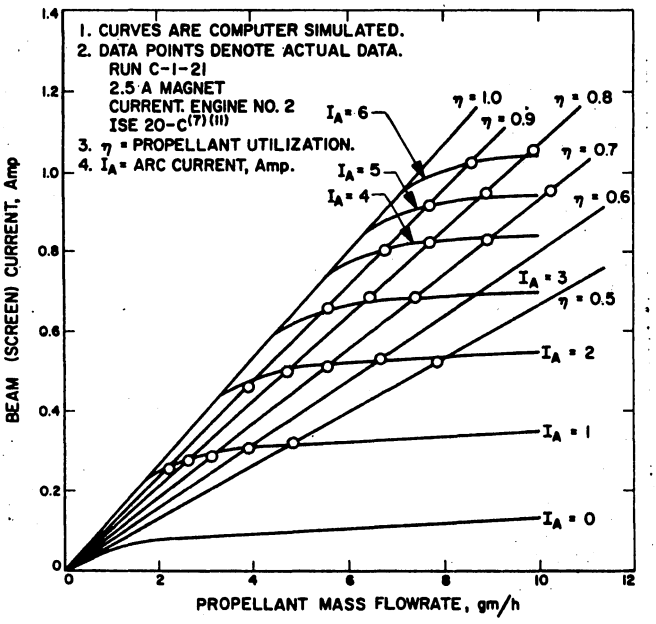

* From Mickelsen, W.R., and Jahn, R.G.: Status of Electric Propulsion. AIAA Paper No. 69-497. June, 1969. Figure 8, p. 21.

Figure 2 Bell Jar Assembly

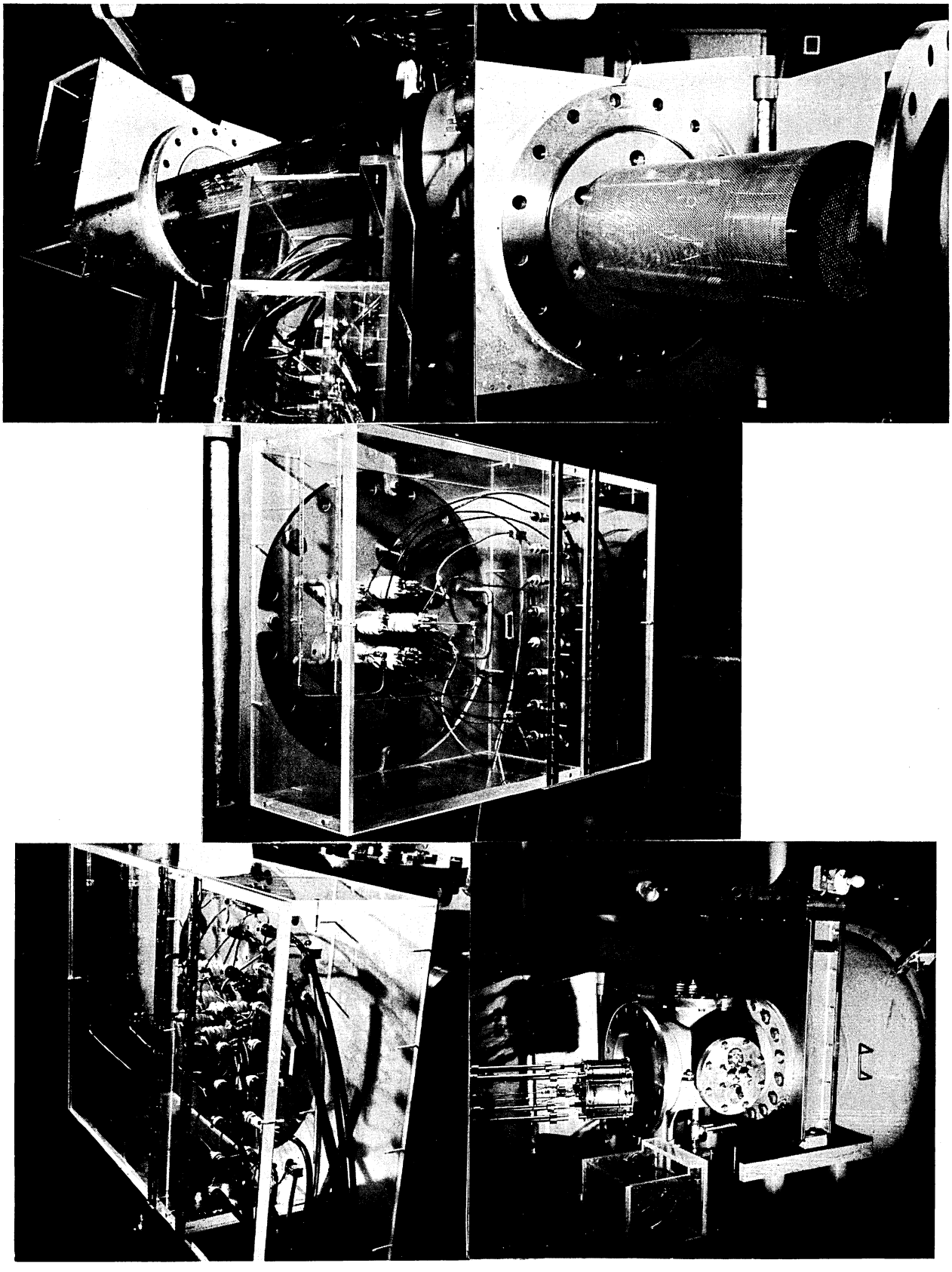

Figure 3 Thruster Setup

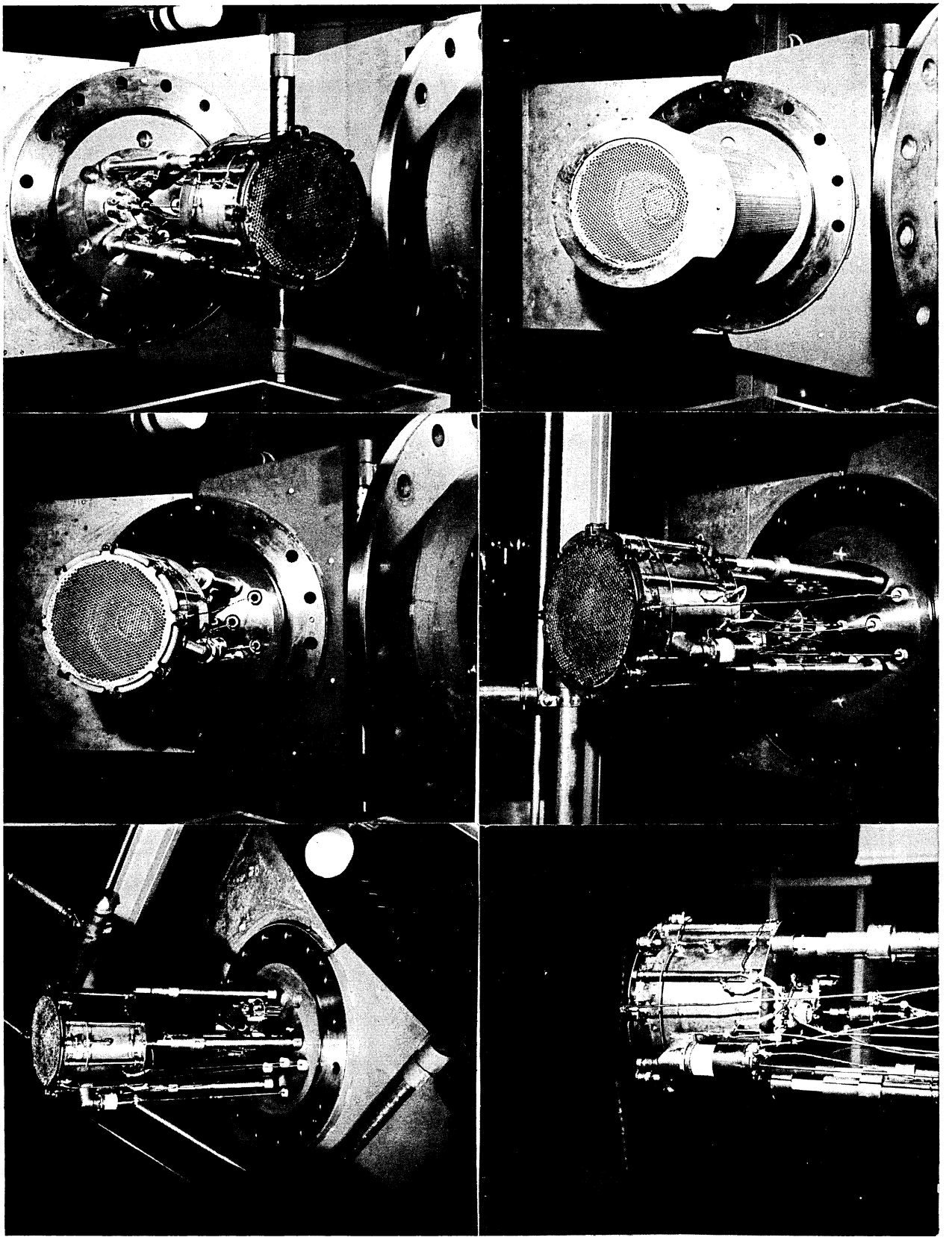

Figure 4 Power Supplies

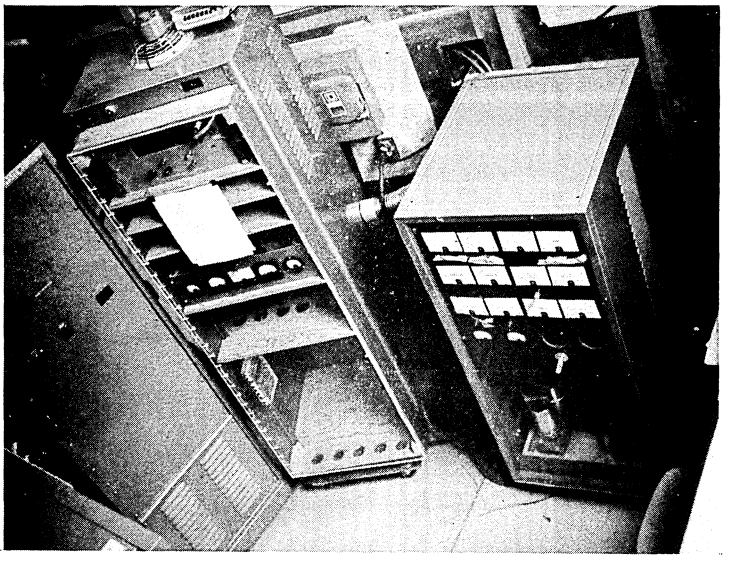

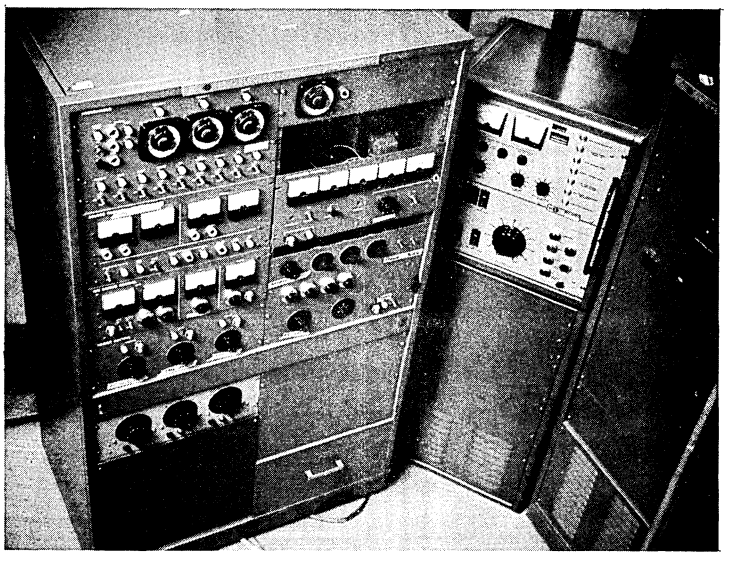

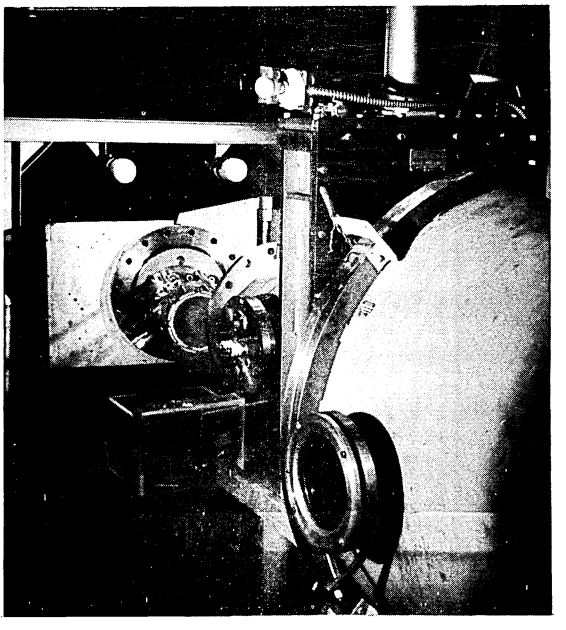

Figure 5

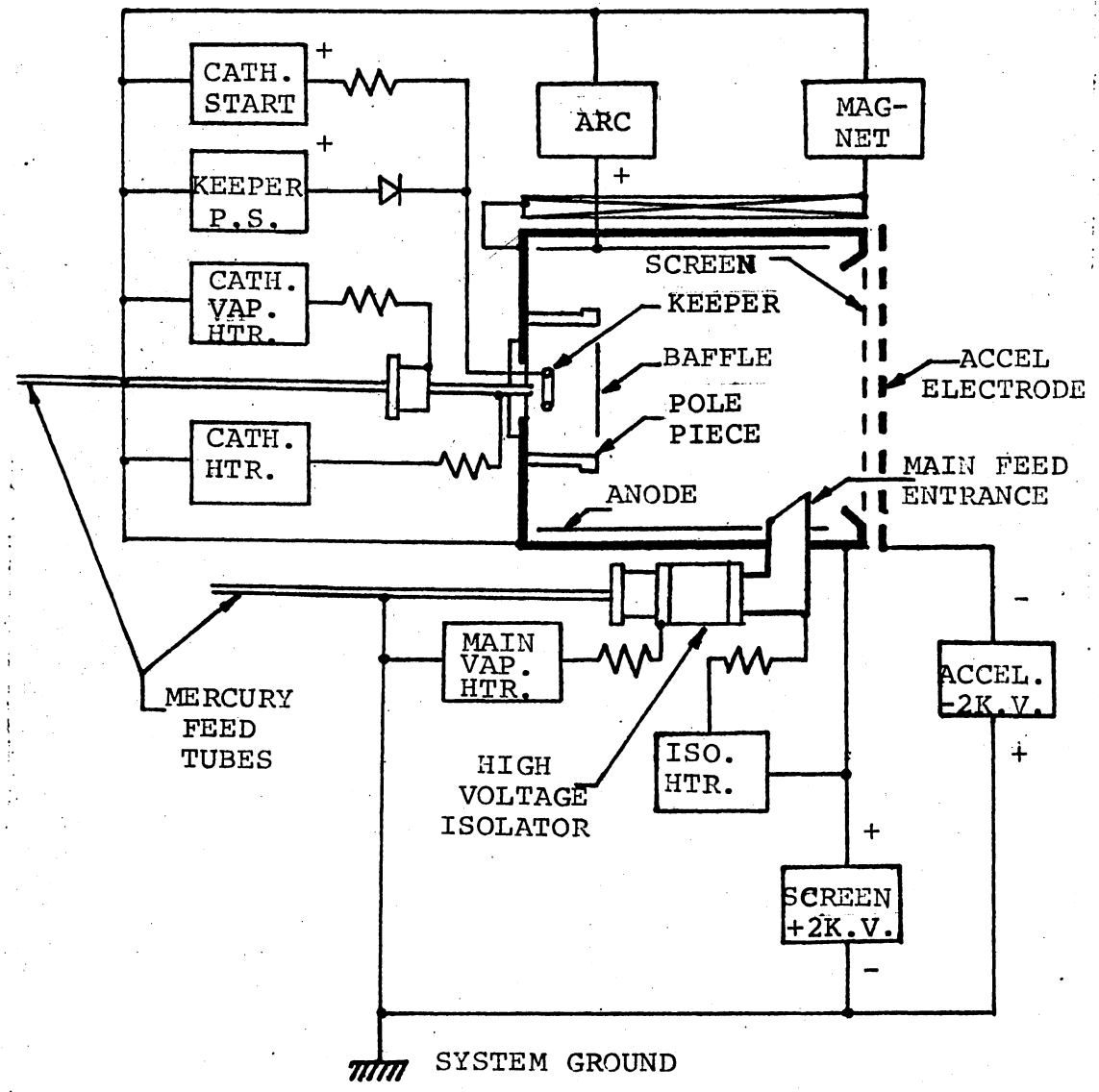
CATH. START
KEEPER P.S.
CATH. VAP. HTR.
CATH. HTR.
ARC
MAG-NET
SCREEN
KEEPER
BAFFLE
POLE PIECE
ANODE
ACCEL ELECTRODE
MAIN FEED ENTRANCE
MERCURY FEED TUBES
MAIN VAP. HTR.
HIGH VOLTAGE ISOLATOR
ISO. HTR.
ACCEL. -2K.V.
SCREEN +2K.V.
SYSTEM GROUND